G-Safety
SCIENCE FOR GLOBAL SAFETY

The 5th International Symposium on Water Environment Systems

---with Perspective of Global Safety

(November 30th - December 2nd, 2017)

Department of Civil and Environmental Engineering

Graduate School of Engineering

Tohoku University

TOHOKU
UNIVERSITY

Sponsors

http://www.g-safety.tohoku.ac.jp/

Tohoku University, Main Administration Office Organization for Leading Graduate School Program of Tohoku University, Sendai, Miyagi 980-8578, Japan

http://www.eng.tohoku.ac.jp/

Tohoku University, Graduate School of Engineering, Sendai, Miyagi 980-8579, Japan

ORGANIZERS

Dr. KAZAMA So (Professor, Tohoku University)

Dr. LI Yu-You (Professor, Tohoku University)

Dr. KOMORI Daisuke (Associate Professor, Tohoku University)

SECRETARIES

Assistant Professor, Toshimasa Hojo
toshimasa.hojo.b5@tohoku.ac.jp

Assistant Professor, Yoshiya Touge
yoshiya.touge.a6@tohoku.ac.jp

DC Student, Jialing Ni
jialing@dc.tohoku.ac.jp

DC Student, Bo Jiang
jiang.bo.t1@dc.tohoku.ac.jp

M Student, Kaoruko Kimura
Kaoruko.kimura.r7@dc.tohoku.ac.jp

PARTICIPANTS

Tohoku university	**Japan**
Name	**Identity**
Prem Rangsiwanichpong	Student
Noriko Uchida	Student
Chang Qing	Student
Miku Sakurai	Student
Danila Aleksandrovich Podobed	Student
Grace Puyang Emang	Student
Mbugua Jacqueline Muthoni	Student
Silva Vasquez Leonardo Alonso	Student
Kentaro Sugii	Student
Hironobu Hirayama	Student
Masafumi Kon	Student
Satoshi Anzai	Student
Koji Iwama	Student
Tao Zhang	Student
Jing Wu	Student
Jialing Ni	Student
Yan Guo	Student
Bo Jiang	Student
Yujie Chen	Student
Aijun Zhu	Student
Siti Nur Fatihah Binti Moideen	Student
Yemei Li	Student
Wataru Ruike	Student
Mribet Chaimaa	Student

National science and technology center for disaster reduction	**Taiwan**
Name	**Identity**
Jun-Jih Liou	Assistant researcher

Institut Teknologi Bandung	**Indonesia**
Name	**Identity**
Mohammad Farid	Lecturer

University of Moratuwa	**Sri Lanka**
Name	**Identity**
Chaminda Samarasuriya	Senior Lecturer

Shanghai University	**China**
Name	**Identity**
	Professor

Venue

Graduate School of Engineering, Aobayama campus, Tohoku University

Lectures and oral presentations

Room 402, Aoba Memorial Hall (青葉記念会館) (C03)

Posters exhibition

Room 402, Aoba Memorial Hall (青葉記念会館) (C03)

Dinner party

Shikisai (四季彩), Aoba Memorial Hall (青葉記念会館) (C03)

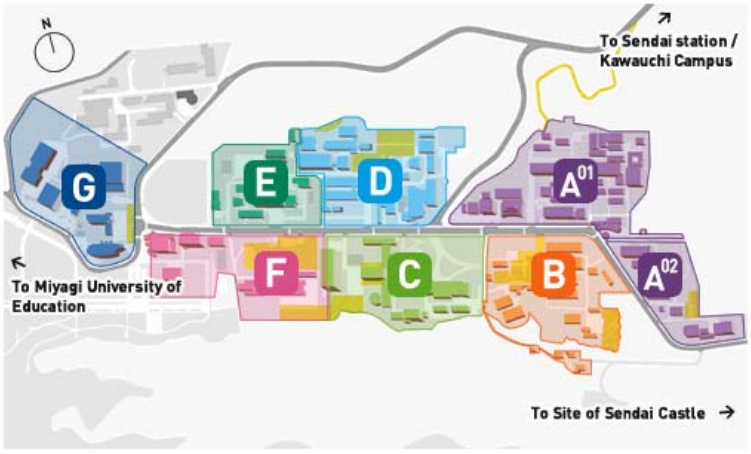

A01 Mechanical and Aerospace Engineering
A02 Quantum Science and Energy Engineering
B Materials Science and Engineering
C Center Square
D Electrical Engineering and Applied Physics
E Applied Chemistry, Chemical Engineering and Biomolecular Engineering
F Civil Engineering and Architecture
G Various Area

Aoba Memorial Hall（青葉記念会館）（C03）

Access to Aobayama Campus

(Subway)

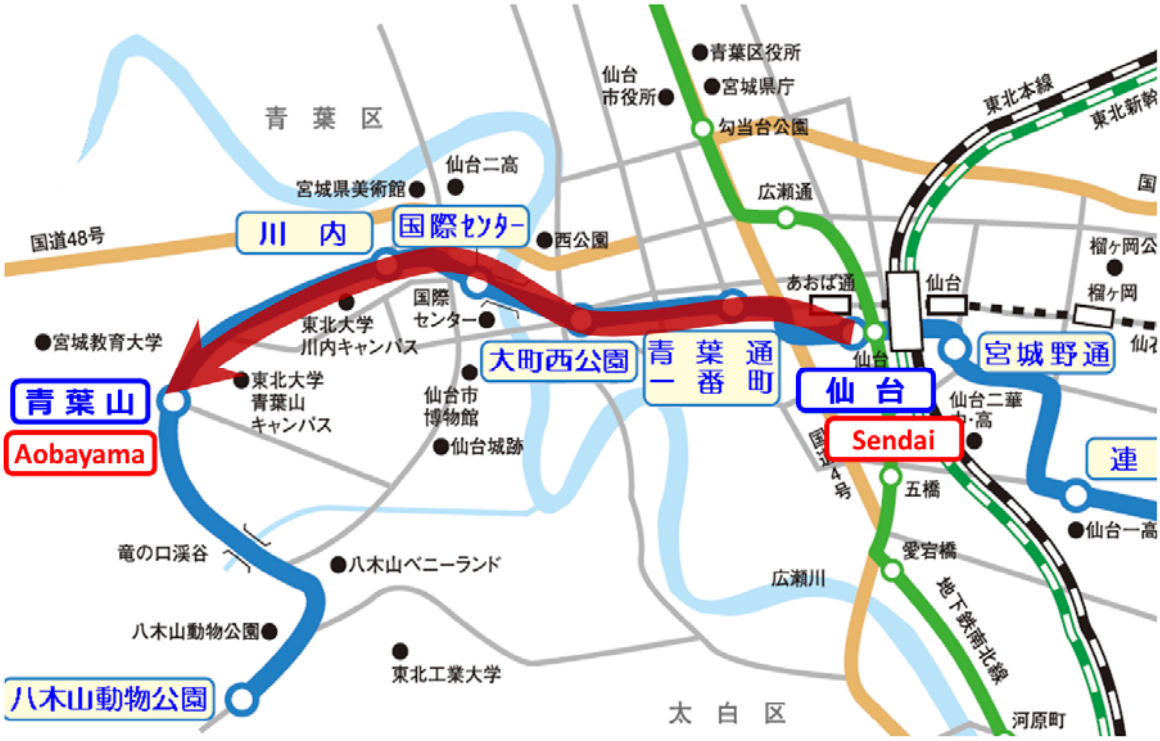

Map of **East-west line subway(地下鉄 東西線)** in Sendai

Please take this subway line and get off on the stop **Aobayama（青葉山）**.

Tips

If you start from Sendai Station, please make sure you are entering **East-west line subway（地下鉄 東西線）** rather than South-north line subway（**地下鉄 南北線**） nor JR station.

Program

Thursday, 30 Nov 2017

Fieldwork

The reconstruction of Minami-gamo sewage treatment plant

・2011/3/11 Tsunami hitting the Sewage Facilities

・Remains of 311-tsunami shocking on the wall of pump station

・Plan view of the sewage facilities

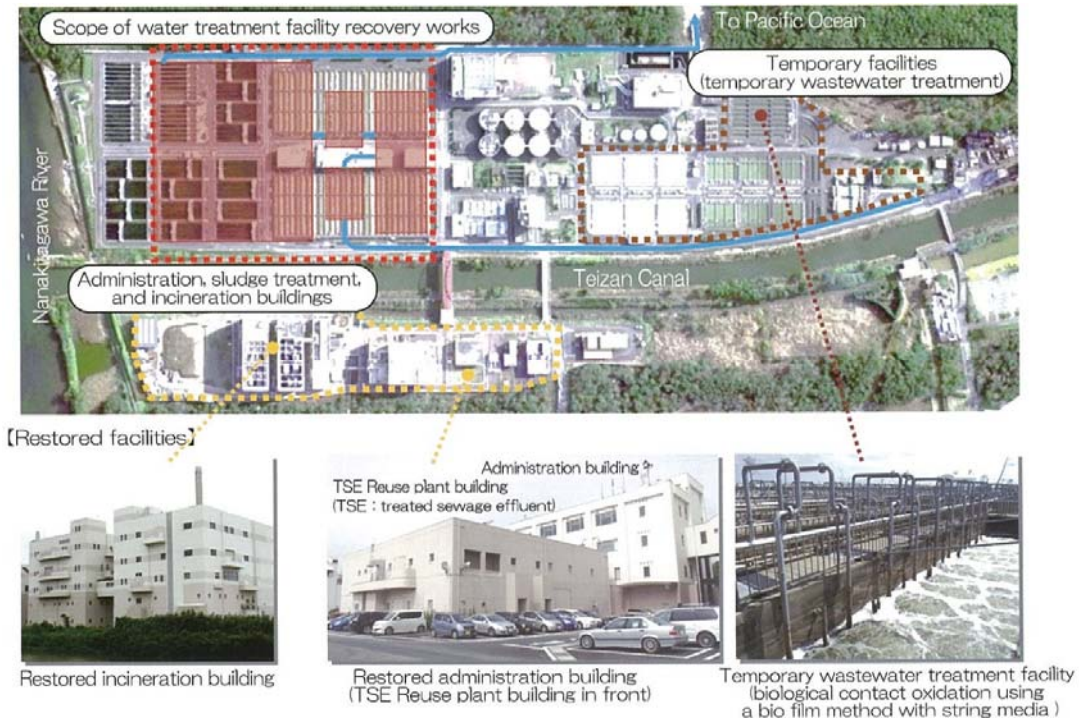

・Location of Minami-gamo sewage treatment plant

Friday, 01 Dec 2017

The 5th International Symposium on Water Environment Systems

Place: Room 402, Aoba Memorial hall, Tohoku University

9:00 ~ 9:10 **Opening address**

9:10 ~ 9:20 **Memorial photo**

Session I

9:20 ~ 9:50 Analysis and web-based mapping of typhoon impacts under climate change: a case study of Tainan, Taiwan
Jun-Jih Liou
National science and technology center for disaster reduction

9:50 ~ 10:20 Hydrological Characteristics of Upper Citarum River Basin
Mohammad Farid
Institut Teknologi Bandung

10:20 ~ 10:50 Development of Hydrological Disaster Index to Assess the Integrated Probability of Flood and Drought
Chaminda Samarasuriya
University of Moratuwa

10:50 ~ 11:00 **Coffee break**

Session II

11:00 ~ 11:30 Attempt of environmental assessment in freshwater using environmental DNABasins
Noriko Uchida
Tohoku University

11:30 ~ 12:00 A sensitivity analysis for Storm Water Management Model in a dense residential area of Japan
Chang Qing
Tohoku University

12:00 ~ 13:00 **Lunch break**

13:00 ~ 14:30 Poster exhibition

Place: Room 402, Aoba Memorial hall, Tohoku University

- Analyzing relationship between ocean index and rainfall in Northern part of Thailand
  Prem Rangsiwanichpong
  Tohoku University

- Understanding of water quality degregation with rapid urbanization - Case study in Yangon city, Myanmar-
  Miku Sakurai

  Tohoku University
- Evaluating the Effect of Afforestation on Groundwater Recharge Using Naturally-Occurring Isotopes
  Danila Aleksandrovich Podobed

  Tohoku University
- Satellite Analysis to Detect Burned Area of Forest Fire in Kamaishi, Tohoku 2017
  Grace Puyang Emang

  Tohoku University
- Remote sensing of irrigation water using different resolution sensors in the Aral Sea Basin
  Mbugua Jacqueline Muthoni

  Tohoku University
- Applying a Land Surface model considering groundwater effect in the Yoneshiro river basin
  Silva Vasquez Leonardo Alonso

  Tohoku university
- Determination critical rainfall using, Infiltration model-infinite slope model: A case of Iwaizumi, Iwate, Japan
  Kentaro Sugii

  Tohoku university
- Development of the Sakikawa flood model enabling estimation of cultural property damage
  Hironobu Hirayama

  Tohoku university
- Dynamics of CO_2 Fluxes Over the Heterogeneous Land Covers

  Masafumi Kon

  Tohoku university
- Analysis on Instagram data to understand people actions during heavy rainfall period
  Satoshi Anzai

  Tohoku university

- The Concentration of Trace Elements in Corbicula Japonica
  Koji Iwama
  Tohoku university
- A Rapid Start-up of a Lab-scale Anammox Reactor Applied for Treating the Domestic Sewage
  Yujie Chen
  Tohoku university
- Effect of HRT on themophilic anaerobic digestion of paper waste containing OFMSW
  Aijun Zhu
  Tohoku university

Session III

14:30 ~ 14:50	The effect of organic matter on one-stage anammox process Yan Guo *Tohoku university*
14:50 ~ 15:10	A research on the mathematical model of co-digestion's synergism mechanism based on coffee ground and wasted activated sludge Tao Zhang *Tohoku university*
15:10 ~ 15:20	**Coffee break**

Session IV

15:20 ~ 15:40	Anaerobic co-digestion of food waste and paper waste: mesophilic vs. thermophilic Jing Wu *Tohoku university*
15:40 ~ 16:00	Start-up of a New Anaerobic Reactor for treating wastewater containing High SS Content Bo Jiang *Tohoku university*
16:00 ~ 16:20	Active microbial population diversity analysis in anaerobic digester by using PMA-PCR Jialing Ni *Tohoku university*
16:20 ~ 16:30	**Coffee break**

Session V

16:30 ~ 16:50	The treatment of synthetic palm oil mill effluent (POME) by Anaerobic Membrane Bioreactor (AnMBR) Siti Nur Fatihah Binti Moideen *Tohoku university*
16:50 ~ 17:10	Carbonation and utilization of basic furnace slag coupled with concentrated water from electrodeionization Yemei Li *Tohoku university*
17:10 ~ 17:30	Analysis of material flow and energy balance in full-scale biogas plant Wataru Ruike *Tohoku university*
17:30 ~ 17:50	Slaughterhouse wastewater treatment plant investigation: a case Mribet Chaimaa *Tohoku university*
17:50 ~ 18:00	**Coffee break**
18:00 ~ 18:20	**Closing speech**
18:20 ~ 20:00	**Dinner party**

Analysis and web-based mapping of typhoon floods for climate change adaptation

Jun-Jih Liou*, Chao-Tzuen Cheng, Hsin-Chi Li, Yi-Chiung Chao, Yi-Hua Hsiao
National Science and Technology center for Disaster Reduction, New Taipei City, Taiwan, R. O. C.

*E-mail: jjliou@ncdr.nat.gov.tw

Abstract

In East Asia, floods caused by heavy rainfall of typhoons are always a big problem to our society. In Taiwan, the impacts of floods seems to be larger after 2000 due to heavier typhoon rainfalls. IPCC reports had reported that the relative frequency of severe typhoons will be increased due to global warming, and it is worthy to study related issues of future typhoon flood and make no-regrets adaptation pathway in time. Images make projected future disaster impacts be experienced or seen by people, and shape the situation affected by global warming. Since last decade, many online websites were constructed to provide images and essential information of climate change, but none (or not many) of them can provide the projection of the situation of future typhoon floods.

In this study, we built a webpages to show geographic information mapped with projected typhoon floods for non-experts and general public. Therefore, all information can be transformed into understandable and useful knowledge for less confusion or misunderstanding. Flooding simulations and their economic-loss estimations were extensively analyzed at earlier studies (Wei et al., 2016). Web-GIS mapping and visualization charts were plotted with any available software. The webpages could help people understand climate change issues and raise more concerns about environment protection.

Preliminary results revealed that a prototype webpages of story-map type were built for general public and composed of essential knowledge and mapping of simulated typhoon floods for distributing the ideas of climate change. Web real-time demonstration could serve many people online and provide a better communicating tool among cross fields or different stakeholders without limits from distances. The preliminary results were only a few mapping webpages. Climate change adaptation, uncertainty issues and users' opinion survey were still needed further studies.

Keywords: typhoon flood, climate change, web-GIS mapping, visualization

1. Introduction

In East Asia, floods associated with heavy rainfall brought by typhoons always cause serious impacts to our society. According to historical records in Taiwan, it seems that the severe magnitudes of natural flooding disasters were increased after 2000 due to heavier intensity and longer duration of typhoon rainfalls (Chen et al., 2011). Since IPCC reports had pointed out that the relative percentage of frequency of severe typhoons will be increased under global warming, it is worthy to pay attention and effort to study related issues of future typhoon flood and make no-regrets adaptation pathway in time. Also, there are two questions we like to know in this study. What will beyond-historical-records typhoon happened in the future look like? How severe will be record-breaking and unexperienced flooding event happened under global warming?

Because future is not yet to happen, how IPCC and former vice president of USA Al Gore had done in their publications to promote the necessary action for climate change adaptation? They used a mass of images, for example, natural disasters' photos and videos related to past climate change, to imply possible future impacts and shape the imagination of world under the condition of global warming (Schneider and Nocke, 2014).

Now, there are many websites established to demonstrate vast amount of data and information related to climate change. These websites can be easily connected or accessed online by people all over the world 24 hours a day. Since last decade, many web-based mapping tools have developed and applied for climate change adaptation (Wrobel et al., 2010; Neset et al., 2016). There are 3 main characteristics could be used to measure the functions of those websites, including the interactive degree between users and webpages, new information/knowledge, and the amount of users. The conventional websites were full of climate information and didn't limited to specific users. But the true is that only climate experts are able to read the climate information. People may be overwhelmed by too much information and don't know what is the essential part. That is why the cross-fields experts are needed to transform information to knowledge for general public. In recent years, there are more and more new websites designed for specific users with more online interaction and necessary knowledge (Bai et al., 2014; Nugent et al., 2017). A good case was demonstrated for homeowners with 3 steps on webpages, which are location, investigation, and action, for climate change adaptation (Johansson et al., 2016).

There are several important questions people might like to know. How can we explore the changing characteristics of future typhoons? Is there any available typhoon data under global warming? Global circulation models (GCMs) were used to simulate climate projection data assuming certain global warming scenarios for years. However, spatial resolutions of most GCMs are coarser than 100 km, which is not high enough to explicitly resolve typhoon information. High-resolution GCMs are more capable of simulating

typhoon activity and their simulation results can be used to meet the need of our studies.

In this study, we focused on making webpages with geographic information mapping and projection of typhoon floods. These webpages are designed not just for non-experts but also for general public. Therefore, all webpages information had been screened or transformed into readable and useful knowledge for less confusion or misunderstanding of people without extra explanation. Flooding simulations and their economic-loss estimations were extensively analyzed at earlier studies (Wu et al, 2014; Wu et al., 2016; Su et al., 2016, Wei et al., 2016; Li et al., 2015). Web-GIS mapping and visualization charts were plotted with any available software. We hoped that the webpages could help people understand climate change issues and raise more concerns about environment protection.

2. Data, Models and tools

In earlier study (Su et al., 2016), MRI-AGCM-20km projection data was dynamically downscaled and bias-corrected to create regional data for Taiwan area with5km resolution. Furthermore, Top ten typhoons of present and future sorted by total rainfall amount at Tengwen-reservoir basin, were selected to simulate floods and to estimate the disaster loss. Rainfall-runoff, channel flow, and flood modules of SOBEK were used to estimate the hourly rainfall-runoff flow in upstream mountain areas, the inundation depth of midstream area, and the inundation depth of downstream area, respectively. Economic loss estimations of top 10 typhoon flood events were calculated with TLAS (Taiwan typhoon Loss System, Wei et al., 2016; Li et al., 2015). Geographic information mapping of total rainfall and inundation depth, and loss statistics charts were established for visualization purposes with portal-of-ArcGIS and TABLEAU software. Story-map type webpages were built and composed of the simulated results for distributing the ideas of climate change.

3. Preliminary results

A prototype webpages of story-map type were built for general public and composed of essential knowledge and mapping of simulated typhoon floods for distributing the ideas of climate change. Web real-time demonstration could serve many people online and provide a better communicating tool among cross fields or different stakeholders without limits from distances. The preliminary results were only a few mapping webpages. Climate change adaptation, uncertainty issues and users' opinion survey were still needed further studies.

References

1) Bai Y., Kaneko I., Kobayashi H., Kurihara K., Takayabu I., Sasaki H. and Murata A. : A Geographic Information System (GIS)-based approach to adaptation to regional climate change: a case study of Okutama-machi, Tokyo, Japan, Mitigation and Adaptation Strategies for Global Change, 19, pp. 589–614, 2014.
2) Chen L. C. et al. : Taiwan Climate Change Science Report, chapter 6, pp. 311, 2011. (in Chinese)
3) Johansson J., Opach T., Glaas E., Neset T., Navarra C., Linnér B-O., Rød J. K. : VisAdapt: A visualization tool to support climate change adaptation, IEEE Computer Graphics and Applications, PrePrints, 2016. doi:10.1109/MCG.2016.49
4) Li Hsin-Chi, Wei Shiao-Ping, Cheng Chao-Tzuen, Liou Jun-Jih, Chan Yong-Ming, Yeh Keh-Chia : Applying Risk Analysis to Disaster Impact of Extreme Typhoon Events under Climate Change, Journal of disaster research, 10(3), pp. 513-526, 2015.
5) Neset T.S. et al. : Map-Based Web Tools Supporting Climate Change Adaptation, The Professional Geographer, 68(1), pp. 103-114, 2016 .
6) Nugent P.J. et al. : A Web-Based Geographic Information Platform to Support Urban Adaptation to Climate Change, In: Griffith D., Chun Y., Dean D. (eds), Advances in Geocomputation, Advances in Geographic Information Science, Springer, Cham, 2017.
7) Schneider B., Nocke, T. : Image Politics of Climate Change. Transcript, London, 2014.
8) Su Y. F., Cheng C. T., Liou J. J., Chen Y. M., Kitoh A. : Bias correction of MRI-WRF dynamic downscaling datasets, Terr. Atmos. Ocean. Sci., 27, pp. 649-657, 2016. doi: 10.3319/TAO.2016.07.14.01
9) Wei H. P., Li H. C., Yeh K. C., Liou J. J., Chen Y. M., Lin H. J. : Using structural measures to reduce flood losses in a future extreme weather event, Terr. Atmos. Ocean. Sci., 27, pp. 757-767, 2016. doi: 10.3319/TAO.2016.07.14.02
10) Wrobel M. et al. : A review of user interface conventions in web applications for climate change information, International Environmental Modelling and Software Society (iEMSs), International Congress on Environmental Modelling and Software, 2010.
11) Wu Tingyeh, Li Hsin-Chi, Wei Shaio-Pin, Chen Wei-Bo, Chen Yung-Ming, Su Yuan-Fong, Liu Jen-Jih, Shih Hung-Ju : A comprehensive disaster impact assessment of extreme rainfall events under climate change: a case study in Zheng-wen river basin, Taiwan. Environmental Earth Sciences, 75:597, pp. 1-17, 2016.
12) Wu Tingyeh, Wei S.-P., Chen W.-B., Li H.-C., Chen Y.-M., Su Y.-F., Liou J.-J., Shih H.-J., Yeh K.-C. : Impact assessment of slopeland, river, urban and coastal areas associated with extreme typhoon floods under climate change, National science and technology Center for Disaster Reduction technical reports, NCDR 102-T19, 2014.(in Chinese)

Hydrological Characteristics of Upper Citarum River Basin

○Mohammad Farid[1*], Arno Adi Kuntoro[1], Muhammad Syahril Badri Kusuma[1]
[1]Faculty of Civil and Environmental Engineering, Institut Teknologi Bandung, Bandung 40132, Indonesia

*E-mail: mfarid@ftsl.itb.ac.id

Abstract
Higher water demand, more frequent of water related disaster, and climate change have made water resources management more complicated. Hydrological characteristics assessment is important to develop a good approach regarding water resources planning and management. Upper Citarum River Basin is selected as a case for the assessment. The environmental degradation and change in variation of hydro-climatology in the basin has caused many problems such as flood and drought. The analysis of datasets and simulation results indicates the change of hydrological characteristics in the basin. Therefore, it is necessary to have policy regarding water master plan which can accommodate land use planning considering water capacity in the basin by using an approach to achieve sustainable river basin development through green planning.

Keywords: Hydrological characteristics, Upper Citarum River Basin, Sustainable river basin development

1. Introduction
Nowadays, water resources management has become more complex with many challenges ahead. Many factors such as economic development, population growth, and also change of lifestyle have made an impact in increasing water demand. More frequent of water related disaster occurrences have been considered to be caused by runoff intensification due to land use/land cover change as a consequence of human activity. Furthermore, climate change has been indicated to make alteration in hydrological regime [1].

Infrastructure development is commonly proposed to tackle water resources problem. A good planning by considering a good land use and water resources management, adequate infrastructure maintenance and operations, climate prediction, hazard mitigation and information dissemination is significant to have an appropriate development [2]. Hydrological parameter plays an important role in the planning. Therefore, it is necessary to conduct the assessment of hydrological characteristics in a river basin related to water resources infrastructure planning. This paper presents the case of Upper Citarum River Basin in order to have good understanding in its hydrological characteristics.

2. Materials dan Methods
2.1. Case Study
Citarum River Basin is the biggest river basin in West Java Province with total catchment area of 12,000 km^2 and 270 km of river length. With three cascade reservoir (Saguling, Cirata, and Jatiluhur), this river basin has an important role for generating around 1,800 MW of electricity, serving more than 237,000 ha of irrigation area, and supplying water not less than 16 m^3/s to 80% population of Jakarta City.

The upstream of Citarum River, called as Upper Citarum River Basin, is located around 6°43'21,8" - 7 °19'38,1" South Latitude and 107°32'2" - 107°53'51,6" East Longitude. The topography elevation is in the range 625-2600 meter above sea level and it is surrounded by mountains and hills [3]. This river basin is the main catchment area of Saguling Dam and covers the area of some districts including Bandung City.

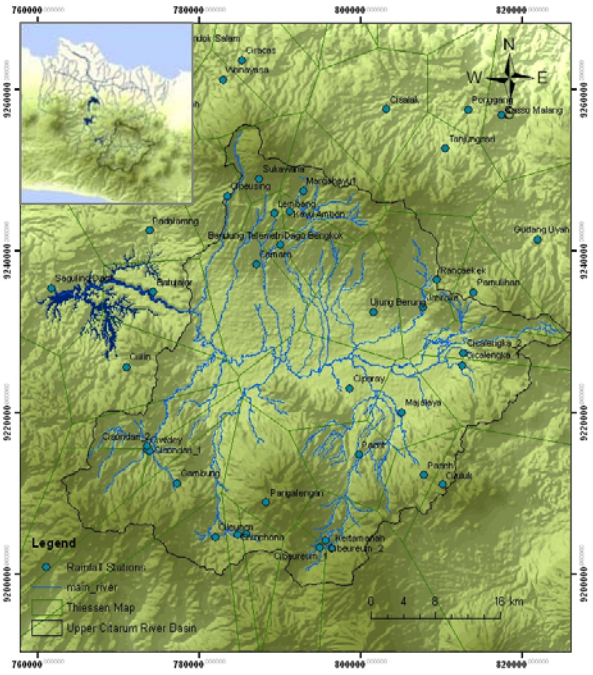

Figure 1. Upper Citarum River Basin

2.2. Problem Statement
In Upper Citarum River Basin, particularly in Bandung City and several districts around it, flood occurs almost every year. The occurrence of flood is usually located in the meeting point of main Upper Citarum River and its tributary.

In these meeting points, the river paths are perpendicular due to its flow regime which is at least critical flow [4]. The topographical condition in the middle part of the basin is flat so that it makes the flood inundation period becomes longer. Furthermore, the river capacity been reduced due to the problems such as sedimentation and illegal building.

Water supply for Jakarta City has been an attention recently related to the condition of Upper Citarum River Basin. The decreasing of water supply to the city caused by prolonged drought will make impact for the potential of loss in national economic activities in Indonesia [5].

Degradation of environmental condition in Upper Citarum River Basin has been considered to cause all of the problems. There was decrease of forest cover due to land conversion to urban area. This phenomenon can result in flood as well as drought. Furthermore, the changes of hydro-climatology variation make it worse.

3. Discussion

The assessment of the river health through river regime and its correlation with the rainfall trend is conducted as well as examination of the correlation pattern of rainfall runoff transformation [6]. The data used in the study obtained from Balai Besar Wilayah Citarum (Citarum River Basin Authority) during the period of 1981-2009 for daily rainfall and river discharge in Nanjung. In order to assess the condition of river regime and river health, flow duration curve is used. The change of curve is analyzed into two period, 1981-1995 defined as before urbanization and 1996-2009 defined as after urbanization.

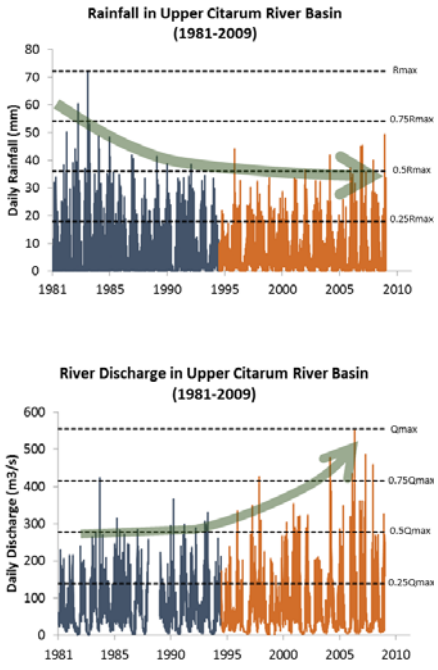

Figure 2. Hyetograph (above) and Hydrograph (bottom) at Upper Citarum River Basin

Figure 2 shows the daily time series graph of hyetograph and hydrograph in Upper Citarum River Basin. It can be seen that there is indication of river basin degradation regarding its carrying capacity which can be assessed by correlate the trend of river discharge and rainfall. The graphs show that there is increasing trend related to high flow while there is decreasing trend related to rainfall in the period of 1981-2009. This asymmetric trend indicates land use change effect.

The pattern change related to rainfall and runoff is shown in Figure 3 which is analyzed in logarithmic scale of exceedance probability. Comparing to the period of 1996-2009, the gradient of rainfall curve in the period of 1981-1995 is steeper while, the gradient of runoff curve in is milder. Furthermore, it can indicate that that during the period of 1981-1995, the land use can store water more and longer than the period of 1995-2009.

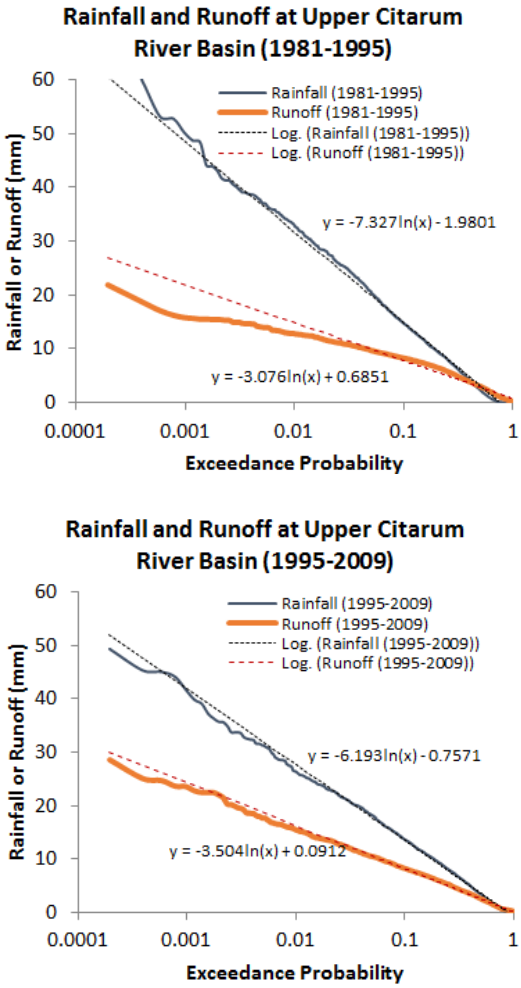

Figure 3. Exceedance Probability Curve of Rainfall and Runoff at Upper Citarum River Basin

The future condition of Upper Citarum River Basin is studied by using Sacramento Catchment Model to simulate river discharge from rainfall and potential evapotranspiration data input [7]. The model is calibrated by using data from 1995-1999 and by using data from 2005-2009. The simulation result of calibration shows an acceptable to good result regarding Nash Sutcliffe Efficiency (NSE) with average number of 0.49 and Correlation Coefficient (r2) with average number of 0.77 compared to the observed data as can be seen in Figure 4.

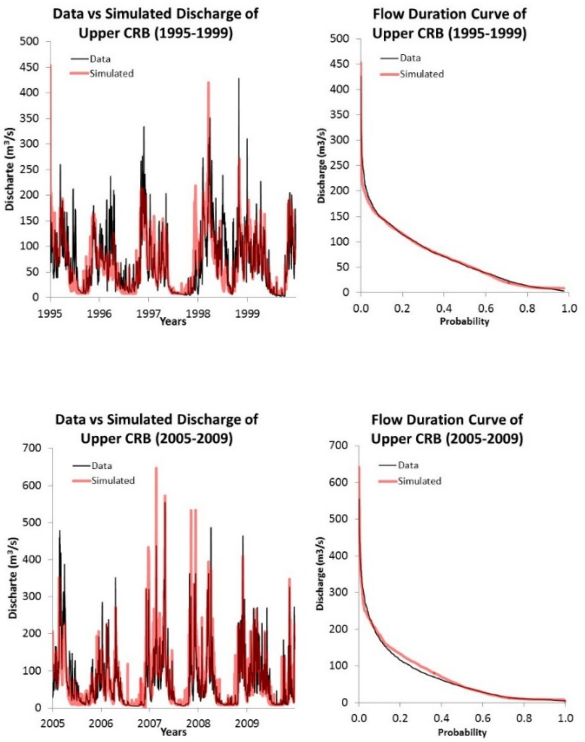

Figure 4. Simulated vs observed river discharge data in Upper Citarum River Basin

In order to simulate future condition of Upper Citarum River Basin, two scenarios is used by using the corrected CMIP5 multi-model mean of rainfall and temperature datasets from 2045 to 2050 and land cover map in 2015 as input for rainfall-runoff model. The first scenario assumes the same impervious land cover in the 2045-2050 as in 2015 while the second scenario assumes linear trend of increase of impervious land cover in the future based on land cover change indication in 1980s to 2015s. The simulation results in Figure 5 shows that related to the average of high flow (Q20%), in "without land use change scenario, there is increasing number of 8% from about 115.9 m^3/s in 2005-2009 to about 124.9 m^3/s in 2045-2050 and in with land use change scenario, there is increasing number of 11% related to the average of high flow discharge (Q20%) from about 115.9 m^3/s in 2005-2009 to about 129.0 m^3/s in 2045-2050. Furthermore, related to the average of low flow (Q80%), in "without land use change scenario, there is decreasing number of 18% from about 10.5 m^3/s in 2005-2009 to about 8.7 m^3/s in 2045-2050 and in with land use change scenario, there is decreasing number of 23% related to the average of low flow discharge (Q80%) from about 10.5 m^3/s in 2005-2009 to about 8.4 m^3/s in 2045-2050. These results indicate that there is climate change effect in decreasing trend of low flow and increasing trend of high flow for both scenarios (with land use change and without land use change).

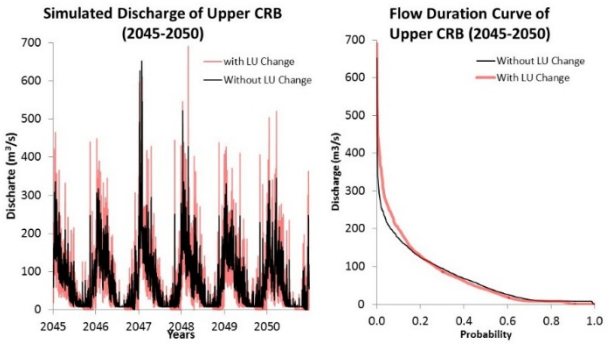

Figure 5. Simulated river discharge data in Upper CRB (2045-2050)

4. Closing remark

In Upper Citarum River Basin, due to urban development and change in land use, there is increasing in regarding high flow in term of flood event and decreasing regarding low flow in term of water supply. The trend of hyetograph and hydrograph and exceedance probability curve of rainfall and runoff show the change of high flow and low flow. Furthermore, in the future, climate change will have impact in change of flow even if there is land use change or not.

Based on the results shown the discussion, it can be seen that there is indication for change of hydrological characteristics in Upper Citarum River Basin. Therefore it is necessary to have policy regarding water master plan which can accommodate land use planning considering water capacity in the basin. Figure 6 shows water resources sustainable development plan framework which can be used as an approach to achieve sustainable river basin development through green planning.

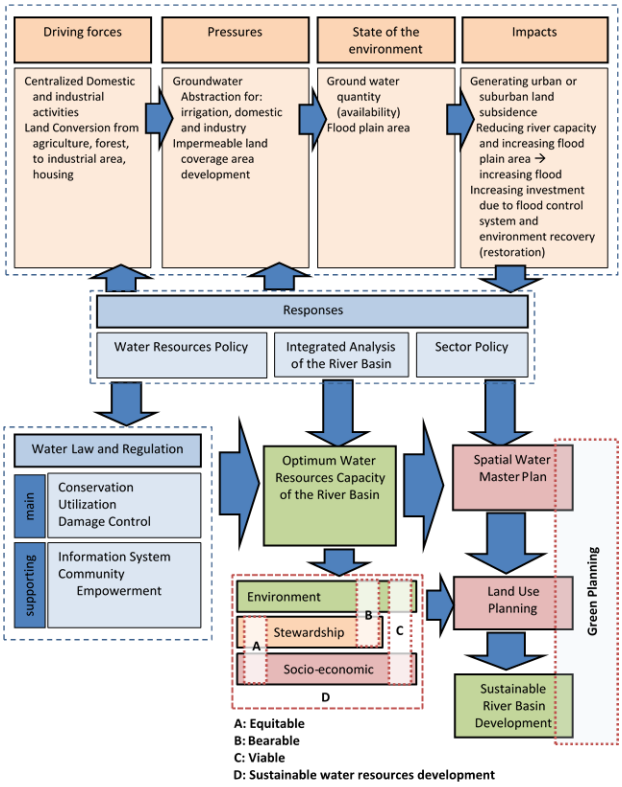

Figure 5. Sustainable River Basin Development Plan [6]

References

1) C. Schneider, C. L. R. Laize, M. C. Acreman, and M. Florke : How will climate change midify river flow in Europe?, Hydrology and Earth System Sciences, 17, pp. 325-339, 2013.
2) Budi Kartiwa, Erni Murniati, Arnob Bormudoi : Application of Hydrological Model, RS and GIS for Flood Mapping of Citarum Watershed, West Java Province, Indonesia, Journal of Remote Sensing Technology, 1Iss. (1), pp. 1-8, 2013.
3) R. I. Siregar, M. Farid, and M. S. B. Kusuma : Assesment of the Contribution of the Flood Hydrograph of Cirasea, Cidurian and Ciwidey River in Affecting Flood Index in Bandung Basin, Proceeding of the Second International Conference on Sustainable Infrastructure and Built Environment, Bandung 19-20 November 2013, pp. 234-245, 2013.
4) I. K. Hadihardaja, A. A. Kuntoro, and M. Farid : Flood Resilience for Risk Management: Case Study of River Basin in Indonesia, Global Aspect, 3(4), pp. 16-19, 2013.
5) M. S. B. Kusuma, A. A. Kuntoro, R. Silasari, : Preparedness Effort toward Climate Change Adaptation in Upper Citarum River Basin, West Java, Indonesia, International Symposium on Social Management Systems, Kochi University, 2011.
6) I. K. Hadihardaja, A. A. Kuntoro, M. Farid, and H. Nurcahyo : River Regime Change and the Basin Land Use Development Regarding to Healthy River Performance, The 5th Environmental Technology and Management Conference “Green Technology towards Sustainable Environment”, November 23 - 24, 2015.
7) A. A. Kuntoro, M. Cahyono, and E. A. Soentoro : Land Cover and Climate Change Impact on River Discharge: Case Study of Upper Citarum River Basin, The Third International Conference on Sustainable Infrastructure and Built Environment, September 26-27, 2017.

Development of Hydrological Disaster Index to Assess the Integrated Probability of Flood and Drought

○Chaminda Samarasuriya [1*], So Kazama[2], Daisuke Komori[3],

[1]Faculty of Engineering, University of Moratuwa, Katubeddha, Moratuwa 10400, Sri Lanka
[2]Graduate School of Engineering, Tohoku University, Sendai 980-8579, Japan
[3]Graduate School of Environmental Studies, Tohoku University, Sendai 980-8579, Japan

*E-mail: chaminda@uom.lk

Abstract

We introduced a new index to identify the seasonal and spatial variation of the integrated probability of hydrological disasters (flood and drought). The flood and drought probabilities were identified by river flow indices that were computed using simulated natural daily runoff from the period 1976 - 2005. The identified flood and drought probability levels were weighted and integrated to develop a new Hydrological Disaster Index (HDI). Validation of the HDI confirmed that it is a reliable index for assessing the seasonal and spatial distribution of integrated hydrological disasters across the country. The computed HDI showed that most of the dry zone river basins have a high probability of hydrological disaster during the northeast monsoon. This index can assess the future seasonal and spatial variation of the integrated probability of hydrological disasters and can be used to identify better future climate change adaptation measures.

Keywords: low flow, high flow, seasonal, spatial, runoff, monsoon.

1. Introduction

The impact of climate change on hydrological systems has received significant attention over the last few decades due to the incidence of hydrological disasters, especially floods and droughts (Nijssen *et al*., 2001; Hirabayashi *et al*., 2008). Recent studies show that the global climate cycle will intensify, creating more severe and more frequent floods and droughts in many regions, resulting in threats to the reliability and quality of water resources, the stability of regional economics and the sustainability of utility infrastructure (Frederick *et al*., 1997; NCAR, 2008). The occurrence and intensity of hydrological disasters (floods and droughts) varies widely across river basins and precipitation seasons because of highly variable seasonal precipitation patterns. Hence, there is now a pressing need to identify the spatial and seasonal variability of the intensity of hydrological disasters so that decision-makers can better understand future regional and seasonal water resource management plans and disaster preparedness and prevention programs.

In recent decades, various drought and flood indices have been derived to characterize drought and flood severity on a regional basis and to provide information for decision makers (Quiring and Papakryiakou, 2003). These drought indices can be classified as precipitation indices, soil moisture indices, water budget indices, and hydrological and various aridity indices (Mika and Dunkel, 2005). Several regional flood frequency analyses have been developed based on the use of the index flood method as a regional model to estimate flood frequency curves (e.g. Robson and Reed, 1999; Bocchiola *et al*., 2003). The above indices are used to identify and assess the characteristics of flood and drought in a river basin as separate event. However, some river basins experience flood or drought as distinct events, while others sustain both a flood

and drought during a given year or season due to erratic precipitation patterns. Moreover, river basins that undergo both drought and flood are more vulnerable to severe hydrological disasters. Thus, it is important to consider the integrated probability of these hydrological disasters. The currently available flood and drought indices are not capable of identifying the integrated probability of these hydrological disasters. Hence, it is necessary to develop a new index to identify and assess the integrated probability of hydrological disasters (flood and drought) along with their spatial and temporal variability across river basins.

Flood and hydrological drought intensity and frequency rely on river flow records and a good understanding of the patterns in river flow and, in particular, in Extreme River flow is important to improve the estimation of flood and drought disaster probabilities in the future. The past studies, successfully used the stream flow indices to identify flood and drought probabilities in a river basin (Dankers *et al.,* 2009; Botter *et al*., 2013). The present study developed a new Hydrological Disaster Index (HDI) as a function of the drought and flood probabilities that were identified using respective stream flow indices from a historical period (1976 – 2005). Then, the developed index was employed to assess the spatial distribution of annual and seasonal hydrological disaster probabilities in Sri Lanka.

2 Study methods

2.1 Study area

Sri Lanka is a tropical island in the Indian Ocean between 79.59^0 E and 81.89^0 E longitudes and 5.87^0 N and 9.84^0 N latitude. There is considerable spatial variation of the mean annual rainfall of 2000 mm. The highest values occur on the western slopes of the central highland with several recorded station values exceeding 5,000 mm. The lowest rainfall occurs in the northwest and southeast lowlands with a minimum value of 935 mm. The island's rainfall is seasonally influenced by the southwest monsoon (May to September) and the northeast monsoon (December to February). In between, tropical cyclones, depressions and thunderstorms influence the climate of Sri Lanka during the intermonsoon seasons, which are caused by the movements of the intertropical convergence zone (ITCZ) (Domroes *et al*., 1992). There are approximately 103 distinct river basins, covering 90 percent of the island. Of the 103 river basins, 12 river basins with 46% of the geographical area generate 72% of the total renewable water resources because these river basins receive rainfall from both monsoons. The majority of the remaining 91 basins, which mainly receive rainfall from the northeast monsoon, are mainly seasonal (Amarasinghe, 2009).

2.2 Data used

The spatial characteristics of the study area are described with three base maps: elevation, land use and soil. The elevation data were obtained from a geometrically corrected Shuttle Radar Topography Mission (SRTM) digital elevation model (LP DACC, 2001). Land use data were derived from geometrically corrected Landsat Enhanced Thematic Mapper (ETM+) images (LP DACC, 2001). Soil data were extracted from the Harmonized World Soil Database (version 1.2). The daily precipitation and temperature were determined from a dataset published by the Meteorological Department of Sri Lanka, 2011. Point weather data were converted to a grid resolution of 1 km x 1 km using the Modified Inverse Distance Weighted (MIDW) method.

2.3 Distributed hydrological model

This study employed the distributed hydrological runoff model developed by Kashiwa *et al*. (2010) under the structure proposed by Kazama (2004) to simulate the natural runoff. As a result, only natural hydrological processes are included (irrigation and reservoir operation are not considered). A detailed description of the model structure, governing equations, model calibration and validation for the study area can be found in the literature (Chaminda and Kazama, 2013; Kashiwa *et al*., 2010). In this study, daily river runoff was simulated for the period 1976 – 2005 at 1km spatial resolution.

2.4 Development of hydrological disaster index

The present study developed the new Hydrological Disaster Index (HDI) as a function of drought and flood probability , which are identified using the low and high river flow indices from a river flow during 1976 – 2005 period.

Identification of drought probability

In this study, the 7Q2 (7 day, 2-year) low-flow statistics were used to identify the annual and seasonal drought probabilities in a river basin. The 7Q2 is calculated as a moving average of seven consecutive days for each year in a given record. These seven-day low flow values are ranked in ascending order. An order number (m) is calculated based upon the number of years of record (n), with a recurrence interval (R) of two years, as m = (n+1)/R, where R = two years. A value of flow corresponding to the mth order is taken as the seven-day, two-year low flow for those simulated river flow data.

The annual and seasonal 7-day low flows at some stream flow-gauging stations used in this study were equal to zero. A conditional probability adjustment for zero flow values (U.S. Interagency Advisory Committee on Water Data, 1982, appendix 5) was used for sites with one or more annual and seasonal 7-day low-flow values of zero. The annual and seasonal low-flow values (7Q2) for all selected river basins were computed using simulated daily runoff for the period 1976 – 2005. The determined low-flow values (7Q2) at each river basin were divided by basin area to compute the area average low-flow value (7Q2) for the basin in order to identify the common threshold for drought probability levels for the study area.

Probabilities of drought at river basins were determined based on derived low river flow values at selected river basin. The determined probability of drought at river basin was relative to the other river basins. The river basin, which has lowest value of area average low flow value (7Q2), is determined as a highest probability for drought out of selected river basins for the study. The probability of drought at the river basins were determined to 5 probability levels (Not high, slightly high, moderately high, very high, and extremely high) based on identified threshold limit of low flow values (7Q2) (**Table 1)**.

Identification of flood probability

Flow duration curves (FDCs) are widely used to analyze the flow pattern changes. FDCs illustrate the relationship between the frequency and magnitude of stream flows. FDCs can produce a number of indices to characterize extreme flows. Here, FDCs were used to assess the extreme annual and seasonal high-flow conditions in the past. Q5 (high flow that exceeded 5% of the time) and Q10 (high flow that exceeded 10% of the time) can be derived from the FDCs and are widely used as high-flow indices (Pyrce, 2004). In this study, we used the Q5 as a high-flow index. The annual and seasonal Q5 values for all selected river basins were manually extracted from the FDCs that were developed at all selected river basins using the annual and seasonal runoff time series for the period

Table 1 Flood and drought probability levels and its assigned weights based on Q5 and 7Q2

Probability levels	High flow (Q5) area average (mm/day)	Low flow (7Q2) area average (mm/day)	Assigned weight
NH – Not high	<6.0	0.25<	0.000
SH- Slightly high	6 - 9	0.20 – 0.25	0.125
MH- Moderatly high	9 - 12	0.15 – 0.20	0.250

VH –Very high	12 - 15	0.10 – 0.15	0.375
EH- Extremly high	15 <	< 0.10	0.500

Table 2 Matrix to compute the hydrological disaster index

	Flood probability	NH	SH	MH	VH	EH
Drought probability		0.000	0.125	0.250	0.375	0.500
NH	0.000	0.000	0.125	0.250	0.375	0.500
SH	0.125	0.125	0.250	0.375	0.500	0.625
MH	0.250	0.250	0.375	0.500	0.625	0.750
VH	0.375	0.375	0.500	0.625	0.750	0.875
EH	0.500	0.500	0.625	0.750	0.875	1.000

1976 – 2005. The determined high-flow values (Q5) values for each river basin was divided by basin area to compute the area average high-flow values for basins in order to identify the threshold level for flood probability. Probabilities of flood at river basins were determined based on derived high river flow values at selected river basin. The determined probability of flood at river basin was relative to the other river basins. The river basin, which has highest value of area average high flow value (Q5), is determined as a highest probability for flood out of selected river basins for the study. The probability of flood at the river basins were determined to 5 probability levels (Not high, slightly high, moderately high, very high, and extremely high) based on identified threshold limit of high flow values (**Table 1).**

Computation of HDI

The probability of flood and drought is derived using the area average low- and high-flow indices categorized into five bands (NH- Not High, SH – Slightly High, MH – Moderately High, VH – Very High, EH – Extremely High) since, it is important to identify and map the hydrological disaster in a different severity level when planning disaster relief, prevention and preparedness programs. However, HDI for the river basin can be calculate from an individual value of probabilities of flood and drought based on the high flow and low flow values too. A weight (0 – 0.5) is then assigned to each band according to probability level for flood and drought (Table 1). A matrix is developed using the weighted values for a given flood and drought probability level, as shown in (Table 2). The range of the computed hydrological disaster index runs from 0 and 1. A values of 0 means no probability of hydrological disaster, and a value of 1 means that the hydrological disaster probability is extremely high.

3 Results and Discussion

The computed annual HDI values show a higher level of hydrological disasters in the wet zone's river basins than in the dry zone's river basins (Figure 2). According to the available record of hydrological extreme events from the Disaster Management Center (DMC), Sri Lanka it is confirmed that most of the wet zone river experience both frequent severe floods and medium to low drought events. However, the spatial variation of the annual hydrological disaster probability in the country is much lower because most river basins undergo a flood or drought during different monsoon season in a given year. Hence, we computed the seasonal HDI values for four different precipitation seasons to compare the seasonal and spatial variation of the HDI. As shown in Figure 2c, 2d, the Kalu river basin (located in SW) shows higher hydrological disaster index values during the southwest and 2nd intermonsoon seasons compared to the other monsoon seasons due to major flood events. The available record from the Disaster Management Center (DMC), Sri Lanka also confirms that major flood events occurred during the southwest monsoon season (May to September) and the 2nd intermonsoon season (October to November) in the Kalu river basin. No major flood events were recorded during the northeast and 1st intermonsoon seasons. Further, the available record from the Disaster Management Center (DMC), Sri Lanka confirms that river basins in the eastern, northern and northwestern regions experience both flood and drought during the northeast monsoon. Hence, it is clear that the computed hydrological disaster index show comparatively higher values during the northeast monsoon in these river basins because of the integrated impact of drought and flood events. However, during the other monsoon seasons, it does not record both extreme drought and flood events in the same river basins and seasons. Both medium to low flood and drought events occur during other monsoon seasons as well. The observed record from the DMC, Sri Lanka confirms that higher flood and zero drought events occurred during the 2nd intermonsoon across the country. The computed hydrological disaster index shows similar disaster probability levels for all selected river basins during the 2nd intermonsoon. According

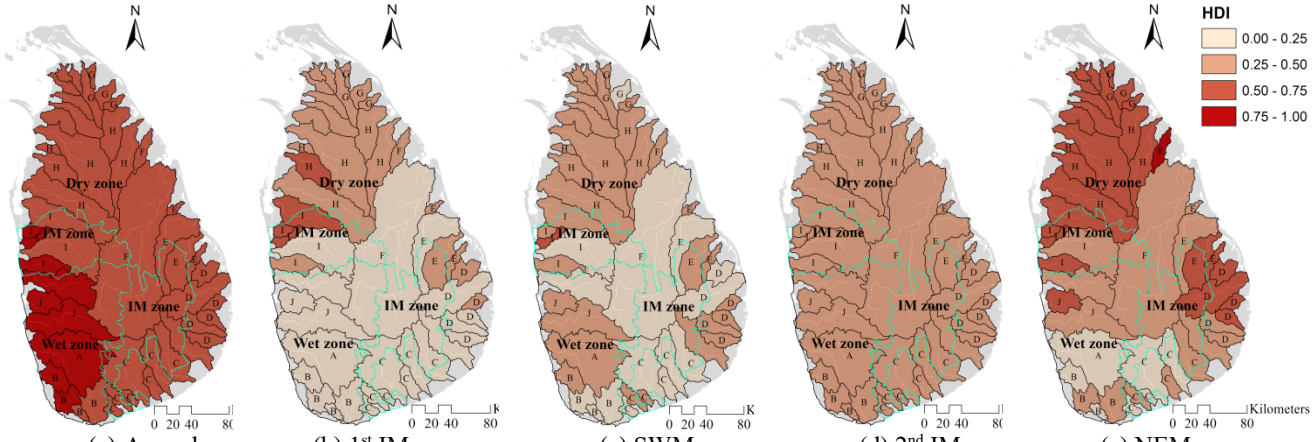

(a) Annual (b) 1st IM (c) SWM (d) 2nd IM (e) NEM

Figure 2 The annual and seasonal (1st IM – first intermonsoon (March – April), SWM – southwest monsoon (May – September), 2nd IM – second intermonsoon (October – November), NEM – northeast monsoon (December – February)) distribution of hydrological disaster index for the past period (1976 – 2005)

to the above qualitative verification of the proposed hydrological disaster index, it is reliable to apply the HDI to assess the spatial and seasonal variation of integrated hydrological disaster probability levels in the country.

The newly developed Hydrological Disaster Index (HDI) is capable to identify the areas which are under the integrated hydrological disaster probability. Hence, new HDI can be successfully used to prioritize the areas and people which are need short time and long time assistance due to the frequent hydrological disasters (flood and drought). Furthermore, it is essential to identify the areas which is under the higher probability in integrated hydrological disasters for many applications such as land use planning, disaster relief planning, climate change adaptation planning, etc…The proposed new HDI needs only a stream flow records for the historical period and it is more convenient to apply for any region under different temporal resolutions. However, HDI is limited to river sub basins scale and cannot apply on grid scale since it is totally depend on stream flow records.

4 Conclusions

The seasonal flood and drought probability of the river basins are well represented by the computed high- and low-flow indices. Most of the dry zone river basins and some of the wet zone river basins have a high probable probability of seasonal drought. The wet zone basins have a high probability of extreme flood events during the southwest and 2nd intermonsoon seasons. The dry zone basins in the eastern and northeastern regions have a probability of extreme drought and flood during the northeast monsoon season. However, the individual drought and flood indices are not capable of identifying the area that has a high probability of integrated hydrological disasters (both flood and drought). The newly developed Hydrological Disaster Index (HDI) is reliable for the assessment of the spatial distribution of the annual and seasonal integrated probability of flood and drought across the country. The annual-scale HDI identified the wet zone river basins under the most severe hydrological disasters because both extreme flood and medium to low droughts existed. The seasonal-scale HDI successfully identified the spatial and seasonal variation of the integrated hydrological disaster probability across the country.

South Asia has been identified as the most hydrologically disaster prone region in the world for the changing climate in the future (UNEP, United Nations Environment Program 2003). Thus, the newly developed HDI can be successfully used to identify the future spatial distribution of annual and seasonal integrated hydrological disaster probabilities using the projected extreme river flow data. Hence, it will be helpful for identifying better climate change adaptation measures for mitigating the impacts of integrated extreme hydrological events at local and seasonal scales.

ACKNOWLEDGMENTS

This study was supported by the Ministry of Education, Science, Sports and Culture, Japan through a Grant-in-Aid for Scientific Research (A), 2010-2013 (30111248, Tatsuo Omura).

References

1) Amarasinghe UA: Spatial Variation of Water Supply and Demand in Sri Lanka. Proceeding of National Conference on Water Food Security and Climate Change in Sri Lanka June 9-11 2009, Colombo, Sri Lanka; 37-47, 2009
2) Bocchiola D, De Michele C, Rosso R: Review of recent advances in index flood estimation. Hydrology and Earth System Sciences **7 (3)**: 283–296, 2003.
3) Botter GS, Basso I, Rodriguez-Iturbe, Rinaldo A: Resilience of river flow regimes. Proceeding of the National Academy of Sciences of the United States of America**110**. 925–12,930. 2013.
4) Chaminda SP, Kazama S: Spatial and Temporal Variability of Surface Water Flow in Sri Lanka. Proceeding of 35th IAHR World Congress September 8 – 13, 2013 Chengdu, China; Vol-07-01, 2013.
5) Dankers RL, Feyen L, Christensen OB: On the benefit of high-resolution climate simulations in impact studies of hydrological extremes. Hydrology and *Earth System* Sciences Discuss **6**: 2573–2597, 2009.
6) Domroes M, Ranatunga E: The orthogonal structure of monsoon rainfall variation over Sri Lanka. Theor Appl Climatol **46**: 109-114, 1992.
7) Frederick KD: Adapting to climate impacts in the supply and demand for water. Climatic Change **37**: 141–156, 1997.
8) Hirabayashi Y, Kanae S, Emori S, Oki T, Kimoto M: Global projections of changing risks of floods and droughts in a changing climate. Hydrological Science Journal **53**: 754–772, 2008.
9) Kashiwa S, Kazama S: Flood analysis Modeling of snow melting and Estimation. Proceedings of the rivers Technology Jun 29-30, 2010 Tokyo, Japan; 289-294, 2010.
10) Kazama S: Uncertainty of morphological data for rainfall-runoff simulation. Proceedings of the International Conference on sustainable Water Resources Management in the Changing Environment of the Monsoon Region November 17-19, 2004 Colombo, Sri Lanka; 400-406, 2004
11) Mika J, Horvath Sz, Makra L, Dunkel Z: The Palmer Drought `Severity Index (PDSI) as an indicator of soil moisture. Physics and Chemistry of the Earth **30**: 223–230, 2005.
12) Nijssen B, O'Donnell G, Hamlet A, and Lettenmaier D: 2001. Hydrologic Sensitivity of Global Rivers to Climate Change. Climatic Change **50**: 143-175, 2005.
13) Pyrce R: Hydrological Low Flow Indices and Their Uses, Watershed Science Centre, Trent University, Canada, 2004.
14) Quiring SM, Papakyriakou TN: An evaluation of agricultural drought indices for the Canadian prairies. Agricultural and Forest Meteorology **118**: 49–62, 2003.
15) Robson A, Reed D: Flood Estimation Handbook. 3: Statistical procedures for flood frequency estimation. Centre for Ecology & Hydrology, Wallingford, UK, 1999.
16) UNEP (United Nations Environment Programme) GEO year book 2003. UNEP, Nairobi, (2003)

Attempt of environmental assessment in freshwater using environmental DNA

○Noriko Uchida[1*], So Kazama[1], Kengo Kubota[1]
[1]Graduate School of Engineering, Tohoku University, Sendai 980-8579, Japan
*Email: noriko.uchida.s8@dc.tohoku.ac.jp

Abstract
Environmental DNA (eDNA) analysis has been known as novel molecular technique used to detect the presence of species, and it could have considerable advantage to estimate the presence of a species. We hypothesize amount of "eDNA-load" should be varied depending on land uses, and tried estimate "the eDNA load units" for different land uses (i.e. forest/ agriculture/ urban river in this report). The target species are freshwater invertebrates in our study area: Natori river basin, Miyagi Prefecture, Japan. As a result, the concentration of invertebrates' DNA are higher at higher water temperature when the water comes from small catchment area. Our observation showed eDNA load units are higher in the order of forest, agriculture and urban river. Our results implied that eDNA can be assumed as area source loads like nitrogen or phosphorus and can be calculated using further numerical models.

Keywords: area source load, aquatic invertebrate, environmental DNA, land use, load unit

1. Introduction

Freshwater is one of vulnerable environments which is easily affected and changed by artificial or climate change. Especially in river ecosystem, where is often used for humans activity, optimal and sustainable biomonitoring survey is required for conservation that ecosystem[1)]. Additionally, in streams, understanding assemblage component (population size or faunal composition) of stream invertebrate is fruitful to assess biological diversity[2)]. Monitoring of aquatic wild life has been practically carried out by visual observation, and fishing in several manners.

Environmental DNA (eDNA) is a novel monitoring method in the field. eDNA is a small fragment of DNA originated from animal bodies and metabolites such as skin cells, feces, saliva, urine of animals occupying water body and it extracts to water like lake, pond, ocean, river[3)]. By detecting species specific genome sequences in a given water samples using molecular biological methods (e.g. PCR, Next Generation Sequencing) presence / absence of a target species can be determined with high accuracy. While conventional survey (e.g. trapping, counting and morphological identification) needs huge man power and cost, and also time consuming, eDNA methods require only a little amount of environmental sample. Remarkably, it is already verified that using eDNA method is more efficient to know species composition or existence than conventional monitoring methods by Minamoto *et al.* [4)]

Using eDNA method is expected to make optimization of biological monitoring, to improve objectification for monitoring results, and also to help financially cost to be lower. Furthermore, there are some reports which find positive correlation between biomass and amount of

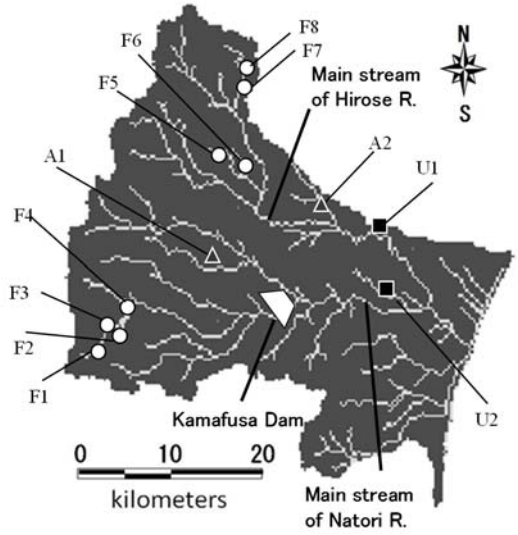

Figure 1: Sampling sites, Natori River Basin
○:Forest river (F1-8), ▲:Agriculture-river (A1-2),
■:Urban-river(U1-2)

observed eDNA collected from closed aquatic habitat such as aquarium, lake and lagoon[5-6)]. On the other hand, there are a few attempts to estimate the concentration of eDNA in river channel because the degradation process is unknown and DNA production rate is difficult to know under natural environment.

In this study, we aim to examine the eDNA concentration using qPCR (quantitative Polymerase Chain Reaction, one of real-time PCR techniques) and estimate their load units to determine the amount of eDNA source from different land

use in Japan. To know which factor is effective to explain eDNA variation, we tested statistical analysis using observed data.

2. Materials and Methods

(1) Field survey

We sampled eDNA at forest-, agricultural-, urban-river to find variations of DNA load units depending on land use types. 8 sampling site for forest-river and 2 sites for agricultural-river, and 2 sites for urban-river were set (Figure 1), Natori River Basin, Miyagi Prefecture in northeast Japan. The samplings were conducted during March to May 2016. In that duration, no agricultural activity was conducted in this area thus we can eliminate the influence of human activity which may cause huge water quality effect to agricultural river. We collected 4L of water from water surface to bleached plastic bottles by gloved hands. For experimental procedures we mainly followed the earlier reports[7]. At the same time to sample water for eDNA analysis, we also measured water temperature using TOA-DKK HM-20P.

(2) DNA analysis

The sampled water was transported to the laboratory and kept in the cold condition on the same day before subsequent filtering process. The water samples were then filtered until clogged by the vacuum filtration with 47mm diameter glass-fiber filters (normal pore size, 0.7μm; Whatman) and GF/D filter (Whatman, diameter 47mm, normal pore size 2.7μm) as a pre-filter. These samples were wrapped in commercial aluminum foil and stored in -20ºC until DNA extraction. DNA was extracted from filters by Phenol-Chloroform-Isoamyl alcohol extraction method and ethanol precipitation with 100μl of final volume. After then, the elution was purified using PCR Inhibitors Removal Kit (Zymo Research) following manufactured protocols. Finally, concentration of the extracted DNA was measured using Qubit 3.0 fluorometer (Invitrogen) following recommended protocols for the dsDNA HS Assay.

Mitochondrial DNA (mtDNA) was employed as the target genetic marker because copy number of mtDNA in stream water could be larger than that of nuclear DNA per cell so that detection rate is expected to be higher. We used a universal primer targeting mtDNA cytochrome *c* oxidase subunit 1 (CO1), which is divergent among invertebrate species (Folmer *et al*., 1994). We amplified the target DNA fragments of the samples using the PCR primers designed to amplify invertebrate-specific loci from the CO1 region. A 658 bp fragment from CO1 region was amplified with the following primer pair; LCO1490 (5'-GGT CAA CAA ATC ATA AAG ATA TTG G-3') and HCO2198 (5'-TAA ACT TCA GGG TGA CCA AAA AAT CA-3')[8]. We initially validated the primers on tissue samples for a larva of the caddis fly species (*Stenopsyche marmorata*) which was also sampled in the study catchment.

The qPCR was performed using SYBR®Premix Ex Taq (TaKaRa) and LightCycler®2.0 (Roche). The condition of qPCR consists of an initial incubation at 95ºC for 20 seconds followed by 40 cycles of 95ºC for 5 seconds, 53ºC for 30 seconds, 72ºC for 1 minute. Fragment size of amplicons was verified with agarose gels electrophoresis. Further, we set a template DNA which was extracted from tissue of *S. marmotara* and amplified it using the above mentioned primer pair. Fragment size of amplicons was also verified with agarose gels electrophoresis and qPCR products were purified using a MicroSpin S-400 Columns (GE Life Science). Then we created a dilution series from the PCR products of as standard DNA thorough $1.0x10^1$ to $1.0x10^7$ (copies/μl). DNA concentration of the dilution series was measured using PicoGreen (Thermo Fisher Scientific Inc).

In subsequent statistical analysis, we defined two words "total DNA" and "Invertebrates' eDNA". The total DNA is meant the weight concentration of DNA (ng/L) measured by Qubit fluorescence meter. This included not only the target taxa, but also non target taxa such as mammals, flora, and bacteria. The invertebrates' eDNA (Inv. eDNA in legends or tables) is meant the number of copied DNA fragments concentration (copies/L) measured using qPCR.

3. Results

(1) Relationship between environmental condition and

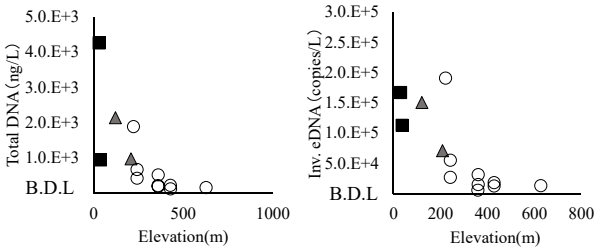

Figure 2: Elevation and eDNA concentrations
Blank circles show forest-river, gray filled triangles show agricultural-river, black filled square show urban-river.

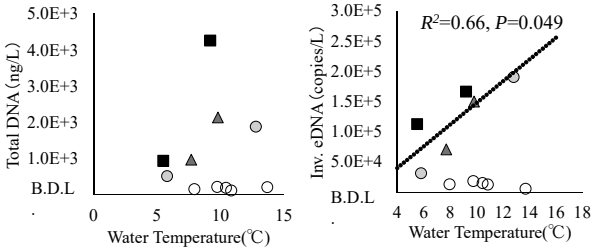

Figure 3: Water Temperature and eDNA concentrations
Correlation was found with invertebrate eDNA (right graph).
Legends are same as Figure2.

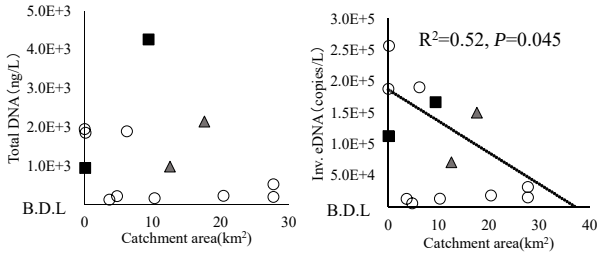

Figure 4: Catchment area and DNA concentrations
Legends are same with Figure 2.

eDNA concentration

Figure2-4 describes the scatter diagrams to find relationship between extracted DNA concentrations of all river samples and environmental factors. There is no correlation between total DNA and 3 factors, namely elevation, water temperature and catchment area. Elevation did not show any correlation with eDNA concentration. It indicate outdoor temperature did not important factor to explain eDNA variation in this study. On the other hands, between invertebrates' eDNA and water temperature and between catchment area has positive/ negative correlation. Furthermore, the general linear model was calculated using static analysis software R 3.4.0 (R core team). The linear model was given as:

$$PCR = 1.56 * 10^4 x_T - 2.78 * 10^3 x_A + 1.86 * 10^4$$

(R^2 =0.81, P=0.038)

where: qPCR: invertebrates'eDNA$(copies/L)$,
x_T : $water\ \ temperature$(℃), x_A
: catchment area (km^2)

This formula explain that invertebrates' eDNA increase at higher water temperature. Higher water temperature generally makes organisms activate their metabolism rates, and consequently more DNAs were produced and exposed to river water. The estimated formula also indicated that eDNA decrease at wider catchment area while the site which has large catchment area seems to put a lot of DNA into that point. One of assumption for it, all of sampling site has small catchment area (< 28km^2). For such as smaller catchment river, the larger discharge gathered from catchment may make dilution effects for DNA concentration rather than collecting and concentrating DNA from catchment area.

The above formula has better R-squared value than one-to-one relationship between invertebrates' eDNA and water temperature (R^2=0.66), and catchment area (R^2=0.52). Water temperature can be higher at smaller catchment area such as urban river and these two environmental factors may be in trade-off relationship. Hence, the formula which has both factors made better expression.

(2) Estimated eDNA load units for 3 land uses

We estimated eDNA load units by multiplication of observed total/ invertebrates' eDNA and daily discharge (m^3/day) and division by catchment area. Daily discharge of each sites were average of 30days in April in 2014, 2015 and 2016. The discharge were calculated by distributed runoff model which is optimized in Natori River basin[10]. Table 1 showed average of eDNA load units of each land uses. As for reference data, nutrient salt load units which is set for water quality conservation planning in 2000 of Kamafusa Dam, Naroti River basin was also shown. According to load units in Kamafusa Dam, total phosphorus load (TP) from agricultural river is larger than 4.6 times of forest and 4.2 times of urban. Total nitrogen load (TN) is also larger from agricultural river than 1.2 times of forest and 1.4 times of urban. Seeing COD (chemical oxygen demand), it becomes larger in the order of forest, agricultural and urban river. Total DNA load unit from agricultural river was 8 times of forest and urban river was 6.6 times of agricultural. Invertebrates' eDNA load units from agricultural was 6 times of forest and urban river was 11 times of agricultural. Therefore the increasing order was same as COD, but contribution from urban was much larger in the cases of DNA load unit. This results contrary to our expectations that DNA load unit should be larger from forest-river because there are rich population and biomass of invertebrates. The population of invertebrates may increase under urbanized condition because there are high supplies of organic matter from atmospheric precipitation or domestic wasted water and they are important feeding source for organisms.

4. Conclusion

This study examined field survey to measure invertebrates' DNA concentration from river water eDNA samples and river environment conditions in 3 different land used river. The results show that:

1) Water temperature and catchment area can be effective factor to explain variations of eDNA concentration while samples.

2) Estimated eDNA runoff load units for each land uses were significantly different from each other. The unit values were higher in the order of forest, agriculture, and urban river. Thus, when we estimate what amount of DNA flow out to river channel like nutrient salt, these

Table-2: eDNA unit loads of different DNA

Land use	T-DNA	Inv. DNA	TN	TP	COD
Forest	0.0012	1.1.E+08	13.8	0.79	127
Agriculture	0.0097	6.8.E+08	62.8	1.01	147
Urban	0.0647	7.5.E+09	14.8	0.71	158

Invertebrates' DNA : copies/ha/day, others : g/ha/day

differences should be considered as the initial input data.

Using eDNA analysis, we can assess the river environment to discuss river design in the future and to consider the relationship between flood and environment. Furthermore, it is indicated that eDNA also can extend the possibility of continual survey to evaluate wasted water and land use change.

Acknowledgements

This research was partly supported by the Ministry of Education, Science, Sports and Culture through a Grant-in-Aid for Scientific Research (grant nos. 25241024, Yasuhiro Takemon, 26630247, Kozo Watanabe, 26820196, Kei Nukazawa) and Japan society for the Promotion of Science (JSPS) Research Fellowship (grant no. 256493).We express deep appreciating for all of supports.

References

1) Hurlbert, A. H., Jetz W.: Species richness, hotspots, and the scale dependence of range maps in ecology and conservation, PNAS, 104 (33), pp.13384-13389, 2007
2) Heino, J.: Biodiversity of aquatic insects: spatial gradients and environmental correlates of assemblage-level measures at large scales, Freshwater Reviews, 2, pp.1-29, 2008
3) Rees, H. C., Maddison, B. C., Middleditch, D. J., Patmore, J. R. M., Gough K. C.: The detection of aquatic animal species using environmental DNA-a review of eDNA as a survey tool in ecology, Journal of Applied Ecology, vol. 51, pp.1450-1459, 2014
4) Minamoto, T., Yamanaka, H., Takahara, T., Honjo, M. N., Kawabata, Z.: Surveillance of fish species composition using environmental DNA, Limnology, 13 (2), pp.193-197, 2012
5) Pilliod, D. S., Goldberg, C. S., Arkle, R. S. and Waits, L. P.: Estimating occupancy and abundance of stream amphibians using environmental DNA from filtered water samples, Canada Journal of Fisheries and Aquatic Sci., Vol. 70, pp.1123-1130, 2013
6) Takahara, T., Minaoto, T., Yamanaka, H., Doi, H., Kawabata, Z.: Estimation of fish biomass using environmental DNA, PLoS ONE, 7 (4), e35868, 2012
7) Fukumoto, S., Uchii, A. and Minamoto, T.: A basin-scale application of environmental DNA assessment for rare endemic species and closely related exotic species in rivers: a case study of giant salamanders in Japan, *Journal of Applied Ecology*, Vol.52, pp.358-365, 2015.
8) Folmer, O., Black, M., Hoeh, W., Lutz, R., Vrijenhoek, R.: DNA primers for amplification of mitochondrial cytochrome c oxidase subunit 1 from diverse metazoan invertebrates, Molecular Marine Biology and Biotechnology, Vol.3, pp.294-299, 1994
9) Ficetola, G. F., Miaud, C., Pompanon, F., Taberlet, P.: Species detection using environmental DNA from water samples, Biology Letters, Vol.4, pp.423-425, 2008
10) Tsuchida, K., Kazama, S., Sawamoto, M.: Relation between land use and allowable population for conservation of river environment, Journal of Hydraulic by Japan Society of Civil Engineers, Vol.48, pp. 475-480, 2004

A sensitivity analysis of Storm Water Managament Model in a residential area

○Chang Qing[1*], So Kazama[1], Yoshiya Touge [1]
[1]Graduate School of Engineering, Tohoku University, Sendai 980-8579, Japan

*E-mail: chang.qing.q3@tohoku.ac.jp

Abstract
This study discusses the sensitivity of main parameters of urban storm drainage system based on Storm Water Management Model. A residential dominated catchment in Sendai city of Japan was chosen as the study area. The parameter sensitivities were considered with different rainfall condition, model spatial scale and infiltration equations.

The parameters about imperviousness, roughness, initial loss and infiltration were considered. Three patterns of rainfall with same total depth were designed: single peak, multi peak and flat continuous rainfall. And the models were built up with 3 different spatial scale to evaluate the scale effect on sensitivity. The Morris method was used for sensitivity analysis. The lower and upper limits of parameter range for sensitivity analysis were set to 50% and 150% of the initial parameter value.

The result showed that that Imperviousness was the most sensitive parameter, afterwards were the surface Manning roughness and depression storage depth. The result of Morris method were: %Imperv 0.73~0.91, N-imperv 0.19~0.26, N-perv 0.06~0.14, Dstore perv 0.18~0.24, Dstore imperv 0.08~0.13. Sensitivities of Green-Ampt and Horton infiltration parameters as well as the initial loss parameters were influenced by rainfall characteristics. These parameters were more sensitive when the rainfall were less intensive. The sensitivity of catchment roughness and conduit roughness are scale dependent. Specifically, with finer spatial scale, the conduit roughness tended to be more sensitive than coarser scale.

Keywords: parameter, sensitivity analysis, SWMM, model scale

1. Introduction
Urbanization is associated with increasing imperviousness of land cover and the concomitant alterations of hydrological cycles. Both the increasing quantity of stormwater runoff and the pollutant washoff from urban surfaces have degrading effects on receiving water bodies, including changes in the eco-hydrological diversity, deteriorating stream water quality, and stress in stream hydrology due to higher peak discharges and shorter travel times. Reduced infiltration due to imperviousness affects both surface and ground waters.

Thus water management of urban system had became an important issue which increased the need of enhancing the modeling for the hydrological and the water quality processes in both the overland flow and the flow in sewer systems. Nowadays many researchers and practitioners studying and managing stormwater sewer systems in urban catchments use semi-distributed models like SWMM, CANOE or MOUSE (Zoppou, 2001; Elliott and Trowsdale, 2007). These models are based on a description of the catchment as a set of subcatchments linked by a drainage network. The runoff generation processes are simulated for each subcatchment, and the network is used to simulate the routing of water to the catchment outlet. Due to the naturally complexity, the amount of parameters of these model are so large that the calibration and validation of such models require a huge amount of data and computation.

In order to discern which parameters have the most influence over model performance and to identify what are the most appropriate parameter values, we need to find a way to screen out sensitive parameters and quantitatively evaluate the influence of each parameter on model performance. Sensitivity analysis (SA) has been used by many people for this purpose (Liu et al., 2004; Borgonovo et al., 2012). SA can identify parameters of which a reduction in uncertainty specification will have the most significant impact on improving model performance measures. Thus, if some noninfluential parameters can be identified and fixed reasonably at given values over their ranges, the computational cost may decrease without reducing model performance.

SA approaches based on design of experiment (DOE) have gained popularity recently because they offer sensitivity measures while maintaining computational efficiency. A typical DOE-based SA method involves two steps: first, generating a sample set of parameters within the feasible parameter spaces using a chosen design; and then, obtaining a quantitative attribution of model output variation due to

the variation of different parameters. There are many sampling techniques, such as MC, Latin Hypercube (LH), Orthogonal Array (OA) and Orthogonal Array based Latin Hypercube (OALH), which are commonly used for DOE-based SA. Some DOE based SA methods, such as Morris One-At-a-Time (MOAT), Fourier Amplitude Sensitivity Test (FAST), and extended Sobol method, require special sampling techniques. More recently, along with the development of response surface methods (RSM), SA based on RSM makes it cheaper for estimating parameter effects.

The EPA Storm Water Manage Model (SWMM) was used as the hydrological model for this study. This model is suitable for urban hydrology analysis and had been successfully applied at various scales. The modified Morris method was used for sensitivity analysis to identify model structure and find key parameters among 8 main parameters.

2. Study site and data

2.1 Study site

We chose the Kunimigaoka Area in Sendai City, Japan for the case study (Fig.1(a)). KA is located in the north-western part of the uptown of Sendai City, which covers approximately 50 hector with a medium gradient slope topography. KA is featured with a temperate monsoon climate and the annual average rainfall and temperature are 1254 mm and 12.4C, respectively. KA is an old uptown where urbanization degree is rather complete and the land use shows little change after 2000. The urban land use accounts for over 90% of the total in this region. The storm water was firstly drained to a regulating pond and then to a downstream river. The drainage system of KA can be divided into two parts, one being the sewer network in the Northern part of KA which accounted for most of the drainage areas; the other is a located in the southern part beside the regulating pond (Fig.1(b)).

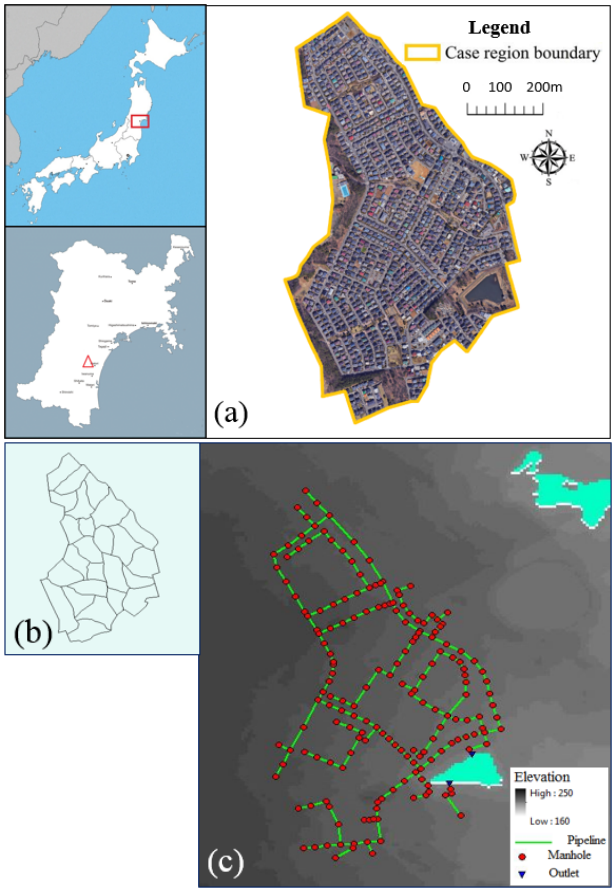

Fig.1. (a) Location of the Kunimigaoka Area; (b) Sub watersheds of the study region delineated by GIS; (c) Top view of the digital terrain model overlaied with swere network.

2.2 Data availability and processing

Topographic data

The DEM of KA was available in the form of a high-resolution (5x5m) elevation data set, which was provided and quality controlled by the Land and Resources Department of Japan. In order to represent the blockage effect of buildings on surface flows, the building profiles were distinguished using the planar graph and Google satellite image.

Sewer network data

The underground pipeline data were obtained from Sewer Administration Office of Sendai City which contained geographic and geometric information of more than 400 pipelines and manholes. Most of the pipes are circular with diameters ranging from 0.3 to 2.4 m, while some pipes are rectangular whose widths and heights vary from 0.4 to 0.8 m. The pipe slops show a wide range, varying from 0.5 to 38%.

References

1) Borgonovo, E., Castaings, W., Tarantola, S. : Model emulation and momentindependent sensitivity analysis: an application to environmental modelling. Environ. Model. Softw. 34, 105-115, 2012
2) Elliott, A.H., Trowsdale, S.A : A review of models for low impact urban storm water drainage. Environ. Modell. Software 22, 394–405, 2007.
3) Liu, Y., Gupta, H.V., Sorooshian, S., Bastidas, L.A., Shuttleworth, W.J. : Exploring parameter sensitivities of the land surface using a locally coupled landatmosphere model. J. Geophys. Res. 109, D21101, 2004.
4) Zoppou, C : Review of urban storm water models. Environ. Modell. Software 16 (3), 195–231, 2001.

Synthesis of Layered Double Hydroxides with Fermentation Liquid of Organic Waste To Extract Short-Chain Fatty Acids as a Biodenitrification Carbon Source

○Jianyong LIU[1], Guangren QIAN[1], Yu-You LI[2*]
[1]School of Environmental and Chemical Engineering, Shanghai University, 333 Nanchen Road, Shanghai 200444, People's Republic of China
[2]Department of Civil Engineering, Tohoku University, 6-6-06 Aoba Aramaki Aoba-ku Sendai city, Miyagi Prefecture, Japan.
*E-mail: gyokuyu.ri.a5@tohoku.ac.jp

Abstract

Short-chain fatty acids (SCFAs) were extracted from artificial and actual anaerobic fermentation liquid of organic waste via the synthesis of layered double hydroxides (LDHs), which was then used as external carbon source in bio denitrification process. Results of X-ray diffraction and Fourier transform infrared analysis indicate that SCFAs were successfully intercalated into LDHs in both artificial system and actual anaerobic fermentation liquid of food waste, with good slow release performance. When using SCFAs-LDH and SCFAs-Na as carbon source with COD/N ratio of 4:1, the nitrate removal efficiency and the utilization efficiency of carbon source were improved from 42.3% and 30.3% to 81.3% and 58.1%, respectively. A dynamic "release-utilization" balance of carbon source was always kept during denitrification process when using SCFAs-LDH, so that higher removal efficiency of nitrate and utilization efficiency of carbon source were obtained simultaneously. This study could help to recover SCFAs from organic wastes efficiently as a denitrification carbon source with slow release performance.

Keywords: Layered double hydroxides, Carbon source, Slow release, Organic waste, Denitrification

1. Introduction

Biological removal of nitrogen is identified as an efficient and economical way, which is used widely in municipal wastewater treatment plants all over the world with nonpolluting nitrogen gas produced. Heterotrophic denitrifying bacteria play a key role in the denitrification process with nitrate as an electron acceptor, but need organic substances (carbon source) for microorganism growth, as well as for application as an electron donor. Therefore, sufficient organic carbon is crucial for biological denitrification.

The objectives of this study were (1) to examine the feasibility of SCFAs-LDH synthesis within artificial anaerobic fermentation liquid and actual anaerobic fermentation liquid of food waste; (2) to evaluate the release performance of SCFAs-LDH; and (3) to investigate the nitrogen removal performance and carbon source utilization efficiency in actual bio denitrification system with SCFAs-LDH tablets as an external carbon source. This study could help to find a better way to recover SCFAs from organic wastes efficiently as an external carbon source of bio denitrification.

2. Results and Discussion

Characterization of SCFAs-LDH Synthesized with Artificial Anaerobic Fermentation Liquid. The structures of synthesized LDHs were examined by XRD. The characteristic diffractions of LDHs materials with 00l peaks were observed, without impurity hydroxide phases. But the ZnO crystal phase discovered all that of ZnAl-LDH. The basal spacing value (d_{003}) of NO_3-ZnAl-LDH was -0.89nm. Compared with NO_3ZnAl-LDH, the (003) characteristic reflection of SCFAs-LDH, C_3H_7COO-LDH, and C_2H_5COOLDH shifted to lower 2θ values, with corresponding d-spacings of 1.47, 1.49, and 1.38 nm, respectively. This suggests that SCFAs, $C_3H_7COO^-$, and $C_2H_5COO^-$ were all intercalated into the interlayer galleries of ZnAl-LDH. While the basal spacing value ($d_{(003)}$) of CH_3COO-LDH was 0.76 nm, which was consistent with the literature, indicating that CH_3COO^- was also successfully intercalated into ZnAl-LDH.

The FTIR spectroscopy of SCFAs-LDH, C_3H_7COO-LDH, C_2H_5COO-LDH, and CH_3COO-LDH can be seen that the broad absorption bands in region of 3450cm^{-1}, which was associated with the O−H stretching vibration arising from the metal-hydroxyl groups in gibbsite layer, and those of the interlayer water with H-bonding. The C−H stretching vibration of ZnAl-LDH appeared at 2973cm^{-1}. The asymmetric and symmetric of the COO- stretching vibrations appeared at 1560cm^{-1} and 1385cm^{-1}, which were consistent with literature. The broad bands observed at about 549cm^{-1} and 429cm^{-1} lattice vibration region indicate the variation in the divalent/trivalent metal composition of the hydroxide layers. The FTIR spectroscopy also confirmed the intercalation of SCFAs anions within inter lamellar region.

Characterization of SCFAs-LDH Synthesized with Actual Anaerobic Fermentation Liquid of Food Waste. The results of X-ray diffraction (XRD) pattern of SCFAs-LDH prepared with actual anaerobic fermentation liquid showed sharp characteristic reflections of hydrotalcite-like compounds with high crystallinity. The interlayer d-spacing of SCFAs-LDH was 0.76 nm at 2θ = 11.7°. The sharp peak at 3379 cm^{-1} was attributed to the O−H stretching vibration from the interlayer water molecules and hydroxyl groups in the brucite-like layers. The weak absorption peak at

1553cm^{-1} was assigned to the COO^- stretching vibrations. The 1350cm^{-1}peak corresponded to the vibrations of the carbonate group. Chemical analysis of the synthesized SCFAs-LDH was performed. It can be seen that the experimental Zn/Al ratio (1.96) was consistent with expected Zn/Al ratio (2:1). The carbon content of SCFAs-LDH was 4.8% by elemental analysis. This carbon content was attributed by SCFAs including acetate (5.7 mg/g), propionate (4.4 mg/g), and n-butyrate (8.8 mg/g), meaning that the SCFAs in actual anaerobic fermentation liquid were intercalated with SCFAs-LDH synthesized successfully. At the same time, carbonate was also found in the synthesized SCFAs-LDH, because there must be a high concentration of carbonate in the anaerobic fermentation liquid. It has been proven that the carbonate anion has a strong affinity with LDH and easily forms CO_3^{2-}-LDH.45 A strong CO_3^{2-} absorption peak can be found obviously. In view of practical application, the large amount of carbonate in anaerobic fermentation liquid must be removed primarily. Alkaline fermentation of organic waste with $Ca(OH)_2$ could be an effective way to increase SCFAs production and remove carbonate ions simultaneously. Of course, a small amount of carbonate must still remain; however, this small amount of carbonate does not affect the utilization of this method.

Release Performance of SCFAs-LDH. It can be found that the larger the particle size, the slower the release content. In addition, the profiles exhibit a gradual two-step release behavior, i.e., a fast release stage in the initial hour, followed by a relatively slow period over the next 1−72h. This trend is consistent with the literature. It is believed that rapid release was related to physical adsorption of SCFAs on LDH surface, and slow release was attributed to the successful extraction of SCFAs intercalated into the interlayer of LDH. The release performances of SCFAs-LDH and SCFAs-Na tablets were investigated in a releasing medium system. It can be found that the SCFAs-LDH tablets exhibited a gradual two-step release behavior: a fast release stage in the initial 6h, with an SCFAs release percentage of 33.1%, followed by a relatively slow period over the next 6−72h, with an SCFAs release percentage of 47.6%. This trend is also consistent with literatures. However, SCFAs-Na tablet exhibited a rapid release, with an SCFAs release percentage of 95% within 30 min. The release tests indicate that a slow release of SCFAs could be achieved via the synthesis of SCFAs-LDH tablets.

Nitrate Removal Performance with SCFAs-LDH as an External Carbon Source. Without any external carbon source added, the final nitrate removal efficiencies were 61.7% and 43.6%, using SCFAs-LDH and SCFAs-Na tablets as an external carbon source with COD/N ratio of 3:1, respectively. This shows that SCAFs-LDH tablets, with slow-release SCFAs, worked much better than SCFAs-Na tablets, as an external carbon source of denitrification. When the COD/N ratio was 4:1, the final nitrate removal efficiencies were 81.3% and 42.3%, using SCFAs-LDH and SCFAs-Na tablets, respectively. With a higher COD/N ratio (4:1), the nitrate removal efficiency increased by 19.6% when using the SCFAs-LDH tablet, but remained stable when using the SCFAs-Na tablet. These two points indicate that the SCFAs-LDH tablet is a promising external carbon source, especially for reactors with long hydraulic retention time or when COD/N ratio is low.

The Variation of COD Concentration during Denitrification. For the control (without any external carbon source added), the COD concentration was ~52 mg/L. This content of COD in liquid was secreted by metabolism of the bacteria from the inoculation. For the test using SCFAs- LDH tablets, the COD concentration was ~100 mg/L, resulting from the balance of SCFAs release from SCFAs- LDH tablets and SCFAs utilization as the carbon source of denitrification. However, for the test using SCFAs-Na tablets, the COD concentrations exhibited an obvious similar trend, with quick consumption in the first 8 h (when COD/N ratio was 3:1) and 12 h (when COD/N ratio was 4:1) and then stable. This one direction trend of COD concentration resulted in overfeeding and an insufficient carbon source at the beginning and in the end of denitrification, respectively. The excessive carbon source must be utilized for bacteria anabolism, leading to sludge growth.

Utilization Efficiency of Carbon Source. The utilization efficiencies of denitrification using SCFAs-LDH and SCFAs-Na tablets as the external carbon source with COD/N ratios of 3:1 and 4:1, respectively. The utilization efficiencies were 58.8% and 41.6% when using SCFAs-LDH and SCFAs-Na tablets with a COD/N ratio of 3:1, and 58.1% and 30.3% with a COD/N ratio of 4:1, respectively.

3. Conclusions

SCFAs were extracted from artificial and actual anaerobic fermentation liquid of organic waste via the synthesis of SCFAs-LDH. SCFAs-LDH had a good slow release performance for serving as an external carbon source of bio denitrification, with an SCFAs release percentage of 47.6% during a relatively slow release period (6−72 h). The nitrate removal efficiency was improved greatly, from 42.3% using SCFAs-Na tablets to 81.3% using SCFAs-LDH tablets as an external carbon source, with a COD/N ratio of 4:1. Using SCFAs-LDH tablets as an external carbon source, the utilization efficiency could be improved by 91.7%, compared with using SCFAs-Na tablets.

The study of simultaneous removal of nitrogen and COD from anaerobic digestate liquid at different COD/NH_4^+-N ratios by anammox-based new process

○Yan Guo[1], Takumi Sugono[1], Qigui Niu[2], Yu-You Li[1]*

[1] Dept. of Civil and Environmental Engineering, Graduate School of Engineering, Tohoku University, Aoba-ku, Sendai, 980-8579 Japan

[2] School of Environmental Science and Engineering, Shandong University, 27# Shanda South Road, Jinan 250100, China

*E-mail: gyokuyu.ri.a5@tohoku.ac.jp

Abstract

The presence of residual organic matter (OM) in the anaerobic digestate liquid brought negative effects to the nitrogen removal by one-stage partial nitrification/anammox process, and the OM removal is also one problem needed to be solved for discharge standard. In this study, the simultaneous removal of nitrogen and COD from synthetic wastewater with different COD/NH_4^+-N ratios through simultaneous partial nitrification, anammox, denitrification and dissimilation (PNADD) process in a CSTR equipped with functional suspended carriers was investigated**.** The results showed until the COD/ NH_4^+-N ratio of 0.8 with a proper aeration rate,the nitrogen removal effciency of above 78.6% and and COD removal effciency of above 87.7% can be achieved. Accodring to the results of activity tests of suspended sludge and biofilm sludge from the reactor , with the existence of organic matter, the denitrification activity increased, and in the system AOB was predominant in the suspended sludge and anammox bacteria was predominant in the biofilm sludge, respectively. It can be concluded that the nitrogen removal was achieved by the synergy of anammox and denitrification and the COD removal was attributed to both dissimilation and denitrification. The activity test results of nitrogen removal of biofilm sludge with high COD/ NH_4^+-N ratio shows that there are no obvious effect on the anammox activity. It was c that the negative effect of organic matter on one-stage PNA process was mainly because of strong competence of the heterotrophic bacteria for DO than AOB, then the subsequensely anammox step was limited that effected the nitrogen removal effciency. It showed that the PNADD process were successfully achieved by using the CSTR equipped with functional suspended carriers.

Keywords: Anammox, digestate liquid, Nitrogen removal, COD removal

1. Introduction

The biogas production through anaerobic fermentation is one utilization way of mass wasted biomass for social sustainable development, but the production of digestate liquid during this process needed to be solved. One of the methods for digestate liquid treatment is as liquid fertilizer for farmland. For the area that the digestate liquid cannot be directly used as liquid fertilizer, the treatment of digestate liquid for discharge meeting the discharge standard is needed.

Compared with the nitrogen content, the organic matter content is obvious low for the digester liquid of various kinds of raw materials after methane fermentation. So the traditional biological nitrogen removal method for this kind of wastewater will face the shortage of carbon source. The anammox process consumes 60% less oxygen and 100% less organic carbon source, produces about 90% less sludge compared with nitrification/denitrification, so there have numerous research focusing on the application of anammox process for high ammonia-containing or low COD/NH_4^+-N ratio wastewater.

Among the over 100 operating installations worldwide, 88% of all plants being operated as one-stage partial itrification anammox (PNA) systems. One of the challenges in the application of the one-stage PNA process is retaining biomass and distinct habitats required for the AOB and anammox bacteria for the aerobic and anaerobic activities. The previous research reported that the biofilm is much simpler and more effective due to the improved ability to retain biomass in the reactor and the large contribution towards total reactor activity. Numerous reports have been reported focused on the various carriers used in the one-stage PNA process. The second is the nitrite oxidizing bacteria (NOB) competes with AOB or anammox bacteria for the substrate. It has been reported that the difficulties could be overcome by washing out NOB under a low dissolved oxygen (DO) concentration (<1.0 mg/L) .

The influent carbon source is proved to be a critical factor for PNA performance. High COD concentration leads to growth of heterotrophic bacteria, resulting in suppression of AOB and anammox bacteria. Meanwhile the enriched heterotrophic bacteria can denitrify the nitrate produced by anammox bacteria, thereby reducing the effluent nitrogen concentration.

In this study, for the simultaneous removal of nitrogen and COD of anaerobic digester effluents at different COD/ NH_4^+-N ratios, through the simultaneous partial nitrification, anammox, denitrification and dissimilation (PNADD) process in a CSTR equipped with functional suspended carriers were investigated**.** Meanwhile the shifting of the microbial community and the metabolic pathway of nitrogen and organic carbon were investigated.

2. Materials and Methods

2.1 The synthetic wastewater and the carrier.

The synthetic wastewater was used and COD was added in the form of the acetate.

The functional suspended carrier applied in this study was a hollow cylinder made of hydrophobic polypropylene (pp) resin with good adherence to the microorganism assured by special porous foam. The carrier was 4 mm $\Phi \times 4$ mm L, with a true specific gravity of 0.98 g/cm^3 and a specific surface area of 1500 m^2/m^3. Before the reactor was dosed with the bio-carriers, they were immersed in a neutral cleaning solution for 24 h, to promote hydrophilic properties and thereby enhance both the flow of the carrier in the reactor and the contact between the carrier and the liquid phase.

2.2 The operation condition

The reactor was operated in six stages with the HRT of 12 h. During the first five stages, the COD/ NH_4^+-N ratios were stepwise increased from 0 to 1.6 by increasing the COD concentration from 0 mg/L to 400 mg/L with a constant substrate concentration of NH_4^+-N to 250.0 mg/L. For the last stage, the COD/ NH_4^+-N ratio was back to 0.8 by decreasing the COD concentration to 200 mg/L.

2.3 The system set-up and control condition

The single-stage partial-anammox process was carried out in a lab-scale CSTR reactor made of transparent polyvinyl chloride (PVC) plastic with a working volume of 5 L and a 1 L clarifier. The temperature in the reactor was set and kept in the range of 25 ± 1 °C by a heater with temperature adjuster set in the reaction zone. Influent was introduced into the reaction zone with a peristaltic pump. Air was supplied using an air pump through a glass tube, serving both to mix and oxygenate the sewage. The porous polypropylene carriers (packing ratio: 30 v%) in the reactor were in a continuous movement with horizontal and vertical mixing due to the air supplied through a glass tube inset into the bottom of the reactor. The aeration rate (AR) was adjusted by a glass rotameter in pace with NLR variations.

The temperature in the reactor was controlled at ±25℃, and the DO concentration was under 0.1mg/L.

2.4 Instrumentation and analysis method

Sensors for temperature, pH, oxidation reduction potential (ORP) (HORIBA D-72, Japan), and DO (HORIBA OM-70, Japan) were installed in the reactor for the on-line monitoring of pH, ORP and DO, respectively.

Samples were taken from both the influent and effluent every other day. Concentrations of NH_4^+-N, NO_2^--N, NO_3^--N were analyzed by capillary electrophoresis (Agilent 7100) after being filtered through a 0.45 μm polyether sulfone syringe filter. The COD, MLSS and MLVSS were determined according to the Standard Methods.

3. Results and Discussion

The results showed that with the improvement of COD/NH_4^+-N ratio from 0 to 0.4, for a favorable nitrogen removal efficiency (NRE), the aeration rate (AR) correspondingly increases. At the first COD/NH_4^+-N ratio of 0.8, with the drop of AFR, the decrease of NRE was sharp than carbon removal efficiency (CRE). At the COD/NH_4^+-N ratio of 1.6, the NRE decreased sharply than CRE, so the COD/NH_4^+-N ratio was back to 0.8. At the second time of COD/NH_4^+-N ratio of 0.8, with a higher AFR, the NRE increases again. It can be concluded that one effect of organic matter on one-stage PNA process was the oxygen competition between COD oxidizing bacteria and NH_4^+-N oxidizing bacteria. Until the COD/ NH_4^+-N ratio of 0.8 with a proper aeration rate,the nitrogen removal effciency of above 78.6% and and COD removal effciency of above 87.7% can be achieved.

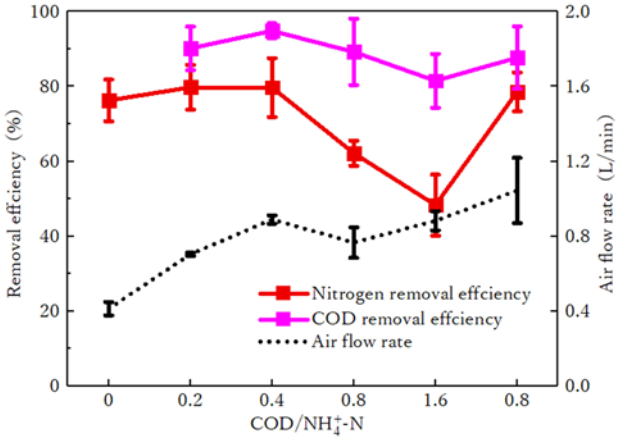

Figure. 1. The variety of NRE, CRE and AR at different COD/ NH_4^+-N ratios.

From the COD/NH_4^+-N ratio of 0.2 to 1.6, the NO_3^--N/ΔNH_4^+-N values were obvious lower that 11.5% of COD/NH_4^+-N ratio of 0, the absent ΔNO_3^--N (11.5%—$NO_3^-N_{-eff}$— NH_4^+-N_{-eff}) can be explained by the enhancement of denitrification activity that transferred this part of the NO_3^--N produced during the anammox process to nitrogen gas.

The results of the activity tests indicated that AOB was predominant in the suspended sludge and anammox bacteria was predominant in the biofilm sludge, respectively. Besides, with the introduction of organic matter into the system, the denitrification activity was obviously enhanced.

From the results of the activity tests of nitrogen removal of biofilm at different COD/NH_4^+-N, the COD/NH_4^+-N ratio up to 5 have no heavily impressed function on the specific anammox activity of the biofilm sludge. It means the COD/NH_4^+-N ratio up to 1.6 in the actual reactor has no effect on the anammox activity. It can be concluded that the negative effect of organic matter on one-stage PNA process was mainly because of competence for DO between AOB and the heterotrophic bacteria.

4. Conclusions

(1) The simultaneous partial nitrification, anammox, denitrification and dissimilation process in a CSTR equipped with functional suspended carriers were achieved with the COD/NH_4^+-N ratio up to 0.8.

(2) AOB was predominant in the suspended sludge and anammox bacteria was predominant in the biofilm sludge, respectively. With the introduction of organic matter into the system, the denitrification activity was obviously enhanced.

(3) The nitrogen removal was achieved by the synergy of anammox and denitrification and the COD removal was attributed to both dissimilation and denitrification.

A research on stoichiometric model of codigestion's synergism mechanism based on coffee gro und and wasted activated sludge

○Tao ZHANG[1]*, Kazuki TONOUTCHI[1], Wataru RUIKE[2] ,Yu-You Li[1*]
*Department of Civil and Environmental Engineering, Graduate School of Engineering , Tohoku University,980-8579 Japan
*E-mail: zhang.tao.q7@dc.tohoku.ac.jp
gyokuyu.ri.a5@tohoku.ac.jp

Abstract

Coffee grounds have been proved difficult to be degraded by thermophilic digestion. An introduction of activated sludge is possible to improve the coffee grounds degradation through synergistic mechanisms. In this research, two 12 L CSTRs which were fed with the mixture of coffee grounds and activated sludge with different ratio,80:20 and 70:30 correspondingly. After startup, the two reactors reached the 30-day-HRT operation and had kept steady biogas production about two times longer than this HRT, which could be reckoned to be a steady operation. During the whole operation, no nutrition supply was implemented. On the basis of ammonia balance, the biomass yield was calculated to illustrate the necessary reproductive ammonia and trace elements for the biomass cell. Biogas methane composition and bicarbonate alkalinity fitted well with the prediction value. After the comparison of theoretical and actual value, it could be concluded that such 2 ratios of WAS could offer enough trace elements for the biomass cell reproduction. The inner synergism mechanism of the co-digestion was achieved in this study.

Keywords: Coffee grounds, wasted activated sludge, co-digestion, synergism, mathematical model

1. Introduction

Nowadays the global coffee consumption kept increasingly growing. According to International Coffee Organization's statistics(International Coffee Organization 2017), the very increasing rate is around 9% and it has amounted to 9.3 million in 2016. Then a multitude of coffee grounding(CG), (the main by-product from the coffee production) would be inevitably produced. A detailed investigation was made by Qiao's research(Qiao, Takayanagi, Shofie, et al. 2013), it demonstrated that the significant characteristic of CG includes high moisture (65.68%) and high organic components in TS (VS/TS is more than 99%). The relatively high moisture makes it less economically via general incineration or land fill. The high VS/TS ratio indicates that it is of a large energy recovery potential. Among the biological processes aiming at reclamation of bioenergy from wastes, methane fermentation is considered to be one of the most suitable choices.

The research concerning laboratory scale anaerobic digestion has been stared ever since 1980s in the form of batch experiments. Dinstale et al. conducted a series of mesophilic and thermophilic experiments both by batch and CSTR reactors, it was demonstrated that VFA accumulation was inevitable for the mesophilic and thermophilic CSTR after 50 days and addition of sodium bicarbonate, nitrogen, phosphorous and trace elements was necessary for the long-term digestion(Dinsdale, Hawkes, and Hawkes 1996). Qiao et al. used AnMBR to dispose CG and the biogas production almost ceased on Day 82d and VFA accumulation and sharply- drop of pH was discovered, owing to a lack of ammonia and nutrition elements(Qiao, Takayanagi, Shofie, et al. 2013).

Therefore, the concept of Anaerobic co-digestion(AcoD) was introduced to overcome the difficult listed above. Neves et al. demonstrated that the CG's AcoD with WAS could achieve a methane yield more than 75% of the theoretical value via a series of batch experiments(Neves, Oliveira, and Alves 2006). Qiao et al. introduced WAS by two different ratios after the mono-digestion of CG's failure, however the propionic acid accumulation and relatively high hydrogen in the reactor made it unsustainable for a long term operation as to both of the ratios(10% and 15%) , external supplement of ammonia and nutrition elements were still necessary(Qiao, Takayanagi, Niu, et al. 2013). Persistent addition of external nutrition would increase additional expense and the maneuverability would be lowered.

On account of the former studies upon the CG's anaerobic digestion, the present study aims at exploring the stable operation possibility of co-digestion with relatively higher WAS ratios (20% and 30%) on condition that no external nutrition supplement was added. Moreover, the synergy mechanism of the co-digestion with WAS would be investigated qualitatively and quantitatively.

2. Materials and Methods

2.1. Characteristic s of coffee groundings and wasted activate sludge

The coffee grounds (CG) samples were collected from a coffee manufacture in Japan, the one Qiao et al.,(2013) sampled from. The raw coffee groundings' TS were 36.3. The wasted activated sludge (WAS) was sourced from the

coffee manufacture's coffee waste treatment unit. TS content of the WAS was 14.7%. On the basis of dry weight, the ratio of CG to WAS for S1 was 80:20, for S2 was 70:30.

2.2. Experimental apparatus

The lab-scale reactor used in this experiment is a traditional CSTR (Completely Stirring Tank Reactor). The reactors had a working volume of 12L and a total volume of 15L. The digester tank was water-jacketed and operated at a constant temperature of 55° C for thermophilic methane fermentation. The scheme of the experimental apparatus was illustrated in Figure.1. The original seed sludge used in this experiment were taken from a food waste thermophilic fermentation digester.

Figure 1 Schematic of the experimental apparatus

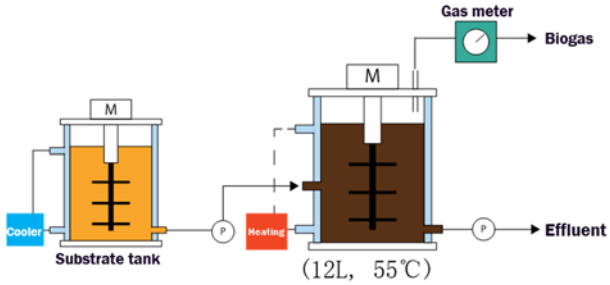

2.3 A method to conclude the stoichiometric model

$C_aH_bO_cN_d + \left(2a + b - c - \frac{9}{20}s\delta - \frac{e\delta}{4}\right)H_2O \rightarrow \frac{e\delta}{8}CH_4 + (a - d - \frac{1}{5}s\delta - \frac{e\delta}{8})CO_2 + \frac{s\delta}{20}C_5H_7O_2N + (d - \frac{1}{20}s\delta)NH_4HCO_3$ **equation 1(McCarty, 1974)**

$\delta = 4a + b - 2c - 3d$ *e is the fraction of* COD_{CH4} *while s is the* COD_{cell}. *for the degraded part, e+s=1*

In1L influent, VS concentration is C_{VS} g/L, molar is n_{VS}, degraded efficiency is α, $C_{ultNH3-N}$ g NH3-N is produced, biomass molar is n_{cell}, nitrogen molar weight is M_N g/mol, VS molar weight is M_{vs}.

$Y_{mol}=\frac{n_{cell}}{n_{VS}} = d - \frac{M_{VS}}{M_N}\cdot\frac{C_{ultNH3-N}}{\alpha C_{VS}}$ **(equation 2)**

3. Results and Discussion

The performance of the two reactors were summarized in Table 1. Generally, the period is required to be more than twice the HRT. After two start-up stages as transition (120-day-HRT and 60-day-HRT), both of the two reactors reached the target phase of 30-day HRT steadily (hereafter would be defined as target phase). Under target phase operation (totally around 75d), some typical operational parameters: pH, methane gas production rate and total VFA concentration were stable in both of the two reactors, which indicated that both of the two reactors were operated successfully without external addition of nutrition under 30-day HRT.

By the equation 1 and 2 and data from Table1, the biomass yield could be worked out and the stoichiometry reaction of the co-digestion could be written as below:

$C_5H_{7.94}O_{2.23}N_{0.419} + 1.63H_2O \rightarrow 0.2564C_5H_7O_2N + 2.19CH_4 + 1.54CO_2 + 0.08NH_4^+ + 0.08HCO_3^-$

$C_5H_{7.97}O_{2.24}N_{0.42} + 1.70H_2O \rightarrow 0.2755C_5H_7O_2N + 2.10CH_4 + 1.49CO_2 + 0.14NH_4^+ + 0.14HCO_3^-$

Table 1 Summary of two series' operation performance

Operation	Unit	R1	R2
pH	-	7.04	7.41
Alkalinity	mg-$CaCO_3$	2160	3820
TS	%	5.4	5.0
VS	%	4.7	4.0
COD	g/L	71.9	73.8
NH_4^+-N	mg/L	482	884
T-VFA	mg-HAc/L	896	724
Acetic acid		241	198
Propionic		165	137
Biogas	L/g-VS_{added}	0.467	0.414
Biogas composition	CH_4	59.37	59.16
	CO_2	39.96	39.60
	N_2		0.67

And then according to the calculated biomass yield, the major value of AD could be predicted as Table 2.

Table 2 Comparison of the model's prediction and actual value

	S1(20%)		S2(30%)	
	Pred.	Actual	Pred.	Actual
GPR(L /g-VS_{add})	0.38	0.467	0.39	0.414
CH_4%	58.62	59.37	58.47	59.16
CO_2%	41.38	39.67	41.53	39.60
Alkalinity mg/L	1861	2160	3476.25	38.20

The model was able to predict the AD's main indexes and then was used to give an explanation of the steady operation without external trace elements supply.

4. Conclusions

(1) Bothe of the 2 reactors would make a steady operation even in spite of no external nutrition supply.

(2) A stoichiometry model was given according to the nitrate balance and then biomass yield was calculated and explained the reason why the co-digestion was self-sufficient under these two WAS ratios.

Anaerobic co-digestion of food waste and paper waste: mseophilic vs. thermophilic

○Jing Wu[1], Yu Qin[2], Benyi Xiao[3] & Yu-you Li[2]
[1]Graduate School of Environmental Studies, Tohoku University, Sendai, Miyagi, Japan
[2]Department of Civil and Environmental Engineering, Graduate School of Engineering, Tohoku University, Miyagi, Japan
[3]Research Center for Eco-Environmental Sciences, Chinese Academy of Sciences, P.O. Box 2871, Beijing, PR China
E-mail: wu.jing.s3@dc.tohoku.ac.jp

Abstract
This study presents the results of anaerobic digestion of food waste (FW), as well as co-digestion with FW and paper waste (PW), which was conducted in two lab-scale continuous stirred-tank reactors (CSTRs) at 37℃ and 55℃ respectively. The effect of FW: PW ratio on co-digestion stability and performance were investigated at around OLR of 10.0 g-VS/L/d and having the FW: PW ratio of 4:1, 2:3, 1:1 and 2:3 (TS). Mesophilic digester (MD) could be operated stably when the PW contents is under 40% (TS), while thermophilic digester (TD) even maintained stable when the PW contents reached 70% (TS). This study confirmed that co-digestion of FW and PW, with the increase of PW content lead to some degree of improvement in biogas yield in TD as a result of mixing substrates while biogas yield decreased in MD. The organic removal of MD and TD were nearly the same under the safe PW contents. MD was superior to TD in terms of effluent quality, while TD has higher solid reduction efficiency than MD. TD is superior to MD in terms of treating FW and PW mixtures for higher stability, particle hydrolysis, and biogas production.

Keywords: Anaerobic digestion; Mesophilic condition; Co-digestion; Food waste; Paper waste

1. Introduction
Food waste (FW) and paper waste (PW) are top two largest fraction of municipal solid waste (MSW) and PW represents the second largest fraction of biodegradable materials in MSW after FW. However, around 37% of PW is still discarded mainly in sanitary municipal landfills.

Anaerobic co-digestion of PW and FW, due to improvement of nutrient balance and system economics, could be a possible solution for reduction and stabilization of PW-contained FW. However, anaerobic digestion concerning PW is limited by the hydrolysis step and there is still a lack of information with reference to the co-digestion of FW and PW. The PW existence may affect the digestion performance by different hydrolysis rate and load bearing capacity of co-substrates. Furthermore, mesophilic and thermophilic anaerobic digestion are two widely applied temperature ranges in industrial. Therefore, this study has two main objects: 1. to better understand the effect of PW existence on the co-digestion of FW and PW; 2. to compare mesophilic and thermophilic condition co-digestion performance.

2. Materials and Methods

2.1 Feedstocks

2.1.1 Food waste (FW)
FW used was made according to the previous work from our laboratory. FW was firstly milled and blended with water in a blender. The disintegrated FW was either supply to the substrate tank directly or blended with shredded PW.

2.1.2 Paper waste (PW)
Three kinds of paper: Newsprint, tissue and office paper, with large daily generation, were chosen. The mixture ratio of three kinds of paper was set as 1:1:1 on TS basis. PW was shredded by a waste paper shredder. After shredding, paper scarps were blended with FW in the blender and fed to the substrate tank. Characterization of substrates used in different Runs are summarized in Table 1.

2.2 Reactors and operations
The co-digestion system used in this study is shown in Figure 1. All tanks were equipped with water bath systems. The substrate tank was maintained at 3℃ in order to prevent putridity. The effect volume of mesophilic and thermophilic digesters was 3.0 L. Both digesters were operated at 37℃ and 55℃ separately. Input of substrates was conducted by roller pumpers which were connected with timers for quantitative supplement.

Table 1 Characteristics of the substrates

		Run 1	Run 2	Run 3	Run 4	Run 5
Day	-	1~127	127~211	212~275	279~293	296~331
PW Content	%	0	20	40	60	50
C/N	-	17.1	20.4	25.8	35.8	29.9
pH	-	4.2	4.8	4.8	5.4	5.2
TS	%	10.9±0.7	10.7±0.7	10.8±0.6	11.1±0.8	10.4±0.2
VS	%	10.3±0.7	10.0±0.8	9.3±0.8	10.1±0.8	9.4±0.2
VFAs	mg-COD/L	1267	1390	1168	1313	1168
COD_{Cr}	g/L	141.8±1.5	138.7±0.8	140.3±0.7	138.7±1.3	133.0±0.7
Carbohydrates	g/L	56.5±7	69.2±16	73.0±10	84.4±5	73.2±5
Protein	g/L	22.2±4	19.0±7	16.7±4	11.1±1	11.8±1
Lipid	g/L	1.3± 0.1	0.95± 0.1	0.82± 0.1	0.64± 0.1	0.57± 0.1

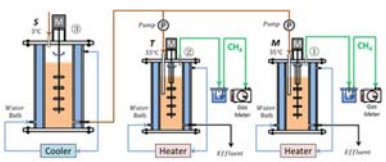

Figure 1 Co-digestion system used in this study

2.3 Analytical methods

Biogas volume was measured daily by a wet gas meter and gas volume was then converted into dry gas volume under 0℃, 1 atm. Biogas content (CH_4, CO_2, N_2) was determined by a gas chromatograph. Sampling of the effluent from the digester was carried out twice a week and the following parameters were analysed: pH, alkalinity, TS and VS, SS and VSS, COD_{cr}, carbohydrates, protein, lipid, TAN and VFAs.

3. Results and Discussion

2.1 Substrate characteristics

FW and PW were represented with formulation of $C_{20}H_{33}O_{12}N$ and $C_{331}H_{508}O_{314}N$. The C/N ratio of FW (17.1) is lower than the number (20-25) recommended in literatures for stable operation. With the increase of PW content in the co-substrate, the high C/N ratio of PW (283.6) may lead to high C/N ratio of the co-substrates.

2.2 Performance and organic removal

MD and TD was stable and well functioned at PW≤40% and PW≤70% with nearly the same level of organic removal efficiency (Figure 3).

For mono-digestion of FW, VFA in TD was about 1000mg/L, higher than that in MD (below 200mg/L). After adding PW, VFA sharply decreased in TD and acetic acid became the major byproduct. With increase of PW contents, pH, TAN and alkalinity gradually decreased in both digesters. However, VFA, as a form of mainly acetic acid started to accumulated (rise from 0mg/L to 932mg/L) at PW=60% in MD, which may cause by inhibition of methanogens due to ammonia deficiency. At PW=70%, when ammonia decreased to about 50 mg/L, TD could still maintain stable, with COD removal around 78%, pH about 6.8 and alkalinity about 1700mg/L. As hydrolysis of protein in FW is thought to provide ammonia and alkalinity in TD, the reason why TD could still be stably operated could be other alkalinity source which came from the alkalinity fillers in PW.

Table 2 Performance of mesophilic and thermophilic digesters (MD Run5: NH_4HCO_3 added)

	Mesophilic				Thermophilic			
	Run 1	Run 2	Run 3	Run 5	Run 1	Run 2	Run 3	Run 5
C/N	17.1	20.4	25.8	29.9	17.1	20.4	25.8	29.9
Biogas Yield (L/g-VS)	0.86	0.81	0.81	0.78	0.86	0.80	0.88	0.91
CH_4 Content (%)	61.0±0.7	58.0±0.8	57.0±2.5	55.8±1.9	62.0±1.1	58.0±0.8	56.2±2.5	54.0±1.9
CO_2 Content (%)	39.0±1.8	42.0±1.0	43.0±3.0	44.2±1.9	38.0±2.8	40.7±1.0	43.8±2.4	46.0±1.9
H_2S (ppm)	1300	1020	273	335	1260	1000	400	287
pH	7.90 ±0.1	7.72 ±0.1	7.44 ±0.1	7.28 ±0.1	8.34 ±0.1	8.30 ±0.1	7.90 ±0.2	7.49 ±0.2
Ammonia (mg/L)	2080 ±309	1700 ±126	970 ±268	630 ±298	2180 ±244	1860 ±112	1140 ±243	520 ±50
Alkalinity (mg/L)	8870 ±220	7920 ±610	5470 ±110	3350 ±950	8350 ±240	7940 ±220	5430 ±610	3360 ±110

2.3 COD mass balance

Figure 4 shows the COD mass balance in MD and TD. With increase of PW content, particle COD (P-COD) in TD is lower than that in MD, which indicate that TD is superior to MD in terms of hydrolysis. Meanwhile, higher soluble COD (SCOD) in TD also means MD has better effluent quality than TD.

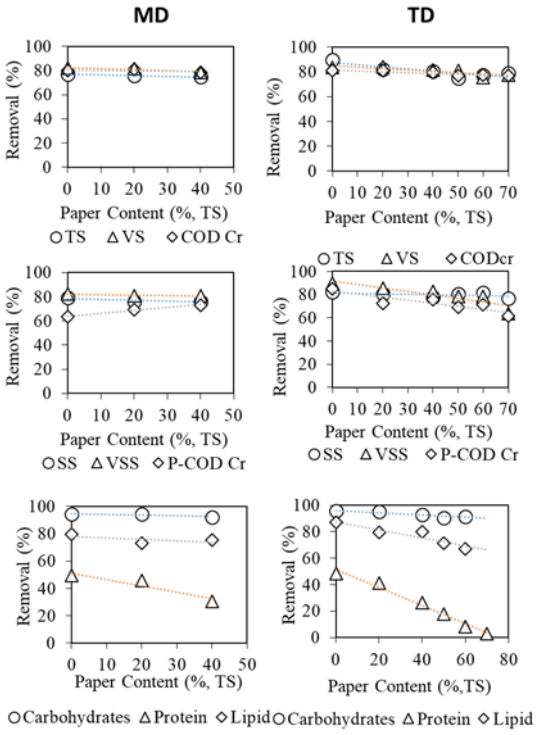

Figure 3 Effect of PW content on organic removal of MD and TD

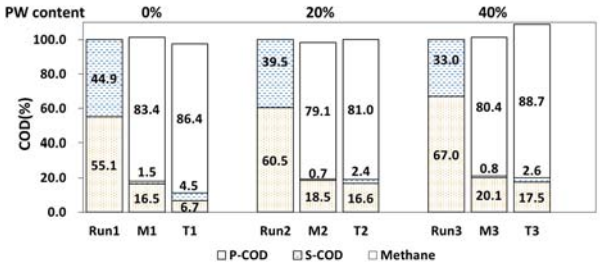

Figure 4 COD mass balance of MD and TD in different Runs (i.e. MD Run1 means M1)

4. Conclusions

(1) PW≤40% and PW≤70% is suggested to ensure good system efficiency for MD and TD at HRT=30 days.

(2) Some degree of improvement in biogas yield was observed in TD as a result of mixing substrates, while biogas yield decreased in MD with increasing PW contents.

(3) MD was superior to TD in terms of effluent quality, TD has higher solid reduction efficiency than MD.

(4) TD is recommended for treating FW and PW mixtures for higher stability, particle hydrolysis, and biogas production.

5. Reference

Sherri M. Cook, et al., A stability assessment tool for anaerobic co-digestion. Water Research, 2017, 112 19-28

Start-up of a New Anaerobic Reactor for treating wastewater containing High SS Content

○Bo JIANG[1], Hong CHEN[1,2], Yuyou LI[1*]

[1] Department of Civil and Environmental Engineering, Tohoku University, Sendai 980-8579 Japan
[2] School of Hydraulic Engineering, Changsha University of Science and Technology, Changsha, 410-004 China

*E-mail: gyokuyu.ri.a5@tohoku.ac.jp

Abstract

The purpose of this experiment research is to analyze the start-up process of a new Anaerobic Suspended Carrier Mixture Reactor (AnSCMR). The new AnSCMR is designed to overcome the disadvantage of traditional UASB reactor against high organic SS wastewater and sludge expansion by using microbial carriers and internal loop. The propeller and inner loop inside the reactor create a water circulation to prevent sedimentation of SS and expansion of sludge. The high SS synthetic wastewater used in the research are starch wastewater (800-1000mg-COD/L, 300-400mg-SS/L). The acclimation period lasts for 230 days, with the HRT has been shorten from 36h to 2h. Limited to its structure, the 4.5L AnSCMR has a lower initial microorganism concentration (20mg-MLVSS/L). With the decrease of HRT and increase of OLR, the removal efficiency of AnSCMR was decreased about 10%(from 65.1% to 54.6%). At the end of the experiment, when the OLD has reached 12g-COD/L/d, the methane production match the S-COD removal rate of the AnSCMR and the organic SS in the AnSCMR was not decomposed or intercepted in the reactor. The results indicated the AnSCMR could be used to remove the S-COD in the wastewater without effect the organic particle in the water.

Keywords: organic SS, methane production, anaerobic methane production

1. Introduction

The starch industry extracts and refines starches from seeds, roots and tubers. The major procedure includes wet grinding, washing, sieving and drying. More than 50 types of plants have been reported to be used for starch production. The most common commercial raw materials are corn, potato and wheat. The starch wastewater is characterized as high organic SS wastewater (Table 1). The SS could be intercepted in the traditional anaerobic reactor, causing sludge expansion and other problems.

Table 1 Starch wastewater status (Unit: mg/L)

Raw material	Water source	COD	SS
Potato	Delivery	60-210	390-2000
	Separation	1550-4800	600-2500
	Precipitation	730-2000	80-170
Sweet potato	Delivery	82-280	273-780
	Separation	7400-9500	2000-3000
	Precipitation	3000-5000	60-90
Corn	Effluent	8000-30000	3000-5000

2. Reactor and Methods

2.1 Reactor and experimental design

The Anaerobic Suspended Carrier Mixture Reactor (AnSCMR) was packed with a rectangular column with an effective working volume of 4.5L (Ø15cm * 25cm). The AnSCMR has a U-shape tube at the top of the reactor to separate effluent from gas produced in the AnSCMR. The SCMR was developed and maintained for 230 days. The SCMR was fed with the synthetic wastewater mentioned below in the way of continuously influent method.

The SCMR was inoculated with 1L granular sludge taken from a standard UASB reactor in the lab operated at 35℃. 3L of blank carrier particles was also added into the reactor. The operational conditions of SCMR in this study are detailed in Table 2. The organic loading rate (OLR) was gradually increased from 0.66g-COD/L/d to 12.0 g-COD/L/d by reducing HRT from 36 (Phase I) to 2 h (phase VII).

Table 2 Operational conditions of SCMR

Phase	Days	HRT (h)	Influent (L/d)	OLD (g-COD/L/d)
I	1-23	36	0.5	0.5
II	24-49	24	1	1
III	50-95	12	2	2
IV	96-143	6	4	4
V	144-183	4	6	6
VI	184-210	3	8	8
VII	210-230	2	12	12

2.2 Synthetic wastewater status

The basic status of the synthetic wastewater is shown in Table 3. The pH and alkalinity of influent was maintained in the similar level in the whole start-up process by controlling the concentration of $NaHCO_3$. The pH and alkalinity in the synthetic wastewater was higher than actual wastewater. This was to make sure the success of the start-up of the reactor. The fluctuation of T-COD, S-COD and SS of the synthetic wastewater had fluctuation because of the stirring situation in the substrate tank. The component of influent COD is only carbohydrate, there are no other form of COD in the influent.

Table 3 Synthetic wastewater status

Item	Unit	Concentration
T-COD	mg/L	800-1100
S-COD	mg/L	200-600
SS	mg/L	300-400
pH	--	7.30-8.10
Alkalinity	mg-$CaCO_3$/L	1200-1500

3. Results and Discussion

The performance of SCMR is exhibited in Figure 1 in terms of gas production rate, methane content, T-COD and S-COD.

The results of SCMR showed that GPR and methane

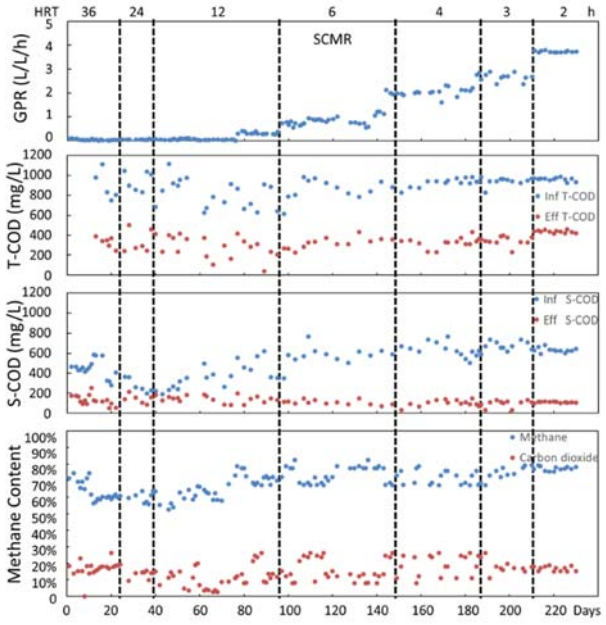

Figure 3 Overall performance of AnSCMR

content of SCMR generally increased when the HRT was shorten. The T-COD in the effluent generally increased when the HRT was shorten. But the S-COD in effluent basically stayed the same. From Figure 1, we can assume that the SCMR can remove the S-COD in the reactor, but not the T-COD in the reactor. The performance of SCMR was basically more similar to that of a stand UASB. The methane concentration in the produced gas is about 70%, The ratio of methane to carbon dioxide is about 3:1 to 3.5:1.

The pH and Alkalinity was measured as a reference of reactor stability. The results were shown in Figure 2. The pH and alkalinity maintained stably during the whole process. In the whole start-up process, the pH of effluent decreased from 8.0 to 6.8, and the alkalinity decreased from 1300 to 1200. The drop between influent and effluent were approximately 0.7 for pH and 1000 for alkalinity.

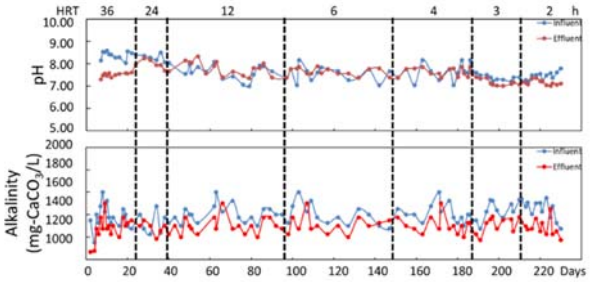

Figure 1 Alkalinity and pH status of the AnSCMR

The results of SS removal were exhibited in Figure 3. The results of SS fluctuated greatly due to the stirring situation and sampling process. On average, The SS concentration is about 300mg/L. In the synthetic wastewater, the SS all came from the soluble starch in the substrate, Thus the SS measured here were purely organic, decomposable suspended particles. In the first two phases, Though the influent SS was high, the SS can be removed and showed visible SS removal from the effluent

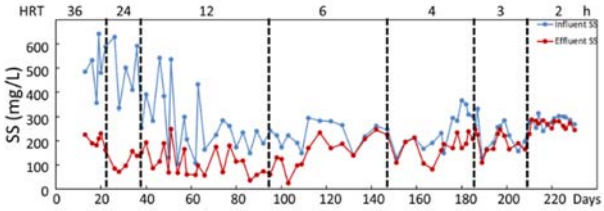

Figure 2 SS removal results of the AnSCMR

wastewater.

But combined the results of gas production, the first two phases showed no gas production, so the removal of SS could be the interception of SCMR. But the later results showed no extra gas production. Thus the results for these two phases are unknown.

The results of phase three to seven (HRT=12h to 2h) was stable and reliable compared with the first and second phases. The influent SS was stable at 200-300mg/L, and the SS of effluent increased from 50mg/L in third phase (HRT=12h) to 300mg/L (HRT=2h). The SS removal ability of SCMR deceased with the shorten of HRT, and when the HRT raised to 2h, the SS in the influent was basically not decomposed and was released through the effluent

4. Conclusions

(1) The AnSCMR had a lower removal efficiency but a higher sludge loading due to its carrier and structure compared with the traditional anaerobic process.

(2) The undegraded SS will not be intercepted inside the SCMR, which could prevent certain negative effects in the reactor, such as sludge expansion or SS sendimentation.

(3) The AnSCMR might be useful in treating certain type of wastewater with SS content, it can removal the S-COD in the wastewater without effect the SS in water.

Active microbail population diversity analysis in anaerobic digester by using PMA-PCR

○Jialing Ni[1], Kengo Kubota[1], Shingo Hatori[1], Yu-You Li[1]
[1]Department of Civil and Environmental Engineering, Graduate School of Engineering, Tohoku University, Sendai, Miyagi 980-8579, Japan.
E-mail: jialing@dc.tohoku.ac.jp

Abstract

12 digester sludge samples were treated with PMA to study actually active microbial community in 5 sludge fed digesters. The microbial community analysis results showed that the obvious decrease of methane-producing bacteria, and the phylum *Proteobacteria* in each digester reduced by 30.6% to 48.2% on average after PMA treatment. Digester sludge samples treated with PMA showed a farther distance than the original ones from primary sedimentation sludge and excess sludge. This study achievably detected the actually active populations in digestion process of environmental samples.

Keywords: Propidium monoazide, 16S rRNA gene sequencing, digester sludge, compromised membrane

1. Introduction

Anaerobic digester wildly used in the world nowadays makes it possible to achieve pollutant removal combined with energy generation and sludge reducing. Next generation sequencing is a very available method that can not only detect the microorganisms connecting anaerobic digestion, but also reveal matter decomposing under anaerobic condition, through microbial community structure analysis. The analysis of 16S rRNA gene extracted from samples without special treatment could not represent the active microbial populations in the certain moment. For instance, in the situation that some microbial populations without activity are remained after aerobic treatment in excess sludge entering into a digester will hardly be proved whether they did make contribution to the digestion process or not.

One method to analyze the DNA from viable cells with intact membrane is a PMA-PCR method. PMA has the characteristic that it cannot get into microbial cells with intact cell membrane (assumed to be live cells). It only penetrates into cells with compromised membrane (assumed to be dead cells) and binds to DNA in the cells. Upon the exposure to bright light, PMA covalently crosslinks DNA, by which dissociation of DNA is prevented even during the thermal treatment during PCR. The cross-linked DNA is not amplified by PCR, so it is not reflected in the community structure analysis result. Our research is to investigate microbial community structure in anaerobic sludge digesters further exploring the actually active microbial community by using PMA-PCR method.

2. Materials and Methods

2.1 Sample collection and PMA treatment

The samples were collected from five different sewage works in Japan (AKT, NGT, NIT, SEN and TNN sewage works). Of all the 46 samples used for this study, 24 were collected from mesophilic sludge digesters, called digester sludge (DS); 12 were collected from primary sedimentation tank, named primary sludge (PS); and the remaining 12 were excess sludge (ES). Table1 shows the detailed information of all the samples including the sampling date and ID for each sample.

PMAxx (Biotium) was added to the DS samples. After incubation in dark, light exposure was performed.

2.2 16S rRNA sequencing and analysis

After DNA extraction, PCR was conducted with the primer set of 341F-806R-mix targeting the V3 -V4 region of the 16S rRNA gene. Sequencing was performed using an Illumina MiSeq platform. Analysis of sequence data was done using the QIIME software with the Greengenes database. Operational taxonomic unit (OTU) was made with the 97% sequence identity.

3. Results and Discussion

At first DS samples were stained with PMAxx and SYTO 9 to ascertain the abundance of dead and viable cells in the samples. Three samples from the SEN treatment plant and two samples from the AKT treatment plant were observed, and we found that approximately 30-50% of cells were stained with PMAxx (recognized as dead cells).

The read numbers obtained after the amplicon sequencing were more than 80,000 for each sample, which was considered to be sufficient for understanding microbial community structures of the DS samples. OTUs with a single sequence read were removed in order to reduce the possibility of sequencing errors. Figure 1 shows the relative abundance of microorganisms in each sample at the phylum and/or class levels. The phyla with the population less than 1.0% are summarized in “Other”.

Microorganisms belonging to the phylum *Proteobacteria* preferentially existed in the ES and PS samples, and the relative abundance of the member was 36-55%. In the DS samples, *Proteobacteria*, *Bacteroidetes*, *Firmicutes* and *Chloroflexi* were dominant members as reported by other researchers. After the PMA treatment, the relative abundance of the phylum *Proteobacteria* reduced by 48.2%, 30.6%, 40.5%, 40.5% and 45.7% on average in AKT, NGT, NIT, SEN and TNN treatment plants, respectively. The class *Betaproteobacteria* existed several percent before the PMA treatment, but it remarkably decreased to less than 1% after the PMA treatment. Many populations whose low

relative abundance were just a few percent also show the same trend in excess sludge. Rivière and colleagues reported that OTUs belonging to the class *Betaproteobacteria* in anaerobic sludge digesters are one of the core groups; nevertheless, our results suggest that the members of the class *Betaproteobacteria* may not be so. In contrast, there were microbial communities that increased their abundance after the PMA treatment, such as the phylum *Bacteroidetes* and candidate phylum WWE1.

The similarity and differences of each microbial community structure are analyzed by principal coordinates analysis (PCoA) (Figure 2). The DS samples treated with PMA showed a structure farther away from the PS and ES samples than the DS samples without treatment.

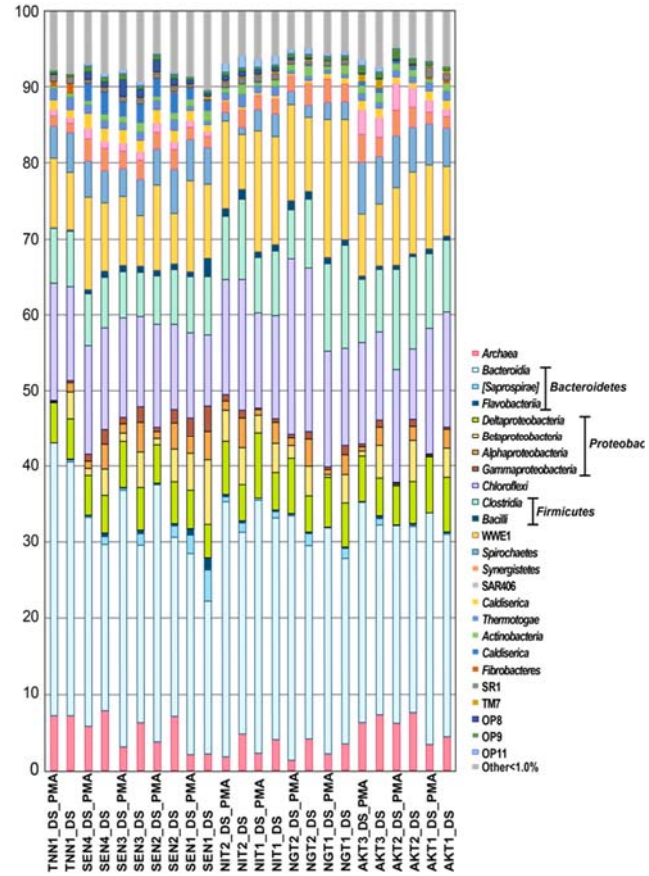

Fig.1 The relative abundance of microorganisms in each sample at the phylum level and class level

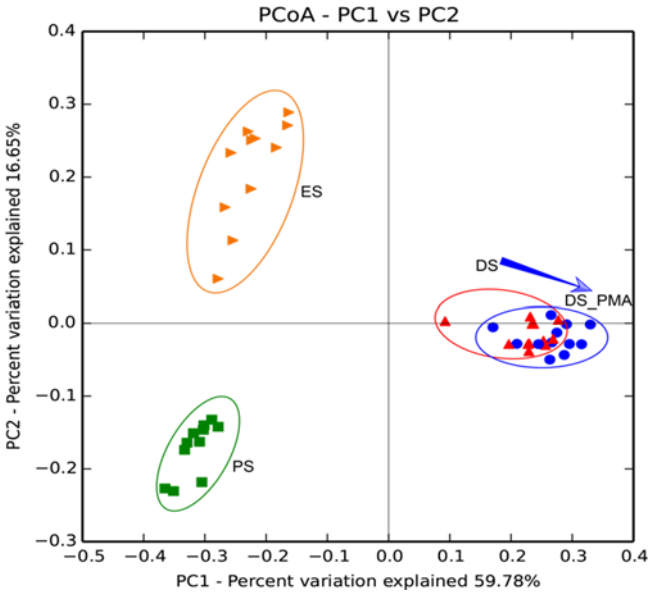

Fig.1 PCoA of sludge samples based on 16S rRNA sequencing

4. Conclusions

Rivière and colleagues reported that OTUs belonging to the *Betaproteobacteria* in anaerobic sludge digesters is one of the core groups, but this study suggests that the members of *Betaproteobacteria* may not be.

The microbial cells assumed to be dead (most likely derived from ES and PS) in the DS samples can be excluded by PMA-PCR, and live microorganisms actively playing functional roles in the anaerobic digestion were detected in this study.

5. Acknowldegments

The authors would like to thank Inter-Graduate School Doctoral Degree Program on Science for Global Safety for the funding support.

Table 1 Samples' information

AKT			NGT		NIT		SEN				TNN
170627	170119	161108	170606	170131	170606	170131	170630	170120		161112	170209
AKT1_DS	AKT2_DS	AKT3_DS	NGT1_DS	NGT2_DS	NIT1_DS	NIT2_DS	SEN1_DS	SEN2_DS	SEN3_DS	SEN4_DS	TNN1_DS
AKT1_DS _PMA	AKT2_DS _PMA	AKT3_DS _PMA	NGT1_DS _PMA	NGT2_DS _PMA	NIT1_DS _PMA	NIT2_DS _PMA	SEN1_DS _PMA	SEN2_DS _PMA	SEN3_DS _PMA	SEN4_DS _PMA	TNN1_DS _PMA
AKT1_ES	AKT2_ES	AKT3_ES	NGT1_ES	NGT2_ES	NIT1_ES	NIT2_ES	SEN1_ES	SEN2_ES	-	SEN4_ES	TNN1_ES
AKT1_PS	AKT2_PS	AKT3_PS	NGT1_PS	NGT2_PS	NIT1_PS	NIT2_PS	SEN1_PS	SEN2_PS	-	SEN4_PS	TNN1_PS

The Treatment of Synthetic Palm Oil Mill Effluent (POME) by Anaerobic Membrane Bioreactor (AnMBR)

○Siti Nur Fatihah MOIDEEN[1]*& Yu-You LI[1,2]
[1]Graduate School of Environmental Studies, Tohoku University, 6-6-06 Aza-Aoba, Aramaki, Aoba-ku, Sendai, Miyagi 980-8579 Japan.
[2]Department of Civil and Environmental Engineering, Graduate School of Engineering, Tohoku University, 6-6-06 Aza-Aoba, Aramaki, Aoba-ku, Sendai, Miyagi 980-8579, Japan.
*E-mail: siti.nur.fatihah.binti.moideen.t3@dc.tohoku.ac.jp

Abstract
Anaerobic membrane bioreactor (AnMBR) is a promising method for palm oil mill effluent (POME) treatment by involving the combination of biological treatment with the aids of activated sludge coupling with the direct solid-liquid separation by membrane filtration. AnMBR is a treatment where two objectives which are energy recovery and better quality effluent for re0use purposes can be achieved simultaneously. POME is a wste generated from palm oil mill industry and having very high content or organic matter which could damage the water body when it been released directly. In addition, POME containing 65% of methane which is 25% more potent than carbon dioxide (CO_2). Thus, anaerobic digestion, is more effective degradation methods in terms of cost and conversion product. Even though there are many approaches of POME treatment anaerobically previously, but, AnMBR may be the best solution since the membrane system helps to retain the bacterial flocs and nearly all suspended solids in the bioreactor. This has contributed to the significantly higher quality water effluent for re-use purposes compared to the conventional anaerobic treatment.

Keywords: Anaerobic membrane bioreactor (AnMBR), palm oil mill effluent (POME), anaerobic digestion, membrane bioreactor, ozonation

1. Introduction

Palm oil is one of the major 17 oils and fats produced globally and the demands on palm oil increasing year by year. China is the largest consumer of oils and followed by the EU, India and the United States. Correlates with this number, it is important to determine the main producer of palm oil worldwide. Indonesia and Malaysia are the main producer of palm oil in the world. These countries produce about 85% of the world's palm oil. Other producer countries contribute to the palm oil production are Thailand, Columbia, and Nigeria. In 2016, Indonesia produces palm oil at the highest percentages with 61% and Malaysia placed in second place with 34% of palm oil production. Indonesia and Malaysia become the main producer of palm oil due to its tropical climate which is marked by all-year-round temperature ranging from 25 to 33^{0}C and having even distribution of rainfall of 2000mm per year (Basiron, 2007).

Malaysia has over 4 million hectares' land covered with oil palm plantation and having impressive export and the production figures increases each year. However, it Is not astonishing that it turned out to be the main source of water pollution. There are around 60 million tons of POME were generated from 426 palm oil processing mill in Malaysia (Liew *et al.*, 2014).

In the palm oil mill industry each tons of fresh fruit bunch (FFB) processed, large quantities of POME are discharged. The process of 1000kg of FFB, about 1.5 cubic meter of water sources are extracted for the operation of boilers and hydroclones separator. During milling process, about 50% of water sources (0.75 cubic meter) eventually became POME while the rest became used water.

Fresh POME is hot, acidic thick and viscous brownish or grey slurry and contains very high organic matter consisting of water, oil and fine suspended components. POME having rich in organic carbon and possessed biochemical oxygen demand (BOD) more than 20 g/L and nitrogen content around 0.2 g/L as ammonia nitrogen and 0.5 g/L totalnitrogen ((Vijayaraghavan, Ahmad and Ezani Bin Abdul Aziz, 2007). The characteristic of POME fluctuating depending on several factors such as, POME collected from different batches or days from different discharge limit, climate as well as the condition of the palm oil processing are thinkable reasons for the dissimilarity. IN addition, different cropping season of palm oil and mill activities may be as the additional factors to the quantity and quality of the POME generated by the mills.

The physico-chemical properties of POME showed that if POME being discharged untreated into the environment will cause pollution, thus, the adverse environmental impacts associated with POME could be prevented through treatment while tapping useful energy resources such as biogas. POME can be treated by aerobic or anaerobic method. Aerobic digestion method of POME involves the use of oxygen during treatment process. Aerobic method has high microbial growth rate, thus lower retention time during biogas production. On the contrary, anaerobic method is a treatment that devoid the utilization oxygen in the process pathway. Anaerobic method having slow microbial growth, hence having far high retention time.

Due to more effective degradation methods in terms of cost and conversion product, anaerobic digestion seems to have better end-product for POME degradation. There are many approaches of POME treatment anaerobically in previous study such as, fluidized bed reactor (FBR), up-flow anaerobic sludge blanket (UASB) reactor, continuous stirred tank reactor (CSTR) and membrane anaerobic system (MAS).

The special features in this study is the treatment of POME using AnMBR. Despite of many research in anaerobic digestion treatment combined with membrane bioreactor, still, the study on POME treatment using AnMBR is limited and not been discussed widely. AnMBR is a great potential application to achieve the two objectives in wastewater treatment technology; energy recovery and better quality effluent for re-use purposes.

2. Materials and Methods

2.1 Synthetic Palm Oil Mill Effluent (POME)

The synthetic POME will be prepared based on the POME characteristics collected from the previous research study as a baseline.

2.2 Reactor set-up

Figure 1 show the AnMBR reactor which will be set up in the laboratory. Hollow fiber membrane with the area of 0.1m^2 will be used in throughout the study. The material of the membrane is polytetrafluoroethylene (PTFE).

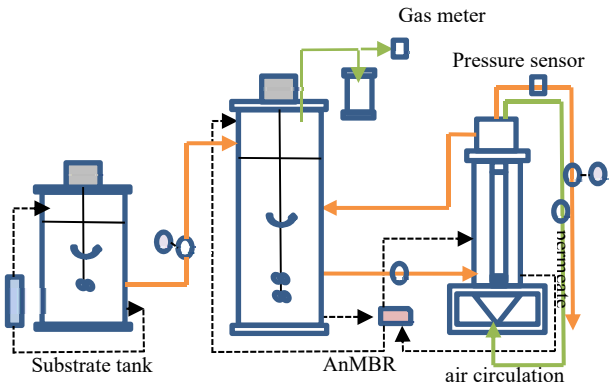

Figure 1: AnMBR reactor

2.4 Analytic Method

The composition of biogas including CH_4, CO_2, and N_2 will be measure using gas chromatography (Shimadzu, GC, 8A, Japan).

Total solid (TS), volatile solid (VS), suspended solid (SS), chemical oxygen demand (COD), carbohydrate, protein and NH_4^+-N concentration is measured by following Japan Standard Testing Method for Wastewater. For volatile fatty acid (VFAs) will be measured using gas chromatograph (Agilent- 6890) and extracellular polymeric substance (EPS) is measured using cation exchange resin method.

3. Expected Results

It is expected that through this study the degradation of POME by AnMBR could increase the production rate of biogas and having high removal efficiency of COD, carbohydrate and protein in POME.

Furthermore, the quality of water effluent aim for re-use purpose also will be significantly higher.

Based on the previous AnMBR studies on food waste, the degradation of food waste by AnMBR having removal efficiency of COD, carbohydrate and protein of 99%,99% and 98% respectively (Cheng, 2017). The removal efficiencies of COD, carbohydrate and protein were based on the organic loading rate (OLR) which also affect the production rate of biogas.

4. Conclusions

(1) The production rate of biogas depends on the OLR.

(2) AnMBR system could significantly improve the degradation of POME.

(3) High quality effluent with less sludge production will be the remarkable results in this study.

Carbonation and Utilization of Basic Oxygen Furnace Slag Coupled with Concentrated Water from Electrodeionization

Yemei LI[1, 2, 3, *], Silu PEI[4], Shu-Yuan PAN[4], Pen-Chi CHIANG[4, 5], Changyi LU[2, 3], Tong OUYANG[2]

[1] Department of Civil and Environmental Engineering, Tohoku University, Sendai 980-8579, Japan
[2]College of the Environment & Ecology, Xiamen University, Xiamen 361102, China.
[3]School of Environmental Science and Engineering, Xiamen University Tan Kah Kee College, Zhangzhou 363105, China.
[4]Carbon Cycle Research Center, National Taiwan University, Taipei City, 10672 Taiwan.
[5]Graduate Institute of Environmental Engineering, National Taiwan University, Taipei City, 10673 Taiwan.
*E-mail: lylym0821@126.com

Abstract

The integrated process of basic oxygen furnace slag (BOFS) recycling coupled with concentrated water from electrodeionization (CW-EDI) was introduced into the direct carbonation process and investigated in this study. The effects of different operating parameters on carbonation conversions of BOFS were studied. The reaction kinetics were determined via surface coverage model, which indicated that the maximum achievable carbonation conversion of BOFS was approximately 60.9% with R^2 of 0.95 to 0.99. Furthermore, we evaluated the performance of BOFS applied as supplementary cementitious materials (SCMs). The properties of the cement that used BOFS as SCMs met ASTM requirements. The suggested substitution ratios for fresh and carbonated BOFS in cement mortars were 15% and 10%, respectively. Lastly, a cost and benefits analysis of the carbonation and cement replacement were conducted. The results revealed the feasibility of the integrated industrial waste treatment and the superiority of the process in CO_2 emission reduction, cost saving and profit gaining.

Keywords: Direct carbonation, basic oxygen furnace slag, concentrated water from electrodeionization, supplementary cementitious materials.

1 Introduction

Mineral carbonation, also called natural weathering, is a CO_2 storage option in which CO_2 is fixed and stored in the form of inorganic carbonates that will not be released back into the atmosphere over a long time. Considering the slow reaction efficiency of weathering, an enhanced version, accelerated carbonation, was proposed.

Naturally occuring silicate rocks and industial solid wastes are suitable for industrial CO_2 fixation due to the existence of alkaline and alkaline earth oxides. Acclerated carbonation can be conducted through direct and indirect approaches. The efficiency of aqueous carbonation at moderate conditions is relatively higher than that of dry carbonation. The performance of the carbonation reaction can be influenced by not only the physicochemical properties of solids but also the reaction conditions and type of reactors. A rotating packed bed reactor applied during the carbonation process also known as HiGCarb produces carbonation results with a shorter reaction time than traditional reactors.

Stable carbonated products can be reused as construction materials such as supplementary cementitious materials (SCMs). Using SCMs can not merely lower cost and environmental impact, especially by decreasing CO_2 emission in cement production, but also improve long-term strength and durability. Besides, using SCMs is also a pathway to utilizing the by-products generated by industrial manufacturing processes.

Basic oxygen furnace slag (BOFS) is a by-product from the steelmaking and refining processes. The free-CaO contained in BOFS will result in volume expansions and structural damages if BOFS is reused as construction materials. On the contrary, the high CaO content is welcome in the carbonation process. Concentrated water from electrodeionization (CW-EDI), which has high levels of Na^+ and Ca^{2+} and whose treatment approaches are rarely discussed, is the effluent generated during the electrodeionization process. Further utilization of products generated from the carboation of CW-EDI may be directly restricted because of its impurity. Howerver, mixing CW-EDI with BOFS before carbonation can improve BOFS properties, utilize CW-EDI and carbon capture simultaneously, and ultimately implement product recycling, which is a strategy of waste control by waste.

Therefore, this study aims to investigate the utilization of CW-EDI in direct carbonation and the feasibility of a comprehensive process for the treatments of industrial sewage, solid wastes, and waste CO_2.

2 Materials and Methods

2.1 Materials

The BOFS provided by China Steel Corporation (Kaohsiung, Taiwan) was ground and dried at 105°C overnight to eliminate moisture. The CW-EDI was used as the liquid phase in the HiGCarb experiments. The synthetic water was prepared using $CaCl_2$ and NaCl (supplied by J. T. Baker) on the basis of the real CW-EDI. High-pressure CO_2

gas with a volumetric concentration of 99.5% supplied by Ching-Feng Gas Corporation (Taipei, Taiwan) was used in carbonation process. Ordinary Portland cement (OPC) and standard sand were supplied by Gao Ching Corporation (Taipei, Taiwan).

2.2 HiGCarb of BOFS Coupled with CW-EDI

The influence of different operating parameters, such as reaction time, reactor rotation speed, slurry flow rate, and L/S ratio, on the carbonation conversion of BOFS coupled with CW-EDI was evaluated. The rotating packed bed reactor used in this study was made of stainless steel with a packing zone filled with stainless steel wire. The BOFS and CW-EDI slurry was pumped into the reactor after adequate mixing in the beaker. Injecting CO_2 into the reactor set off the carbonation process. The reactor rotated and the slurry circulated in the reactor-beaker system with continuous stirring in the beaker during the experiment. After the solid-liquid separation, the solid and liquid samples were analyzed using TGA and ICP-OES, respectively.

2.3 Utilization of BOFS as SCMs in the Cement Mortars

Fresh and carbonated BOFS were used to partially replace OPC at substitution ratios of 0%, 5%, 10% and 15% by weight. Autoclave expansion ratio and compressive strength after curing ages of 3, 7, 28, and 56 days were regarded as the primary indicators with which to evaluate the performance of the BOFS used as SCMs. The autoclave expansion and compressive strength tests were implemented in accordance with ASTM C151 and C109, respectively.

3 Results and Discussion

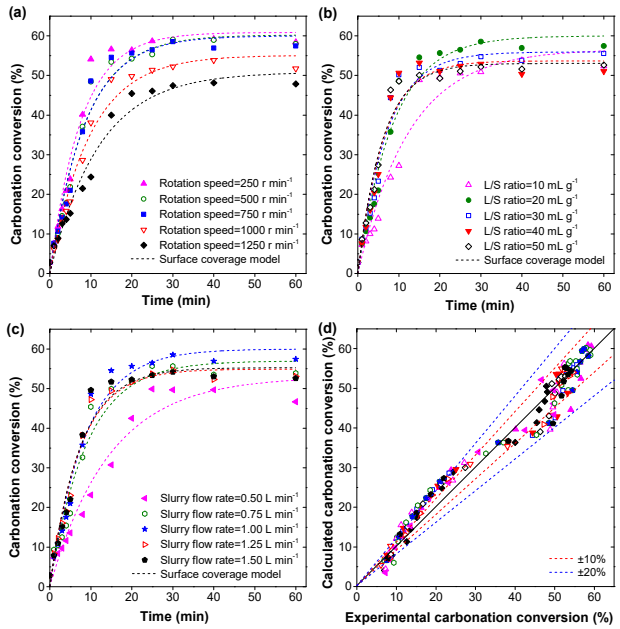

Figure 1. Effect of (a) rotation speed, (b) liquid-to-solid (L/S) ratio, and (c) slurry flow rate on carbonation conversion of BOFS coupled with CW-EDI and (d) comparison of calculated carbonation conversion (surface coverage model) with experimental data.

Figure 1(a), 1(b) and 1(c) show the influence of reaction time on the carbonation conversion of the BOFS under different operating conditions. The surface coverage model was used to describe the reaction kinetics. Figure 1(d) presents the comparison of the calculated carbonation conversion based on the surface coverage model with the experimental data shown in Fig. 1(a), 1(b) and 1(c). The calculated conversions were higher than the experimental ones early on due to the liquid phase used in this study. The abundant Ca^{2+} in the liquid phase caused the generation of solitary $CaCO_3$ thus decreasing the actual conversion of the BOFS. However, the theoretical values, which agreed with the experimental data in the last phase of the experiments, suggested the suitability of the surface coverage model for the HiGCarb of the BOFS in CW-EDI with R^2 of 0.95 to 0.99.

As shown in Fig. 1, different operating conditions had different effects on the reaction. On the premise of sufficient feedstock, Ca^{2+} and CO_3^{2-}, good maximum carbonation conversion could be approached when the rate of carbonation reaction was faster than that of surface coverage. With the syntheizing effects of rotation speed, L/S ratio, and slurry flow rate, δ_{max} could reach 60.9% with an L/S ratio of 20 mL g^{-1}, rotation speed of 250 r min^{-1}, slurry flow rate of 1.00 L min^{-1} and reaction time of 60 min at room temperature.

The autoclave expansion results indicated that adding fresh and carbonated BOFS effectively reduced the expansion of OPC. The cement replaced by 15% of the carbonated BOFS had the capability to restrain expansion. The stable expansion of the cement substituted by the carbonated BOFS with different ratios showed the stabilization of the BOFS after carbonation.

The compressive strength of all the cement mortars continuously increased with curing age. Mortars substituted by 10% of the carbonated BOFS and 10% or 15% of the fresh BOFS achieved better compressive capacity than pure OPC did. This suggests that the substitution ratios for the fresh and carbonated BOFS as SCMs should be 15% and 10%, respectively, to ensure the engineering performance as well as economic and environmental benefits.

A cost and benefit analysis of carbonation of BOFS and displacement of cement by carbonated BOFS in China situation was conducted. Based on the experimental results in this study, when the carbonated BOFS was used in cement replacement, without considering the cost of transportation, compared with the traditional treatment of BOFS, the HiGCarb process with subsequent reutilization at least reduced 124.3 million tonnes of CO_2 emission, saved 7728.7 million USD of cost, and gained 1006.8 million USD from carbon credit.

4 Conclusions

(1) The maximum achievable carbonation conversion of the BOFS with CW-EDI was approximately 60.9%.

(2) The surface coverage model described the carbonation kinetics sufficiently.

(3) The suggested substitution ratios for the fresh and carbonated BOFS in cement mortars were 15% and 10%, respectively.

5 Acknowledgements

The authors would like to thank the Ministry of Science and Technology (MOST) of Taiwan under Grant Number MOST 106-2811-M-002-018 for the financial support.

Analysis of Material Flow and Energy Balance in Full-scale Biogas Plant

○Wataru RUIKE[1]*, Kazuki TONOUCHI[1], Toshimasa HOJO[1] & Yu-You LI[1]
[1]Department of Civil Engineering, Tohoku University, 6-6-06 Aoba Aramaki Aoba-ku Sendai city, Miyagi Prefecture, Japan.
*E-mail: wataru.ruike.q8@dc.tohoku.ac.jp

Abstract
In order to evaluate the waste reduction effect, recycling and energy productivity in Full-scale biogas plant that processes food waste, the material flow and energy balance within the plant were analyzed. As a result, the reduction ratio of solids was as high as 81.3%, 77.9% of organic matter and 95.0% of carbon were used for biogas and 88.5% of nitrogen was effectively used for compost. Biogas production amount was as large as 70,100 m^3 / month, equivalent to 4.03 billion kcal in calorific value. The power self-sufficiency ratio in the plant was 94.8%, the power generation efficiency of the cogeneration facility was 30.2%, the total efficiency including the exhaust heat utilization efficiency was 66.3%, and it was found that there is available heat quantity of about 3.7 to 13.7%.

Keywords: Food waste, Full-scale biogas plant, material flow, energy balance

1. Introduction
The annual amount of food waste produced in Japan is about 19 million tons, but recycling has not progressed much. Methane fermentation targeting food waste has attracted attention due to the Food Recycling Law and the FIT (Feed-in Tariff) Law, and energy use of the produced biogas is expected. In food recycling law, a business operator that generates 100 tons or more of food waste per year should report the amount of generated food waste and action of recycling of food circulation resources to government. If these efforts by business operators are inadequate, government recommendations and orders are made, in the worst case penalties are imposed on business operators. Food Recycling Law promotes the reduction and recycling of food waste. And FIT law is a system that determines the purchase price of energy (mainly renewable energy) by law. Unit price of electricity generation by methane fermentation is 42 yen per 1 kW, which is significantly more expensive than other renewable energy such as solar power, wind power, hydro power, geothermal. Therefore, Methane fermentation of food waste has attracted attention in Japan.

Methane fermentation is a system that decomposes organic wastes such as a raw garbage, livestock manure, sewage sludge by the metabolic action of microorganisms, at the same time collects the generated biogas, and uses it for energy. Residues after fermentation can be used for agriculture as compost. Current research trends on methane fermentation of food waste are fundamental study and improvement of efficiency. There are very few papers on the operation status, material balance, and energy balance of Full-scale biogas plant in operation.

By clarifying the material flow and energy balance within the biogas plant actually in operation, it becomes possible to clarify process problems and improvement points, and to lead optimization of the entire plant. Proper dissemination of biogas plant promotes circulation of resources in the region and leads to revitalization of regional economy as regional energy project. However, with regard to biogas plants, there are few cases where such surveys and analyzes are conducted. Therefore, in this research, we conducted a research of Full-scale biogas plant in S city, clarified the specific material flow and the energy balance of the whole biogas plant and evaluate the waste reduction effect, recycling and energy productivity in Full-scale biogas plant.

2. Outline of investigation

2.1 Target biogas plant
The target biogas plant treatments 16 tons of food waste collected as industrial waste per day when we were conducting the investigation. This 16 tons of food waste is diluted to 40 tons in material input unit. Since there are four fermenters, the input amount after dilution into one fermenter was 10 tons. The maximum input amount is 160 tons / day. Methane fermentation unit has four fermentation tanks, one fermentation tank is 1,200m^3. The inside of the plant was divided into 6 processes (units) shown in Fig. 1, samples were taken from each process and analyzed.

2.2 Analysis items and methods
Analysis was carried out on six items of solid matter (TS), organic matter (COD_{Cr}), carbon (TOC), nitrogen (T-N), phosphorus (T-P), and potassium (K), and each flow was organized. TS was measured based on sewage test method (Ver. 2012, JAPAN SEWAGE WORKS ASSOCIATION). COD_{Cr} was measured based on Standard Methods 5520D: Closed Reflux, Colorimetric Method. TOC and T-N were measured by TOC-L, TNM-L (SHIMADZU). T-P and K were measured by ICP-MS (Agilent 700).

3. Results and Discussion
Fig. 1 ~ 5 show the material flow of each substance. In Fig. 1 ~ 5, the upper number is the amount per month, the lower number is the ratio when the raw material is taken as 100%. As a result of waste mass (Fig. 1), dilution water almost equal to the raw material is mixed. Therefore, the amount of treated water was increasing. From this result, it was found that reduction of dilution water is necessary in order to

reduce environmental impact. Fig. 2 shows material flow of total solids (TS). The notation of the part of the water treatment unit means the possibility of sampling when the water treatment did not succeed, because the value on the outflow side of the water treatment unit is increasing. Total solids reduction ratio in the methane fermentation unit was 81.3%. Therefore, very high weight reduction effect of this biogas plant was revealed. Fig. 3 shows material flow of organic matter (COD_{Cr}). In Methane fermentation unit, 77.9 % of organic matter is decomposed and converted to biogas. Methane fermentation was in good condition, because organic matter is also high decomposition ratio. Fig. 4 shows material flow of carbon (TOC). 95.0% of carbon is converted to biogas. From the viewpoint of carbon resource recycling, most carbon is effectively used for biogas. Fig. 5 shows material flow of nitrogen (T-N). 88.5% nitrogen is used for compost. Regarding nitrogen, it is important to recycle resources as compost. As for material flow, it is necessary to accumulate analysis results in order to investigate seasonal fluctuation in future.

Table. 1 shows the energy balance in this biogas plant. Biogas production is about 70,000 m^3/month, calorie equivalent to 4.03 billion kcal. Currently 30.2% of calories are used for power generation and 36.1% are effectively used for heating fermentation tanks. Electricity self-sufficiency ratio was 94.8%. The total efficiency including the exhaust heat utilization efficiency was 66.3% (30.2%+36.1%). Generally, the total efficiency including the exhaust heat utilization efficiency of the cogeneration facility is 70 to 80%. Therefore, it was found that the heat quantity which can be used for this biogas plant but not yet effectively utilized is about 3.7 to 13.7%. From now on, it is necessary to consider efficient method of unused heat quantity to improve plant efficiency.

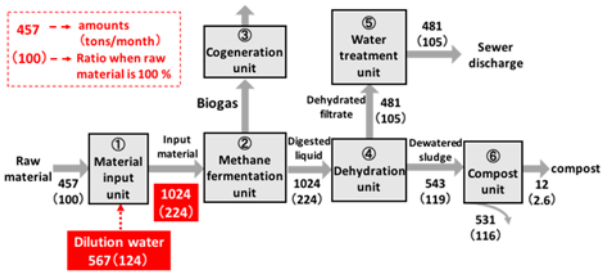

Fig.1 Material flow of waste mass

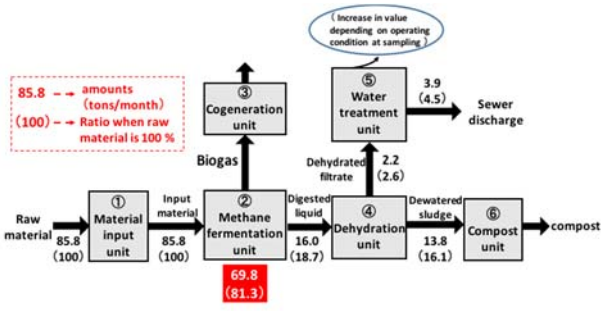

Fig.2 Material flow of total solids (TS)

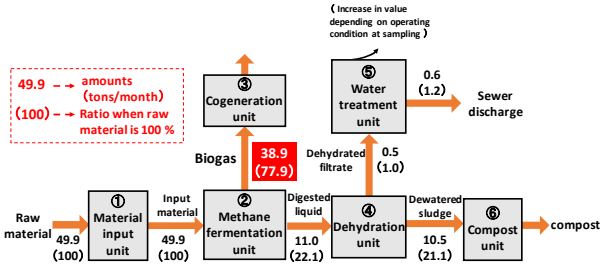

Fig.3 Material flow of organic matter (COD_{Cr})

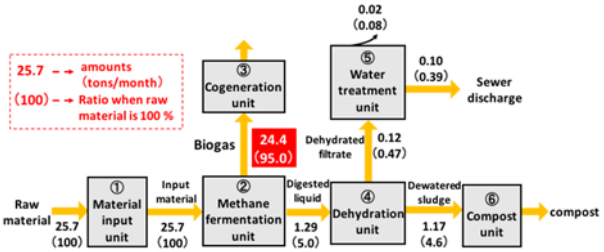

Fig.4 Material flow of carbon (TOC)

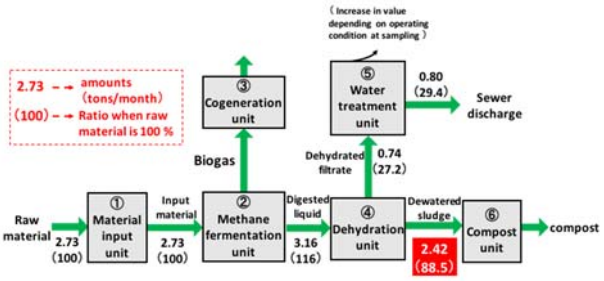

Fig.5 Material flow of nitrogen (T-N)

Table.1 Energy balance in biogas plant

Biogas production	70,100	m^3/month
Methane contents	60.5	%
Calorie conversion (①)	4.03	billion kcal
Generated electricity (②)	141,600	kWh
Power generation efficiency (conversion of calorie in ② / ①)	30.2	%
Power sale amount (③)	34,500	kWh
Percentage of power sale (③ / ②)	24.4	%
Purchased electricity	42100	kWh
Electricity consumption at plant (④)	149,300	kWh
Electricity self-sufficiency ratio of plant (② / ④)	94.8	%
Amount of heat required for warming the fermenter (⑤)	1.46	billion kcal
Heat utilization ratio (⑤ / ①)	36.1	%

4. Conclusions

As a result of analyzing the material flow and energy balance in the biogas plant, the solids reduction ratio and the organic matter biogas conversion ratio are high and the biogas production amount is as high as about 70,000 m^3/month. Furthermore, it was found that the heat quantity which can be used for this biogas plant but not yet effectively utilized is about 3.7 to 13.7%. In the future, as for material flow and energy balance, it is necessary to estimate seasonal fluctuation and consider efficient method of unused heat quantity to improve plant efficiency.

Slaughterhouse wastewater treatment plant: a case study

○Mribet Chaimaa[1]*, Jiang Wu[2], Hong Chen [3] Bo Jiang [2], Yu-You Li[1,2]

[1]Graduate School of Environmental Studies, Tohoku University, 6-6-06 Aoba, Sendai 980-8579, Japan

[2]Department of Civil and Environmental Engineering, Graduate School of Engineering, Tohoku University, 6-6-06 Aza-Aoba, Aramaki, Aoba-ku, Sendai, Miyagi 980-8579, Japan.

*E-mail: mribet.chaimaa.q7@dc.tohoku.ac.jp

Abstract

Meat and poultry industries use a huge amount of water. The wastewater coming out of these factories has a complex composition and is very harmful to the environment. It is strong compared to domestic wastewater. After the initial screening of coarse solids, slaughterhouse wastewater is mainly composed of diluted blood, fat and suspended solids. It may also contain some manure. In this study, a wastewater treatment and biogas production plant performance is being investigated. Both aerobic and anaerobic processes are used for the treatment.

Keywords: UASB, Activated sludge, Biogas, Slaughterhouse wastewater, removal efficiency

The influent of the wastewater treatment plant comes mainly from a meat factory (50%), poultry feathers (30%) and other sources with an average flow rate of 350 m^3/d. The current treatment process consists of a Dissolved Air floatation unit, followed by a UASB and an Activated Sludge unit.

The plant treatment process was updated during January 2017. The first scenario (before the year 2017) included a dissolved air flotation unit followed by an activated sludge unit. Starting 2017, the plant added the anaerobic treatment unit (UASB). The investigation involves the analysis and interpretation of the variations in the performance of the three main treatment units (DAF, UASB and Activated sludge), along with the treatment efficiency of the whole process. Monitoring involves temperature, pH, DO, ORP, biogas production, daily flow and pressure. COD, SS, VSS, MLSS, MLVSS, NH4+, NO2- and NO3- are analyzed in the laboratory in a weekly basis.

The plant's removal efficiency has got an average of 94%, where 84% of the removal occurs in the activated sludge system that removes most of the COD, while the UASB's average removal rate is 48%. The Dissolved air floatation system being the least efficient (24%), a new process is planned in the next scenario that consists of eliminating the Dissolved Air Floatation treatment unit and improving the UASB performance, along with the comparison of the energy costs between the three scenarios.

From a whole scale level, COD analysis results show an improvement in the removal efficiency to 97%, while due to different parameters variations (Temperature, oxygen levels, loading rate), the performance of UASB and activated sludge process faces some difficulties. In the UASB digester, the temperature decreased remarkably, leading to a decrease in the reduction of the organic matter and affecting the color and sludge density, as well as the biogas production rate. During the first 100 days, biogas wasn't generated from the UASB. After that abrupt variations in the daily volume of production are noticed. The COD removal rate of the UASB and biogas production graphs show a similar variation. From the biogas composition analysis, methane rate is around 80%.

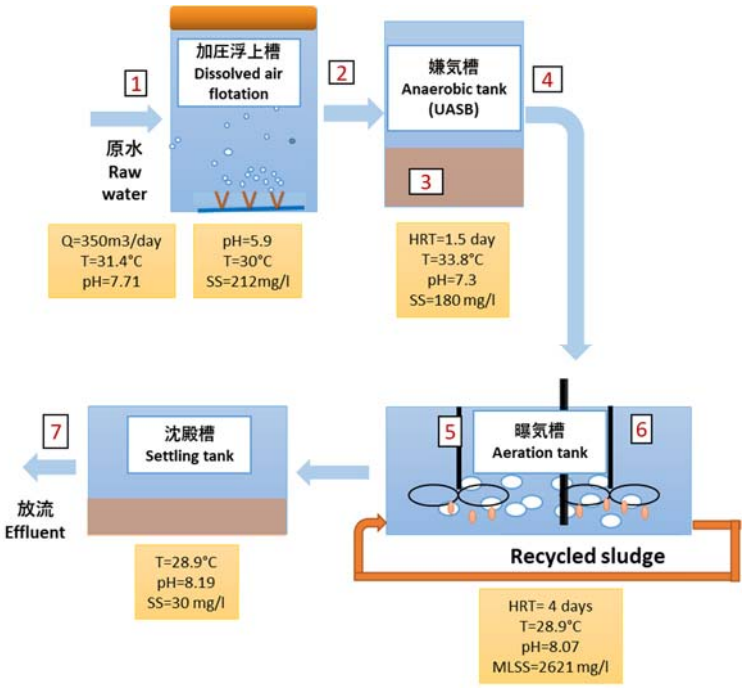

Figure 1: Wastewater plant treatment process characteristics and sampling points

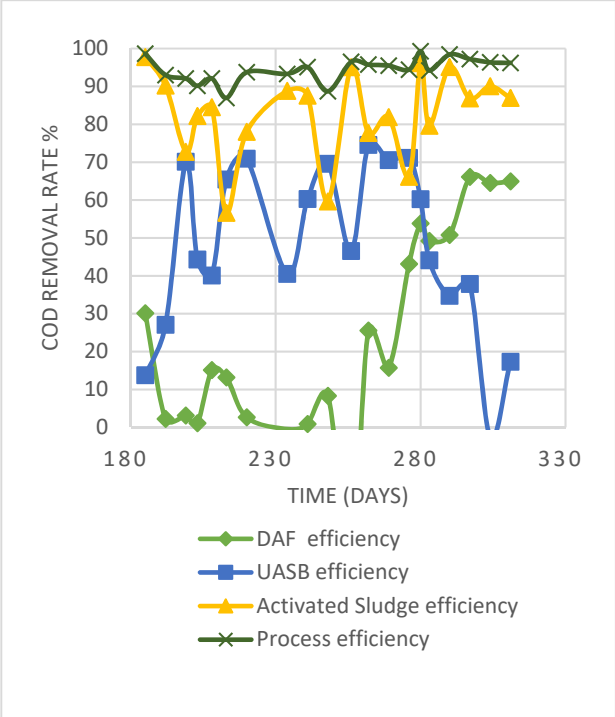

Figure 2: COD removal efficiency in different treatment units

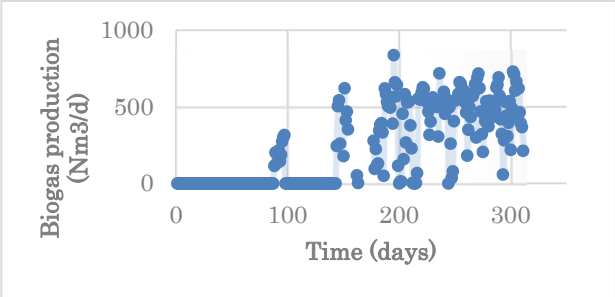

Figure 3: Biogas daily production

Meanwhile, in the activated sludge process the DO concentration variations affect both the COD removal efficiency and the nitrogen removal process. DO levels were as low as 0.1 mg/l, then reached an 8.1 value during the 277th day of the process Ammonia concentrations are quite stable and seem to sustain at high levels, while nitrates and nitrites are almost inexistent. Nitrification and denitrification reactions doesn't seem to occur, leading to an effluent with high ammonia concentrations.

MLSS levels are also increasing in both UASB and Activated Sludge units, but a recent dropping level in the UASB lead to a noticeable decrease in the efficiency. Optimal conditions are not yet obtained for the three units, which need to be determined and applied for a better optimization of the energy consumption, thus reducing the process cost.

Analyzing relationship between ocean index and rainfall in Northern part of Thailand

○Prem Rangsiwanichpong[1*], So Kazama[2]

[1]Graduate School of Environmental Studies, Tohoku University, Sendai 980-8579, Japan
[2]Graduate School of Engineering, Tohoku University, Sendai 980-8579, Japan

*E-mail: prem.rangsiwanichpong.q8@dc.tohoku.ac.jp

Abstract

Rainfall variability is an important factor on flood event in Thailand especially in the northern part of country. Thailand are prone to seasonal flooding due to tropical savanna climate. The floods often occur in the north and spread down the Chao Phraya River through the central plains. This research, aimed to analyze rainfall variability in the upstream of Chao Phraya River basin using the ocean indices. Which we use numerous ocean indices consisting of the NINO sea surface temperature indices (NINO1+2, NINO3, NINO4 and NINO3.4), the Southern Oscillation Index (SOI) and the Dipole Mode Index (DMI). The results show that rainfall variability in the northern part of Thailand was affected by climate variability in the Pacific Ocean more than in the Indian Ocean. Moreover, rainfall in the northern part of Thailand was strongly related with SOI index.

Keywords: Chao Phraya River, ENSO, Ocean index

1. Introduction

In recent years, great flood was occurred in Thailand with enormous damage to economic system of this country. Which rainfall variability in the northern part of country is a one of important factor to flood event in Thailand. Many research have investigated the effect of ocean index on rainfall variability (Geethalakshmi et al., 2009; Juan et al., 2013). Ocean index is a one of tools of analyze climate variability in the ocean such as the El Nino-Southern Oscillation phenomenon (ENSO) and the Indian Ocean Dipole (IOD). ENSO and IOD phenomenon are occurred from fluctuation of ocean temperature in the Pacific and Indian Ocean respectively. Thailand are prone to seasonal flooding due to tropical savanna climate. The rainfall has impacted by monsoon including ocean climate variability. Therefore, method for analyzing rainfall variability is a necessary to flood protection and water resource management. In Southeast Asia, several research analyze impact of ocean index on rainfall variability (Singhratana and Babel, 2011). In 2016, Gobin et al. analyzed the relationship between rainfall and ENSO phenomenon in Vietnam. They found that the ENSO phenomenon have a significant effect on rainfall patterns in Vietnam.
Furthermore, Rangsiwanichpong et al., (2016) used ocean index for assessing flood and drought in the Chao Phraya River Basin of Thailand. In this study, we use the Rescale Adjust Partial Sums method for analyzing relationship between rainfall and ocean index.

2. Study area

Northern part of Thailand is bound by the Salawin River in the west and the Mekong in the east. The basins of rivers Ping, Wang, Yom, and Nan, all tributaries of the Chao Phraya River, in the central part run from north to south and are mostly very wide. The basins cut across the mountains of two great ranges, the Thanon Range in the western part and the Phi Pan Nam in the eastern. Their elevations are generally moderate, a little above 2,000 metres (6,600 ft) for the highest summits.(Fig. 1.)

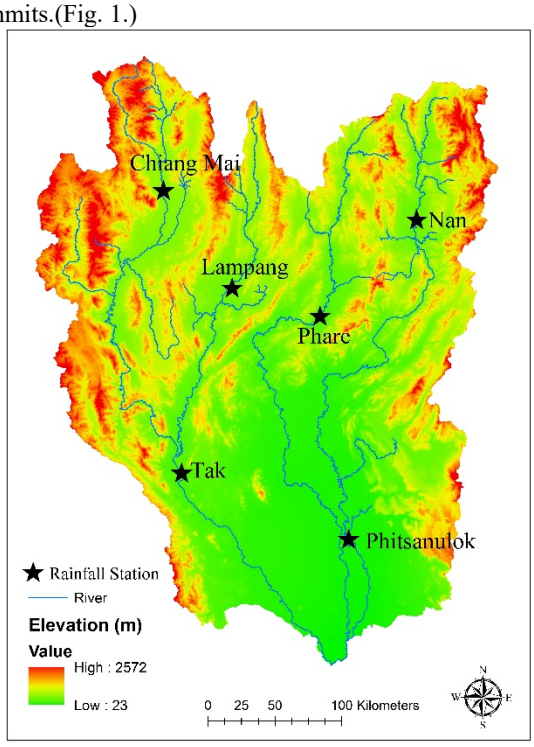

Fig. 1. Upstream of Chao Phraya River Basin and rainfall station

3. Data

Monthly rainfall data from 6 stations were collected by the Royal Irrigation Department of Thailand with continuous data 54years (1958 – 2011). These stations were located on the upstream of the Chao Phraya River Basin. We use

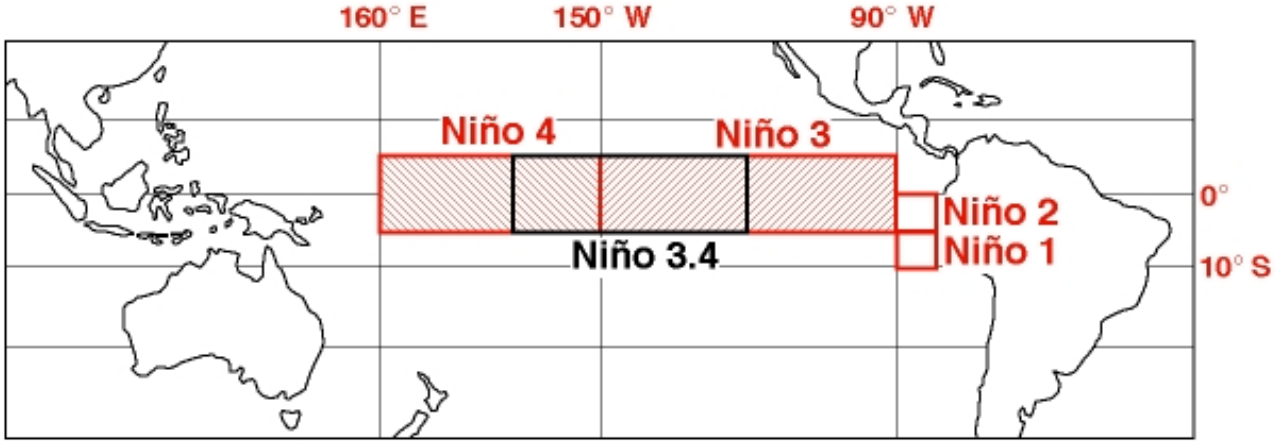

Fig. 2. Map of NINO index

numerous ocean indices consisting of the NINO sea surface temperature indices (NINO1+2, NINO3, NINO4 and NINO3.4), the Southern Oscillation Index (SOI) and the Dipole Mode Index (DMI). Which these indices were collected by the National Oceanic and Atmospheric Administration (NOAA). NINO index is an indicator of climate variability in the central of Pacific Ocean. Mostly, NINO index was used for predicted the ENSO phenomenon. The map of NINO index was show in Fig. 2. The SOI was used to indicate fluctuations in air pressure between eastern and western of Pacific Ocean (Fig. 3.). Furthermore, The DMI index was used for measured climate variability by difference temperature between eastern and western of the Indian Ocean. (Fig. 4.)

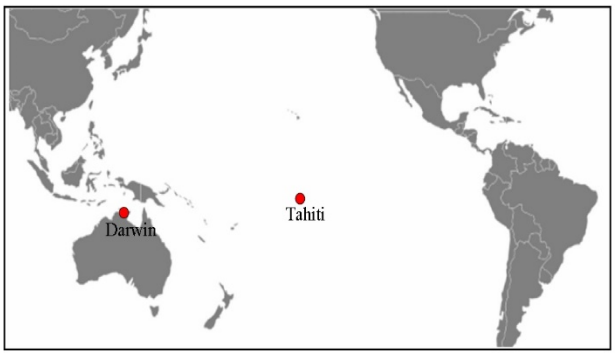

Fig. 3. Map of SOI index

Fig. 4. Map of DMI index

4. Methodology

To analyze the relationship between variability of rainfall and ocean indices, we used the Rescale Adjust Partial Sums method (RAPS) (Garbrecht and fernandex, 1994). The RAPS was used to visualize trend of series data with long term (Bonacci et al., 2008). This method is calculated by Equation as below:

$$RAPS_n = \sum_{n=1}^{i} \frac{A_i - A_{AVG}}{S_d}$$

where A_i represents the mean value of the measured parameter in the year i; A_{AVG} is the average mean value in the period of observation; S_d is the standard deviation of A_{AVG} and n = 1…i is the counter limit of the current summation.

5. Results and Discussion

The results shown that rainfall variability in the Chao Phraya River Basin had related with the ENSO phenomenon events. In 1988, rainfall in the Chao Phraya River Basin was occurred more than the average value corresponding with strong Lanina event. Furthermore, rainfall occurred less than the average value when the El nino period (Fig. 5). The Upper Chao Phraya River Basin has a mean annual rainfall approximately 1400 mm. The rainfall in the study area occurs during the monsoon season. From the results, relationship of ocean indices and rainfall in the Upper Chao Phraya River Basin during the wet season. We used the Rescaled Adjusted Partial Sums (RAPS) to investigate the relationship of ocean indices and average rainfall at six stations. Fig. 6A and Fig. 5b show the fluctuation between RAPS of the time series of ocean indices and rainfall in the Upper Chao Phraya River Basin. Rainfall in this study are had a strong correlation with SOI and NINO3. SOI had a strong positive relationship with average rainfall during the wet season (R =0.9, Fig. 6B). Other indices had negative correlations, especially the NINO3 index which had a strong negative relationship (R =-0.8, Fig. 6C).

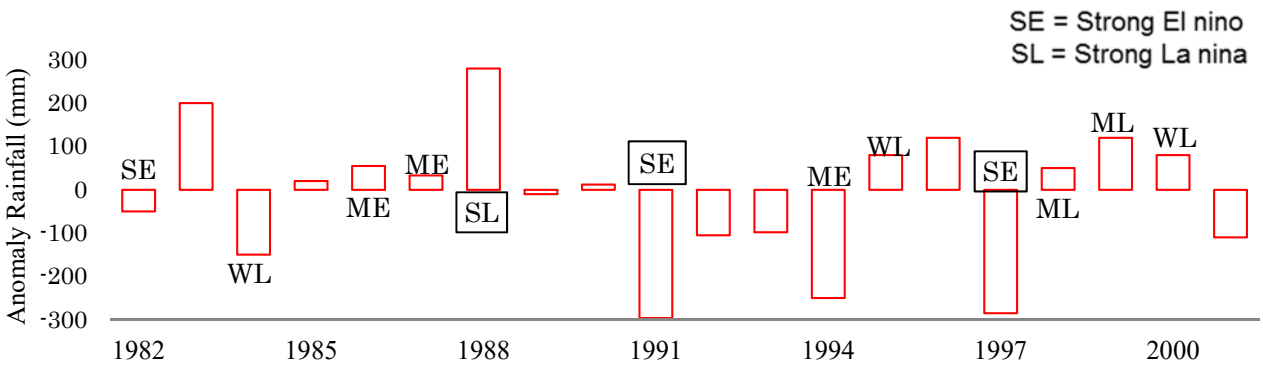

Fig. 5. ENSO and Variability of rainfall in the Chao Phraya River Basin

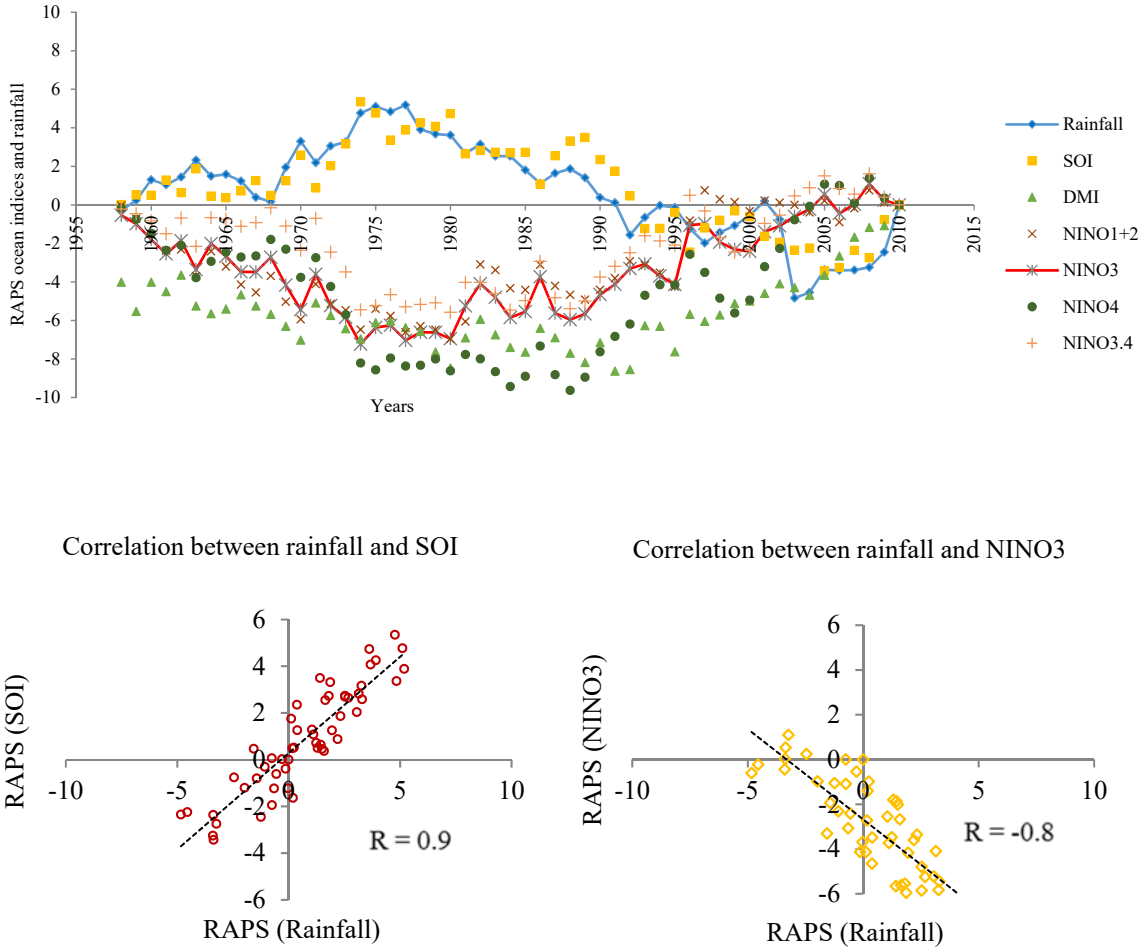

Fig. 6. Values of RAPS of ocean indices and rainfall in the Upper Chao Phraya River Basin (A), and the correlation between the RAPS of SOI and NINO3 with rainfall (B, C, respectively).

6. Conclusions

The rainfall in the Upper Chao Phraya River Basin is influenced by the ENSO phenomenon and this effect is related to the variability of ocean indices. The rainfall in the Upper Chao Phraya River Basin was most strongly related with the SOI index. Furthermore, we found that NINO3 index also had significantly relationship to rainfall in study area with negative direction. We successfully analyzed the relationship between ocean index and rainfall in the Upper of Chao Phraya River Basin using RAPS method. These results open new probabilities for understanding and estimating the rainfall in the Upper Chao Phraya River Basin for flood prediction and water resources management in the future.

Acknowledgements

The present research was supported through the Program for Leading Graduate Schools, Tohoku

University, "Inter-Graduate School Doctoral Degree Program on Global Safety," by the Ministry of Education, Culture, Sports, Science and Technology.

References

1) Bonacci O, Trninić D, Roje-Bonacci T : Analysis of the water temperature regime of the Danube and its tributaries in Croatia, Hydrol. Process, 22, pp. 1014–1021, 2008.
2) Garbrecht, J, Fernandez GP : Visualization of trends and fluctuations in climatic records, JAWRA Journal of American Water Resources Association, 30, pp.297-906, 1994.
3) Geethalakshmi V, Yatagai Akiyo, Palanisamy K, Umetsu Chieko : Impact of ENSO and the Indian Ocean Dipole on the north-east monsoon rainfall of Tamil Nadu State in India. Hydrol. Process., 23, pp. 633–647, 2009.
4) Gobin, A, Nguyen HT, Pham, VQ, Pham HTT : Heavy rainfall patterns in Vietnam and their relation with ENSO cycles, Int. J. Climatol, 36, pp. 1686–1699, 2016
5) Juan Bazo, María de las Nieves Lorenzo, Rosmeri Porfirio da Rocha : Relationship between Monthly Rainfall in NW Peru and Tropical Sea Surface Temperature, Advances in Meteorology, 2013, 9 pages, 2013.
6) Prem Rangsiwanichpong, So Kazama, Chaiwat Ekkawatpanit : Assessment of Flood and Drought Using Ocean Indices in the Chao Phraya River Basin, Thailand, Proceeding in The 7th International Conference on Water Resources and Environment Research; ICWRER2016, Kyoto University, Kyoto, 2016
7) Singhrattna N, Singh Babel M : Changes in summer monsoon rainfall in the Upper Chao Phraya River Basin, Thailand, Clim Res, 49, pp. 155-168, 2011.

Elucidate the relationship between coliforms estimation model and household consumption expenditure in Yangon city,Myanmar

○Miku Sakurai[1], Daisuke Komori[1]
[1]Graduate School of Environmental studies, Tohoku University, Sendai 980-8579, Japan

*E-mail: miku.sakurai.s3@dc.tohoku.ac.jp

Myanmar has now rapid economic growth since the military government changed to a democratic administration in 2011. Yangon City, a commercial city is planned for large-scale and rapid development However there are many concerns that Yangon City's low water supply and sewerage completion rate, the increased flood risk due to climate change and rapid urbanization and the burden on the catchment basin due to population increase will adversely affect residents' lives. Therefore, we incorporate the pollution degree of the coliform bacteria in Yangon City, which has a low percentage of water supply and sewerage systems, in the flood inundation model and quantitatively show the behavior of the coliform bacteria group in the rainy season and the dry season. In addition, we aim to quantitatively show the relation between water pollution and poverty by using Engel coefficient and knowing the ratio of food expenses to the income of the surrounding residents.

Keywords: Yangon, uebanization, flood, coliform, Engel's coefficient

1. Background,Aim

Yangon City's water supply penetration rate of water supply as of 2014 is as low as 38%, and properly updated aged water pipes, water supply and distribution pipes are not enough. Therefore, out of the 520,000 m 3 of the daily amount of water, the amount of non-revenue water is about 66%.Regarding water quality,about 90% of the water source is used regardless of the usage of surface water, two-thirds Has been directly distributed without purification treatment, water purification plant Chlorine treatment has not been carried out sufficiently in the present situation. The low penetration rate of such water supply is one of the factors hindering the spread of sewers. Although YCDC (Yangon municipal development committee) is promoting the spread of the corruption layer, it is estimated that the penetration rate is also 43% of the total population, and the corruption layer can only handle toilet drainage, Miscellaneous wastewater is untreated and directly discharged to neighboring rivers, and deterioration of water quality is conspicuous. In developing counry,Water pollution is going to important problem but There are no research that rerationship between water pollution and economic situation.

The purpose of this research is to elucidate between coliform and household comsumption.

2. Research area

Research area is Yangon river basin(**Figure 1**) I select the Bahan are Lake Inaja used by locals for downtown with high population density,dala area on the opposite shore, Hlaing thayar area where about 5,000 people have migrated in recent years.The climate is tropical monsoon climate, it can be roughly divided into three. The heat season is from on March to May the. rainy season from June to October, and the dry season from November to Febrary.

Figure- 1 (Yangon city,Myanmar

3. Method

Sampling points of domestic wastewater, elevation data was downloaded from USGS landsat data and lowlands considered as water catchment areas were extracted on GIS. It is selected coliform bacteria and Heavy metals as items of water quality survey in Yangon City.

3.1 Coliforms

Shibata Science has issued a method for measuring coliform bacteria group [Collagen group test paper reduced in pack]. This is a simple test method of bacteria by specially treated test paper, 1 ml of the test solution (2000-fold diluted raw water with commercially available bottle water)

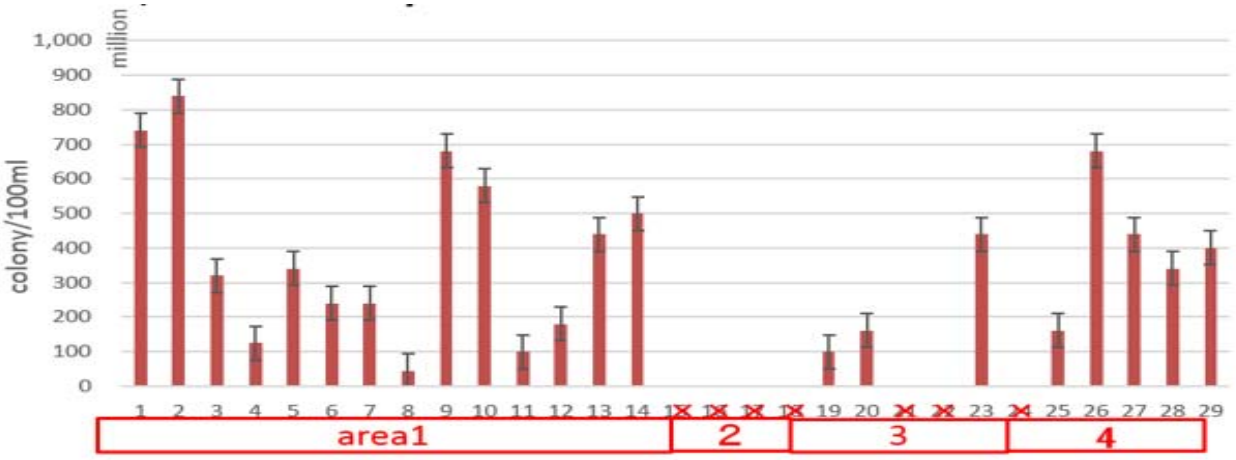

Result.1:coliform bacteria Feb,2017

was immersed in the test paper and then incubated in a thermostat (37 ° C) for 15 hours. After cultivation, count the number of spots (colonies) appearing on the test paper. Five sheets of test paper per point were used and the average number of colonies was taken as the number of coliform bacteria groups.

3.2 Hearing observation

We interviewed to residents ,hotel,retail and restaurant 1st～9th in October ,2017. We made preparations in advance that we need to ask question items. We went to resident, hotel, retail and restaurant and interviewed some queation about water consumption and relate to economic consumption at randam in Yangon city for 9 days

In this observation, We pair off with YTU(Yangon technological University) students and they acted us as interpreter.

The question items are as follows.:

Family structure,income,water resource,water consumption,food consumption,non-food consumption,electric fee,eat out,public tranceportation, happiness

4. Result

4.1 coloform

It can be said that the coliform pollution level is high in a wide area(**Result.1**). In particular, the population density of downtown Hlaing thayar area is incomplete in the improvement of water supply, as nearly 5,000 poor people have moved in recent years. In addition, coliform bacteria in the water supply was examined, and colonies of the coliform bacteria group were detected in a small amount. This water is water used not only for washing dishes and bodies, but also for washing raw vegetables people talk about Yangon. It can be said that The residents living in the city are in an environment where they ingest coliform bacteria from food and tableware everyday.

4.2 Hearing observation

We can correct 72 samples.This is the results of water resource(**Result.2**). YCDC is a short for Yangon City Deverpment Committee.The more close to downtown area, The more water supply rate is tend to high.. However, water supply from YCDC is limited the time zone,we found that They also use tube well.

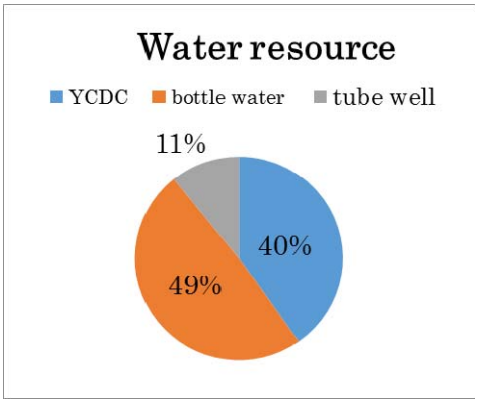

Result.2: Water resource

5. Future work

I am going to make coliform transport model using Coliform date in Febrary and Cotober 2017.We will continue field observation in the rainy season and dry season and newly add Engel coefficient (ratio of food and beverage cost to household consumption expenditure: hereinafter abbreviated as ECF) to the method. This was proposed by Ernst Engel and has been used as an indicator to estimate the level of community living. this is. This is because it is known that the richness of communities can be a common indicator for raising awareness of environmental problems. Information on the richness of communities that can not be estimated by income can be obtained andcomparison with different countries becomes possible. As for the Engel's coeffisiant, I use local interview observation data from 1st to 9th October.It is forcus on family composition,income,food expenditure and water consumption. I summarize these data and analyze the characteristic of each area based on the results of this analysis and the results of the coliform transport model. Its needs obtain a correlation between the floods and the local characteristics of residents.

Reference

1) Population of the Republic of the Union of Myanmar, Provisional Results, Census Report Volume (I), Population and Housing Census of Myanmar, August 2014.
2) JICA,The project for the strategic ueban development plan of the Greater Yangon,2014
3) So Kazama, Terumichi Hagiwara, Priyantha Ranjan and Masaki Sawamoto, Evaluation of groundwater resources in wide inundation areas of the Mekong River basin, Journal of Hydrology, Vol.340, No3-4, pp.233-243, 2007.
4) Sendai Framework for Disaster Risk Reduction 2015-2013, UNISDR, 18th March ,2015.
5) Ayako Amano, Taisuke Sakuma and So Kazama, Spatial-temporal distribution of waterborne infectiotious disease risk using the hydraulic model and out patatient data,Hydraulic engineering,Vol.67,No.4 201
6) Toshiki Aizawa, So Kazama, Toru Watanabe and Masaki Sawamoto, Analysis of seasonal variation in the patients of waterborne infectious diseases by the hydraulic innundationsimulation,hydraulic engineering,vol.51,2007

Evaluating the Effect of Afforestation on Groundwater Recharge Using Naturally-Occurring Isotopes

○Danila Podobed[1*], Daisuke Komori[1], Kei Yoshimura[2]

[1]Graduate School of Environmental Studies, Tohoku University, Sendai 980-8579, Japan
[2]Institute of Industrial Science, the University of Tokyo, Tokyo 277-0882, Japan

*E-mail: danila.aleksandrovich.podobed.r1@dc.tohoku.ac.jp

Abstract

The objective of this research is to produce comparative estimates of groundwater recharge for different kinds of land cover across a variety of climactic and soil conditions. The research is modeled on prior studies by Allison and Hughes (1983), Saxena and Dressie (1987), Gaye and Edmunds (1996), Kudo et al. (2013), and other similar studies focused on estimating recharge of groundwater by measuring ratios of stable isotopes (oxygen-18 and deuterium) in soil water or groundwater and comparing them to the seasonal patterns of isotopic content in precipitation. The speed of movement of water particles through the soil column can thus be estimated. The rate of permeation of water can in turn be used to estimate groundwater recharge volumes under different kinds of land cover.

Keywords: Natural isotopes, land cover, hydraulic conductivity, groundwater recharge

1. Introduction

Primary data for the study comes from moisture gathered from soil samples in the unsaturated zone of the soil profile. While groundwater (saturated zone) samples may be taken in the future, the current aim of this research is to focus on soil moisture in the unsaturated zone, dominated by vertical flow. So far, disturbed soil samples of volumes between 300 and 800 cm^3 have been collected with a hand auger and a percussion sampler to depths of 1-4 m. The samples represent contiguous sections of a soil column of 10 cm (percussion sampler) or 15 cm (hand auger) length; the soil moisture values and isotope values represent an average across the whole 10-15 cm section rather than exact point values. Soil moisture content is determined by evaporation of three 20-gram subsamples at 110 degrees Celsius over 24 hours. Water for isotope analysis is extracted from two subsamples by means of centrifugation at 30,000 Gs for 30 minutes, then extracted from centrifuge tubes with a syringe fitted with a .45 micron filter and frozen in 14 ml storage tubes. Water sample volumes are typically between 1-4 ml, but occasionally as low as 0.4 ml for samples that have already been partially tapped for isotope analysis.

Sampling has been carried out across a variety of sites, but these generally fall into two categories: sites with little or no tree cover, and forested sites. The ideal condition for site selection is the availability of recent land cover change (deforestation or afforestation) nearby an area that has not undergone land cover change for some time, with soil and topographical conditions of each site being kept as close to constant as possible. Four of the sampling locations meet this condition based on a qualitative analysis. Soil moisture data indicates much heterogeneity across different locations owing to differences in soil characteristics, and may suggest soil type plays a larger role in moisture retention and hydraulic conductivity that land cover.

Additional sampling of precipitation of two kinds will be carried out. Firstly, comparative sampling of precipitation volumes at forested and cleared sites will take place to determine the amount of throughfall. Secondly, sampling of rainfall for subsequent measurement of daily precipitation isotope ratios will take place over a 1-2 month period, in addition to aggregate monthly precipitation sampling over a one-year period, to validate external precipitation isotope data.

Oxygen-18 and hydrogen-2 (deuterium) content of the soil moisture and precipitation samples is being carried out using a Picarro Isotopic Water Analyzer at the Yoshimura Laboratory of the Institute of Industrial Science, Tokyo University. Preliminary results of the analysis will be submitted for discussion at the symposium. Results are expected to indicate matching isotope profiles across matching land cover/soil types, and to reflect seasonal patterns of enrichment and depletion. For determining seasonal variations in local precipitation isotope rations, the research will refer to Dr. Yoshimura's IsoGSM1 data for the Sendai-Miyagi area. The IsoGSM1 data will be validated by direct observation data on precipitation isotopes available from JMA's Ryori Observatory for certain years, and by on-site precipitation sampling. Soil water isotope values will be additionally compared to values generated by the Iso-Matsiro coupled isotope-land surface model.

Ongoing analysis makes a conclusive evaluation of results difficult at this stage. However, if the distinct contribution of land cover types to hydraulic conductivity and groundwater recharge can be estimated from soil moisture isotope data, the method can be utilized as a simplified means of evaluating the effects of afforestation and artificial groundwater recharge initiatives across a variety of landscapes and climactic conditions.

References

1) Allison, G. B., & Hughes, M. W. (1983). The use of natural tracers as indicators of soil-water movement in a temperate semi-arid region. *Journal of Hydrology*, *60*(1-4), 157-173.
2) Bengtsson, L., Saxena, R. K., & Dressie, Z. (1987). Soil water movement estimated from isotope tracers. Hydrological sciences journal, 32(4), 497-520.
3) Gaye, C. B., & Edmunds, W. M. (1996). Groundwater recharge estimation using chloride, stable isotopes and tritium profiles in the sands of northwestern Senegal. Environmental Geology, 27(3), 246-251.
4) Kudo, K., Shimada, J., Maruyama, A., & Tanaka, N. (2016). The quantitative evaluation of groundwater recharge rate using Displacement Flow Model with stable isotope ratio in the soil water of difference vegetation cover (Japanese Title: 異なる地表面植生に対する地下水涵養量の定量的評価). Journal of Groundwater Hydrology, 58, 31-45.
5) Yoshimura, K., Kanamitsu, M., Noone, D., & Oki, T. (2008). Historical isotope simulation using reanalysis atmospheric data. Journal of Geophysical Research: Atmospheres, 113(D19).

Satellite Analysis to Detect Burnt Area of Forest Fire in Kamaishi, Tohoku 2017

○Grace Puyang Emang[1], Yoshiya Touge[2], So Kazama[2]

[1]Graduate School of Environmental Studies, Tohoku University, Sendai 980-8579, Japan
[2]Graduate School of Engineering, Tohoku University, Sendai 980-8579, Japan

* E-mail: grace.puyang.emang.r2@dc.tohoku.ac.jp

Abstract

In May 2017, several fire broke out in three prefectures in Tohoku region due to dry weather especially in eastern coast of Japan commonly in East Japan and strong wind in Tohoku region. This dry weather was because of sixty (60%) lower precipitation in winter compared to normal year and strong wind from western blowing into Tohoku region. A large fire broke out in Kamaishi, Iwate Prefecture located in the Tohoku region on 8 May 2017. The burnt out area was larger than the total burnt area for the whole of Japan in 2016. The extensive fire was due to strong presence of wind and low accessibility of vehicle into the burnt area. Satellite analysis to detect the burnt area and the extent of burnt area using surface temperature and Normalized Difference Vegetation Index (NDVI) from three different satellites were used; namely Himawari-8, Terra and Landsat. The result of the analyses will be validated against ground truth obtained through field survey.

Key words: Forest fire, surface temperature, NDVI, Himawari-8, Terra, Landsat

1. Introduction

Annually fire occurrence in forest and field has been reported in Japan with an average of 1635 cases for the period of 2014 till 2010 and the average value of loss annually approximately 576 million yen [1]. A large fire broke out in Kamaishi on 8 May 2017 and was suppressed on 22 May 2017 with estimated total burned area, 413 hectares, which was larger than the total burned area in Japan for 2016, 384 hectares (Fig. 1).

Fig. 1. Area affected by fire (Kamaishi Forestry Association)

Information on burnt area can be used for calculation cost of damage and estimation of pyrogenic gaseous and aerosol emissions [2] which give impact on the Earth's radiation budget [3]. This study aims to detect burnt area of forest fire in Kamaishi using surface temperature and NDVI from three satellites namely Himawari-8, Terra, Landsat and validating the analysis through ground truth.

2. Weather Overview

Prior to May 2017, the precipitation in Tohoku region was low in winter and this dry condition continued into spring. Total precipitation record by Automated Meteorological Data Acquisition System (AMeDAS) from January to April 2017 showed low total precipitation for Kamaishi compared to other area (Fig. 2(a)) and 60% lower precipitation from normal year (Fig. 2(b)) [4]. On 7th May a dry warning report was issued nationwide for the northern Kanto, Chubu and Chugoku region as well as Tohoku region.

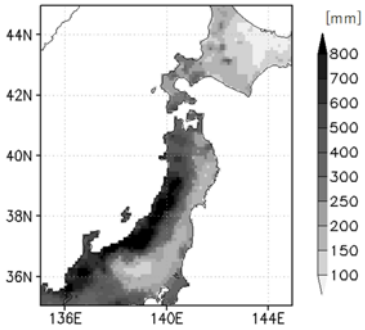

Fig. 2(a) Total precipitation

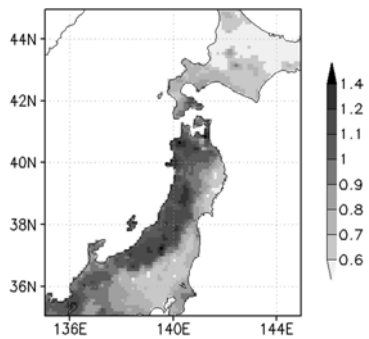

Fig. 2(b) Ratio of total precipitation from normal year

Strong wind was recorded in late April to early May. The maximum wind speed, 14m/s recorded by

Kamaishi Observatory Station on 8 May 2017, was the highest for May 2017. Fig. 3 shows the hourly average of wind speed at 12 to 13 o'clock when the fire occurred [4]. The fire spread extremely extensively due to the weather condition and low accessibility of vehicle which delayed the firefighting activities.

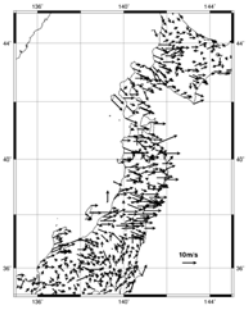

Fig. 3 One hour average wind speed and direction

3. Methodology

Satellite has been use worldwide to detect forest fire and is use as a tool in fire management. Himawari-8 launched in 2015 offers spatial resolution up to 500 meter and temporal resolution of every 10 minutes of Japan, Terra launched in 1999 offers spatial resolution up to 250 meter but temporal resolution of every one and two days while Landsat 7 and 8 launched in 1999 and 2013 respectively offers spatial resolution up to 30 meter with more than 650 scenes a day. Fig. 4 below shows NDVI image from Landsat before (Fig. 4(a)) and after (Fig. 4(b)) fire event.

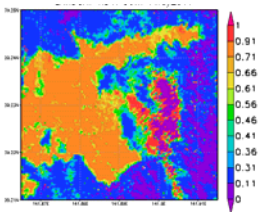

Fig. 4(a) NDVI distribution on 7 May 2017

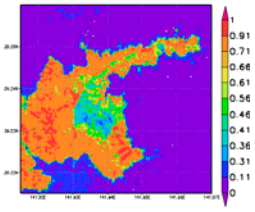

Fig. 4(b) NDVI distribution on 24 June 2017

Thermal infrared band which can detect surface temperature and NDVI which can detect the changes in vegetation were used in detecting burnt area. Thermal infrared of band 14 Himawari-8, band 10 of Landsat and product MOD11A1 from Terra was used to detect surface temperature before and after the fire event. Land surface temperature of Landsat was calculated from At Satellite Brightness Temperature expressed by the following equation [5].

$$T = \frac{T_b}{\left[1 + \left(\lambda \times \frac{T_b}{c_2}\right) \times \ln(e)\right]}$$

$$c_2 = h \times \left(\frac{c}{s}\right)$$

Where T is land surface temperature, T_b is at satellite brightness temperature, λ is wavelength of emitted radiance, c_2 is 1.4388×10^{-2}m K, h is Planck's constant, 6.626×10^{-34} J s, c is velocity of light, 2.998×10^{8} m/s, s is Boltzmann constant, 1.38×10^{-23} J/K and e is emissivity.

NDVI from spectral reflectance of near infra-red and red bands from Himawari-8, Landsat and product MOD13Q1 from Terra were used in detecting burnt area in Kamaishi by analyzing the changes of vegetation before and after the fire event. These bands were used in the calculation of NDVI values. The NDVI formula is expressed by the following equation.

$$NDVI = \frac{(NIR - R)}{(NIR + R)}$$

Where *NDVI* is Normalize Difference Vegetation Index, *NIR* is spectral reflectance of near infra-red band and *R* in spectral reflectance of red band.

The surface temperatures and NDVI images from these satellites were compared to analyze the image differences in before and after fire incident. Next the time series for surface temperatures and NDVI from these satellites were compared with four different locations (Fig.5 (a) – (d) in Kamaishi burnt area and one point outside of burnt area.

Fig.5(a) Ozaki Shrine area

Fig. 5(b) Small burnt area

Fig. 5(c) Slope of burnt area

Fig. 5(d) Trees in burnt area

References

1) Fire and Disaster Management Agency and Statistics Bureau, Ministry of Internal Affairs and Communications, Retrieved from http://www.stat.go.jp/data/chouki/29.htm 2016
2) L. Giglio, T. Loboda, D. P. Roy, B. Quayle, C. O. Justice, An active-fire based burned area mapping algorithm for the MODIS sensor, Remote Sensing of Environment 2009 vol: 113 (2) pp: 408-420 2009
3) R. H. Fraser, Z. Li, J. Cihlar, Hotspot and NDVI Differencing Synergy (HANDS): A New Technique for Burned Area Mapping over Boreal Forest, Remote Sensing of Environment vol: 74 (3) pp: 362-376, 2000
4) Y. Touge, G. P. Emang, S.Kazama, 2017-Nen Tōhoku sanrin kasai no higai gaiyō - Iwate ken Kamaishi-shi Miyagi ken kuribarashi no jirei - (A Summary of the Damage in Tohoku Forest Fires in 2017 - Case Study of Kamaishi City and Kurihara

City), Dai 36-kai Nihon shizen saigai gakkai gakujutsu kōen-kai kōen gaiyō-shū (Proceedings of 36th Annual Conference of Japan Society for Natural Disaster Science-), p83-84, 2017.

5) Q. Weng, D. Lu, J. Schubring, Estimation of land surface temperature–vegetation abundance relationship for urban heat island studies, Remote Sensing of Environment 2004 vol: 89 (4) pp: 467-483

Remote sensing of irrigation water using different resolution sensors in the Aral Sea Basin

O Mbugua Jacqueline Muthoni*[1], Yoshiya Touge [2], So Kazama[2]

[1]Graduate School of Environmental Studies, Tohoku University, Sendai 980-8579, Japan
[2]Graduate School of Engineering, Tohoku University, Sendai 980-8579, Japan

*E-mail: mbugua.jacqueline.muthoni.s8@dc.tohoku.ac.jp

Abstract
The Union of Soviet Socialist Republics (USSR) installed a massive scale irrigation project in the Aral Sea basin. This led to a rapid expansion of irrigation in the region from the late 19th century until the collapse of the USSR in 1991. In turn, the Aral Sea began to shrunk as a result of expanding irrigation that diminished the inflow from the two influent rivers. Currently, the area of the Aral Sea is less than 30% of the level recorded in 1960. Irrigation water is an important part of the hydrology cycle and has thus been included in recently developed hydrological models both at the basin and global level. Despite the large area of land under irrigation in the Aral Sea basin, getting a correct report of irrigated land in the region is a challenge. It is difficult to know the irrigation regime in the Aral Sea basin because collecting data in a wide region is difficult. This has proven to be a challenge even to the local agricultural institutes. It is important to clarify the irrigation regime in order to;(1) Estimate the water demand. An explanation of water demand through climate variables will enable the understanding of climate change impact on water demand. (2) Understand human decision making in irrigation application. This human science aspect is vital as it explains the logical aspect based on the good understanding of the climate. Remote sensing facilitates an efficient and cost effective approach for longer observations of irrigation practices.

Key words: Remote sensing, Irrigation water requirement

1. Introduction

Irrigated land has increased from 50 million hectares in 1900 to 267 million hectares today [1]. Currently, the total area in Aral Sea Basin equipped for irrigation is around 9.76 million ha [2,3].

Fig.1 (A) Typical furrow irrigation in Uzbekistan (Forkutsa 2002) . (B) Accumulated salinity on surface soil in winter wheat field JIRCAS(2016) .

Salinized soils are also a significant problem in the basin. Central Asia is regarded as the most saline-rich area in the world in irrigated farms. In 1994 about 40 percent of the irrigated land in Central Asia was estimated to be saline. Excessive irrigation, has resulted in rising groundwater levels and secondary soil salinization [4].

In order to prevent salinity in the soil from affecting crops, leaching water is applied and it increases water demand in the spring.

Previous studies to detect irrigation water do not consider annual changes due to variations in regional precipitation and air temperature. In addition, some studies do not isolate irrigated land [5,6] instead, they are only part of a broader classification.

2. Satellite analysis

Satellite sensors with different resolutions will be employed for this study. These include; MODIS (Moderate Resolution Imaging Spectro-radiometer) sensor from NASA onboard Aqua and Terra satellites. These satellites are polar orbiting. The sensor has a time resolution of 12 hours. Its spatial resolution for visible channels is 1km for surface temperature. MODIS collects daily global observations from Terra ~11:30 a.m. and 11:30 p.m. and Aqua at ~1:30 a.m. and 1:30 p.m. equatorial crossing time.

Secondly, MODIS NDVI (Normalized Difference Vegetation Index). The product MOD13Q1 is used for this analysis. This vegetation index is produced on 16-day intervals and at a 250m spatial resolutions. It provides consistent spatial and temporal comparisons of vegetation canopy greenness, a composite property of leaf area, chlorophyll and canopy structure.

3. Methodology

Fig.2 Irrigation observation sites in Aral Sea Basin (P. Micklin, 2006).

Water has a higher heat capacity than land. This means that a layer of water added to the ground does not immediately respond to changes in temperature. This could therefore be used to detect irrigation water. Fig.2 shows the study area of this research. There are three testing farms in Uzbekistan. Bayavut, Kyzylkesec and Nukus collaborating with ICARDA. In these farms, soil Moisture is kept at a specific level. Nukus was instated as a testing farm in 2015. It is located in a severely arid region and is the most sensitive to climate change [8]. Satellite based Land Surface Temperature(LST) is used.

$$LST\ (DIF) = LST\ day - LST\ Night$$

Where:
LST day is satellite based day time recorded temperature
LST Night is satellite based night time recorded temperature
LST (DIF) is the difference between day time and night time satellite recorded temperature.

Since water has a higher heat capacity than land. A layer of water added to the ground does not immediately respond to temperature changes. This can be used to detect; (1) Change in Temperature difference over time. (2) Trend in Land surface temperature distribution.

To Estimate irrigated area. 2 indices are used.

1. LST(DIF)
2. LST (DIF) – Average LST(DIF) of surrounding area.

For the first index, a threshold is set corresponding to the map legend indicative of irrigated land. This is based on the computation and observation of the LST(DIF) time series of different points in the basin.

The second index is used to remove climatic influence of the surrounding. The function of this index is to distinguish the aspect of land use management and the effect of land cover.

4. Reference

1. Gleick, Peter H. "A look at twenty-first century water resources development." Water International 25.1 (2000): 127-138.
2. Sokolov, V. 2009. Future of irrigation in Central Asia. IWMI-FAO Workshop on trends and transitions in Asian irrigation. What are the prospects for the future? 19–21 January 2009 Bangkok.
3. Horsman, S. 2008. Afghanistan and transboundary water management on the Amu Darya: a political history.
4. Ikramov R (2004) Present salinity and drainage condition, and salinity control measures in Uzbekistan. Proceedings of the IWMI conference "Materials for meeting on development of the salinity, Land degradation and Drainage—Waste Water Reuse. Research program for Central Asia". May 11–17, Tashkent, 2004
5. Bontemps, S., Defourny, P., Bogaert, E. Van, Kalogirou, V., & Perez, J. R. (2011). GLOBCOVER 2009 Products Description and Validation Report. *ESA Bulletin*, *136*(0), 53. https://doi.org/10013/epic.39884.d016
6. Bontemps, S., Defourny, P., Bogaert, E. Van, Kalogirou, V., & Perez, J. R. (2011). GLOBCOVER 2009 Products Description and Validation Report. *ESA Bulletin*, *136*(0), 53. https://doi.org/10013/epic.39884.d016
7. TOUGE, Y., TANAKA, K., KHUJANAZAROV, T., TODERICH, K., KOZAN, O., & NAKAKITA, E. (2015). Developing a Water Circulation Model in the Aral Sea Basin Based on in situ Measurements on Irrigated Farms. 沙漠研究, 25(3), 133-136.
8. Micklin P. (2007): The Aral sea disaster. Annu. Rev. Earth Planet. Sci., 35: 47-72.

Development of Coupled Land Surface Model with groundwater representation for the Yoneshiro river basin

○Leonardo A. Silva-Vasquez.[1*], Yoshiya Touge [1], So Kazama
[1]Graduate School of Engineering, Tohoku University, Sendai 980-8579, Japan

*E-mail: *silva.vasquez.leonardo.alonso.p1@dc.tohoku.ac.jp*

Abstract

Soil exerts control on both energy balance and water on the surface. In the water balance, soil moisture controls the partitioning between infiltration and surface runoff. Regarding the energy balance, it affects the albedo, that in turns controls the net amount of incoming solar energy on natural land surfaces. Also, soil exerts influence on plant evapotranspiration that affects both the water and energy balance. Land surface models (LSM) are used as boundary conditions for atmospheric models. In these models, soil moisture is represented by means of a column model, but without taking into account the effect of the ground water table (GWT). This misses the important fact that the groundwater table acts as a boundary condition on the shallow soil moisture; therefore, exerting influence on both the water balance and the energy balance on the land surface. This is particularly important in place where the GWT is just a few meters below the surface. In this study, a ground water representation will be added to SiBUC, a land surface model, to improve the representation soil moisture spatial distribution and the seasonal variation of plant evapotranspiration.

Keywords: Groundwater effect on land surface processes Land surface model, Groundwater model, SIBUC,

1. Introduction

Land Surface models (LSM) were originally developed to provide land surface boundary conditions for Global Climate Models GCM during 1960s. Since then, they have advanced considerably by incorporating sophisticated schemes to take into account physical and biological process on the land surface. Despite their advancement, they have not included explicitly the influence of the ground water table (GWT) on the land surface processes.

LSM are based on the concepts of water balance, and energy balance. Consequently, for these models to be representative of the reality, they need to model all relevant elements of the water cycle, including GWT. The influence of GWT in soil moisture is particularly important in places where it is located at a shallow depth. (Yeh and Eltahir, 2005).

In the last two decades, several studies have been done to study the connection between GWT and land surface processes. These studies have ranged in complexity from one dimensional column model (Yeh & Eltahir, 2005; Maxwell & Miller, 2005) to models that included three dimensional representations of GW flow (Kollet & Maxwell, 2008).

In this study, a ground water representation will be added to Simple Biosphere including Urban Canopy (SiBUC) a land surface model which doesn't have GWT representation. The performance of SiBUC with GWT representation will be evaluated in the Yoneshiro river basin.

2. Importance of Ground Water Table (GWT) representation and limitations

The GWT representation is important because a) it controls the stream flow (base flow), b) influences soil moisture distribution c) influences the energy transfer processes in the land surface d) provides a lower boundary condition for soil moisture and e) allows the representation of upward capillary flow. The influence of the GWT is particularly important in humid climates, where it lies near the surface, and ground water runoff is often the dominant streamflow generation mechanism. Under deep water table conditions, there is a relatively uniform soil moisture profile in the unsaturated zone. But in location where the GWT is shallow, its presence changes this profile at least in the lower part of the unsaturated zone. This, in turn, results in a decrease of infiltration and an increase of evapotranspiration (Yeh and Eltahir, 2005).

If the GWT is not represented in the LSM, specifying the lower boundary condition for soil-moisture is difficult. The most common practice is to apply the free drainage condition: the drainage flux equals the unsaturated hydraulic conductivity at the bottom of the lowest soil layer. SIBUC uses the unsaturated hydraulic conductivity multiplied by factor depending on the mean slope of the grid (Tanaka, 2005).

There are two important problems with the free drainage boundary conditions. First, this condition cannot model a negative ground water recharge (upward flow from the saturated zone to the unsaturated zone). And it makes the soil column incapable of maintaining wet conditions over time causing the soil column to dry too quickly (Zeng et al. 2009). This critical issue has been evidenced in the Amazon river basin, where models predict vegetation stress in the dry season, but observations indicate that dry season evapotranspiration is no less than during the wet season (Shuttleworth, 1988).

3. Methodology

3.1 Land Surface model: SiBUC

SiBUC is a land surface model (Tanaka, 2005). It is heavily influenced by both SiB1 and SiB2, but it also includes two extra sub models: urban canopy and Water body model because surface fluxes mechanisms are different under these conditions. Additionally, it also has a module to represent irrigation in arid and semi-arid areas to study the effect of large scale irrigation on surface fluxes.

3.2 Improvement of Soil Moisture representation

Current SiBUC soil moisture representation will be changed to a multilayer column soil moisture content. The basic equations for this multilayer column model are the unsaturated porous media equations:

$$\frac{\partial \theta}{\partial t} = -\frac{\partial q}{\partial z} - Q \qquad (1)$$

$$q = -K(\theta)\frac{\partial(\Psi + z)}{\partial z} \quad (2)$$

Where:

- θ: Volumetric soil moisture content
- q: soil water flux
- t: time
- z: Elevation
- Q: Sink term (ET loss)
- Ψ: Soil matric potential

An approximate solution of this set of equations can be obtained by using a mass conservative, implicit scheme, leading to the following discrete version:

$$\left(z_{i-\frac{1}{2}} - z_{i+\frac{1}{2}}\right)\frac{\left(\theta_i^{n+1} - \theta_i^n\right)}{\Delta t} = -q_{i-\frac{1}{2}}^{n+1} + q_{i+\frac{1}{2}}^{n+1} + Q_i \quad (3)$$

- i: denotes the space index
- n: denotes the time index

This discretization leads to a tridiagonal systems of equations that can be solved using the Thomas algorithm.

To relate soil moisture and matric potential, the Clapp-Hornberger relations (Clapp and Hornberger, 1978) are used.

$$K = K_{sat}\left(\frac{\theta}{\theta_{sat}}\right)^{2B+3} \quad (4)$$

$$\Psi = \Psi_{sat}\left(\frac{\theta}{\theta_{sat}}\right)^{-B} \quad (5)$$

4. References

Chapra, Steven C., Canale Raymond P. "Numerical Methods for Engineers, fifth edition", McGraw-Hill, 2006.

Clapp, R. B., and G. M. Hornberger, 1978: Empirical equations for some soil hydraulic properties. *Water Resour. Res.,* **14** (4), 601–604.

Fan, Y., and G. Miguez-Macho (2010), Potential groundwater contribution to Amazon dry-season evapotranspiration, Hydrol. Earth Syst. Sci., 14, 2039‑2056, doi:10.5194/hess-14-2039-2010.

Koirala, S., P. J.-F. Yeh, Y. Hirabayashi, S. Kanae, and T. Oki (2014), Global-scale land surface hydrologic modeling with the representation of water table dynamics, J. Geophys. Res. Atmos., 119, 75–89, doi:10.1002/2013JD020398.

Kollet, S. J., and R. M. Maxwell (2008), Capturing the influence of groundwater dynamics on land surface processes using an integrated, distributed watershed model, Water Resour. Res., 44, W02402, doi:10.1029/2007WR006004.

Maxwell, R. M., and N. L. Miller (2005), Development of a coupled land surface and groundwater model, J. Hydrometeorol., 6, 233-247.

Miguez-Macho, G., Y. Fan, C. P. Weaver, R. Walko, and A. Robock (2007), Incorporating water table dynamics in climate.

Miguez-Macho, G., and Y. Fan (2012), The role of groundwater in the Amazon water cycle: 1. Influence on seasonal streamflow, flooding and wetlands, J. Geophys. Res., 117, D15113, doi:10.1029/2012JD017539.

Sellers, P. J., and Coauthors, 1996: A revised land surface parameterization (SiB2) for atmospheric GCMs. Part I: Model formulation. J. Climate, 9, 676–705.

Oleson, K. W., and Coauthors, 2004: Technical description of the Community Land Model (CLM). NCAR Tech. Note

Shuttleworth (2012), W. J., Terrestial Hydrometeorology, First edition, Jhon Wiley & Sons, Ltd.

Shuttleworth W. J., Evaporation from Amazonian rainforest, Proceedings of the Royal Society of London, B233, 321-346, 1988.

Strang, Gilbert. *Computatinal Science and engineering.* Wellesley-Cambridge press, 2007.

Tanaka, K.: Development of the new land surface scheme SiBUC commonly applicable to basin water management and numerical weather prediction model doctoral dissertation, Kyoto University, 2004

Walko R. L., et al. (2000), Coupled atmosphere-biophysics-hydrology models for environmental modeling. J. Appl. Meteorol., 39-931-944.

Yeh, P. J.-F and E. A. B Eltahir (2005a), representation of water table dynamic in a Land Surface Scheme, part 1.

Yeh, P. J.-F (2002). Representation of water table dynamics in a land surface scheme: Observations, models, and analyses. Ph.D. dissertation, Dept. of Civil and Environmental Engineering, Massachusetts Institute of Technology, 212 pp.Model development, J. Clim, 18, 1861-1880

Zeng, X., and M. Decker (2009), Improving the numerical solution of soil moisture-based Richards equation for land models with a deep or shallow water table, J. Hydrometeorol., 10(1), 308–319.

Determination Critical Rainfall using Infiltration model-infinite slope model: A case of Iwaizumi, Iwate prefecture, Japan.

○Thapthai Chaithong[1], Kentaro Sugii[2], Daisuke Komori[3]

[1]Graduate School of Environmental Studies, Tohoku University, Sendai 980-8579, Japan
[2]Graduate School of Environmental Studies, Tohoku University, Sendai 980-8579, Japan
[3]Graduate School of Engineering, Tohoku University, Sendai 980-8579, Japan
*E-mail: kentaro.sugii.s4@dc.tohoku.ac.jp

Abstract

Landslide are occurred by rainfall. The connection is complex so various approach has been in some assumption. This study uses Infiltration model-infinite slope model for estimation of risk of landslide in Typhoon Lionrock on 30 August in 2017. Lionrock damaged in Iwate prefecture is over 700 million dollars, moreover 20 lives were lost and 3 persons are missing. In Iwaizumi, 870 people and 430 houses were isolated because landslides blocked roads. This paper applied the model into Iwaizumi region in Iwate prefecture in Japan. This region had much cumulative rainfall so API for three days was high. Rainfall Triggered Landslides(RTL) was less than 1 in the majority of the area, especially in the middle, which suggest this region were in danger of landslides. The region critical rainfall applies the infiltration process and the infinite slope analysis model that can apply in this case.

Keywords: Critical Rainfall, Landslide, Rainfall, Typhoon,

1. Introduction

Landslide killed many people every year and causes great damages to firm land and infrastructure and cities. In most cases, landslide is caused by rainfall. Especially in Japan where has many steep slopes, Typhoon inflicts property damages by strong rainfall each time. However, the study of *Rainfall Triggered Landslides*(RTL) is still developing and need more researches to connect with risk of landslide. Numerical studies proposed a model to depict relationships between landslide and rainfall for early warning and reduction of crisis and estimation of damage. Landslides are influenced not only by rainfall but also by many factors such as land's angle, cumulative and Antecedent rainfall, characteristic of soil. This study aims to determinate critical rainfall using Infiltration model-infinite slope model due to the typhoon Lionrock in Iwate prefecture, Japan.

2. Theory

There are two approaches to depict relationship between landslide and rainfall. One is the spatial analysis that applies to areas widespread proneness to landslide and homogeneous area. Another is the temporal analysis that applies to a single site or small site. This paper takes a former way and homogenizes geographical features and use physical model on a simple assumption. This paper investigates relationship between RTL and landslides by Lionrock using Infiltration model-infinite slope model. The critical rainfall thresholds in a region scale considers the physical properties such as soil permeability, soil strength, and failure mechanism. The cumulative rainfalls were considered to calculate the amount of water the soil has.

3. Method

The critical rainfall threshold is based on two main assumptions. The first assumption is the failure type of landslides is the infinite slope and the saturation of hillslope would destabilize a hillslope. The second assumption is the soil moisture initial condition prior to rainstorm is equal to the volumetric water content at field capacity.

The wetting front of sloping surface is defined as:

$$z_w = \frac{I}{(\theta_s - \theta_f)\cos\beta} \tag{1}$$

So,

$$I = z_w\ (\theta_s - \theta_f)cos\beta \tag{2}$$

The critical rainfall threshold is defined as:

$$I_{cr} = z_w\ (\theta_s - \theta_f)cos\beta \tag{3}$$

z_w is the wetting front, I is the amount of rain infiltration, θ_s is the volumetric water content as saturation, θ_f is the volumetric water content at field capacity, I_{cr} is the critical rainfall thresholds, z_{cr} is the critical depth, and β is the slope angle. The factor of safety for an infinite slope model is based on the Mohr-Coulomb failure creation. The safety factor is defined as:

$$Fs = \frac{c'}{\gamma_t z sin\beta cos\beta} + \frac{tan\phi'}{tan\beta} \tag{4}$$

So,

$$z = \frac{c'}{\gamma_t \sin\beta\cos\beta} \times \frac{1}{Fs - \frac{\tan\phi'}{\tan\beta}} \quad (5)$$

When *Fs* is less than 1, a rainfall classified as the critical rainfall. So (3) and (5) leads the critical rainfall thresholds.

$$I = \left[\frac{c'}{\gamma_t \sin\beta\cos\beta\left[1 - \frac{tan\phi'}{tan\beta}\right]}\right] \times \left[(\theta_s - \theta_f)\cos\beta\right] \quad (6)$$

Rainfall Triggered landslides(RTL) is defined as:

$$RTL = \frac{z_{cr}}{API} \quad (7)$$

The antecedent precipitation index(API) is the amount of cumulative rainfall for three days in this paper. In this area, Soil cohesion is 10.3kPa, Soil units 15.2kN/m^3, Friction angle 28.7 degree.

4. Model applicability

4.1 Typhoon Lionrock

According to Japan Meteorological Agency(JMA) Low Pressure where it was in 580km to the west of Wake Island in the western Pacific Ocean developed a tropical depression 16 August 2016. It was classified Tropical Storm on August 21 that central pressure was 992 hPa and the max winds near center was 18m/s. It was classified Typhoon and the diameter became over 800km on August 28. JMA reported the typhoon Lionrock made landfall near the city of Ofunato which this unusual typhoon to directly land on Tohoku because of typhoons usually approach Japan from the south and south west before moving northward across the archipelago. It was first that typhoon land from Tohoku region since JMA have recorded typhoon since 1951. Finally, Lionrock was absorbed with cold low pressure on August 31.

4.2 Iwaizumi, Iwate, Japan

Iwate prefecture locates the northeast main island of Japan. There is warm and humid climate. Iwaizumi has 5 rang gauges when Lionrock came on August 30 in 2016. API is calculated from it. The geological conditions in these areas were formed an accretionary complex (Mesozoic and Palaeozoic) and some plutonic rock. The landslide scars data is from Geospatial Information Authority of Japan and Google Earth website(Fig.3). The failure occurred on slope ranging from 19 to 58 degrees. Field investigation showed most of the slope failures were complex that can be classified into debris flow, surficial erosion, and soil slide. The range of critical depth is 2-5 meters for a large debris flow and soil slip and 0.7-1.2 meters for small soil slip and local failure. This region's soil was classified as loamsand (LSa) so the volumetric water content at field capacity and the volumetric water content at saturation can be calculated.

Figure 1 shows the Critical rainfall thresholds in Iwaizumi town. Figure2 shows the regional API for three days in this region. Figure 3 shows the RTL and black area shows where landslides occurred by Lionrock.

5. Conclusion

Infiltration model-infinite slope model is approach depict relationship between landslide and rainfall. Using Infiltration model-infinite slope model, The RTL was depicted in the figure. The critical rainfall is defined by the method. The region had stocked rainfall in these mountains by Lionrock. RTL were under 1 in the region during the typhoon. The region critical rainfall applies the infiltration process and the infinite slope analysis model that can apply in this case.

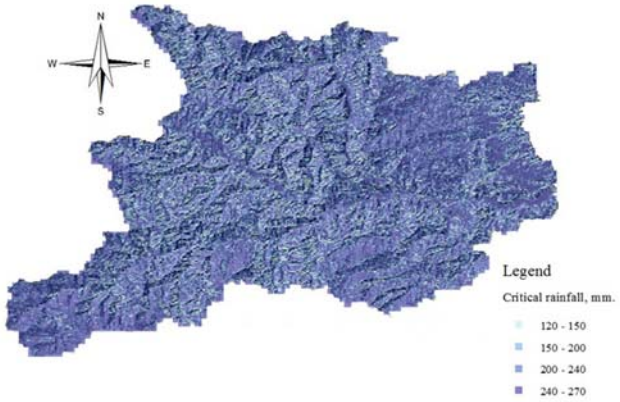

Fig.1 Regional critical rainfall threshold for Iwaizumi town.

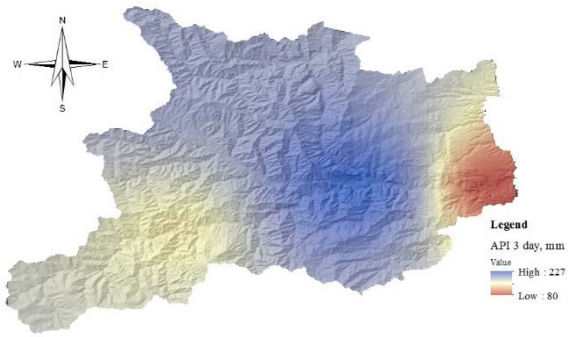

Fig2. Regional API in Iwaizumi town

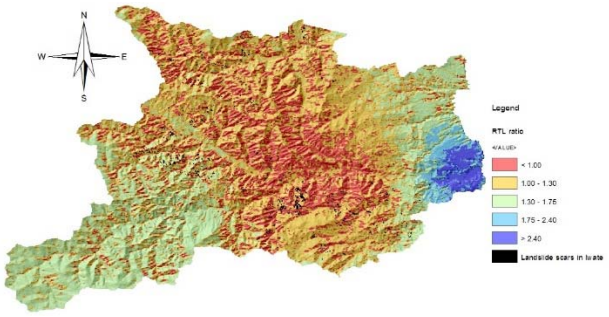

Fig3. Rainfall Triggered Landslides in Iwaizumi town

Development of the Sayo river flood model enabling estimation of cultural property damage

○Hironobu Hirayama[1], Kenichiro Kobayashi[2]
[1]Graduate School of Engineering, Tohoku University, Sendai 980-8579, Japan
[2] Graduate School of Engineering, Kobe University, Kobe 657-8501, Japan
E-mail : hironobu.hirayama.t5@dc.tohoku.ac.jp

Abstract
A severe flood disaster was occurred in Sayo river due to heavy rainfall in August 2009. Thus, this researchs attempts to reproduce the situation of the Sayo river flooding by DRR/FI model. The inundation situation is simulated by a 2D shallow water equation of DRR/FI. 50m and 10m resolution elevation data are used so that it can represent the river explicitly. I thought that by comparing them I can see the differences in resolution and precision depending on the computer I used. As the result, the flow from the river inundated over the houses with cultural properties was reproduced.

key words ArcGIS, flooding, disaster, DRR/FI model

1. Introduction

In this research, we dealt with the Sayo river which is the upstream branch line of the class B river Chikgusa river flowing in the southwestern part of Hyogo Prefecture. The novelty is a model aimed at integrally tracking the rain outflow process and the flooding process and it is necessary to calibrate, but conceptually, the water depth at any point in the watershed, and the river way At the position you can calculate the flow rate and water level. On the afternoon of August 9, 2009, due to Typhoon No. 9, it became a heavy rain that recorded the maximum in Sayo's observation history . As a result, the Sayo and Chigusa rivers, the Makuyama river of small and medium river flooded, the damage of 1878 people, two people missing, human damage of 189 houses including 139 full destruction and 269 large-scale semi-collapse occurred . Floods occur most frequently among the world's natural disasters, and the risk of human injury (drought 1st, windbreak 2nd, flood 5th) is a high disaster. Damaged by Typhoon No 9 of Sayo, the designated cultural assets in Sayo were damaged. However, plans to restore the damages themselves are out of application and they are not actually done, and we spent more time receiving assistance from the Hyogo prefectural board of education to protect the damage situation of the designated cultural property earlier . In this research, we aim to protect cultural properties from inundation damage, so we believe that it is effective to construct a flood assumption model. By using the inundation model, we identify areas where the possibility of flooding is high and lead to protection of cultural properties. In addition, to confirm the relationship between the anticipated inundation area and creating a database of cultural assets, to improve the likelihood that gets to consideration of the cultural property protection at the time of river improvement by estimating the cultural property losses It is set as the final target. In this study, the entire Sayo river catchment area of Hyogo prefecture was used as a calculation target of inundation model, and each resolution model of 10 m , 50m was constructed. For calculation of the 10 m resolution model, Kei-computer is used. We compare the analysis results of this 10 m resolution and 50 m resolution.

2. Materials and Methods

2.1.DRR/FI model

In this study, a distributed rainfall-runoff / flood-inundation model (DRR / FI model) was used as a numerical analysis method .This model shows the rainfall runoff process at the wide area basin level. It is a model that can track internal and external water inundation processes in a unified manner, and the water flow in the protected inland is tracked by the secondary shallow water flow analysis, the flow of the river and rainwater trunk is tracked by one-dimensional uncertain flow analysis, It is made efforts to follow the laws of physics as far as possible as to the equation and

constitutional rule. The connection between the protected land area and the river network is made by exchanging water by inflow / overflow. As a model connection between the two, first one-dimensional unsteady flow calculation is performed on a line connecting the central nodes of the river network. In next, within the basin protected inland, it is an entire drainage basin covering the orthogonal grid to form a two-dimensional orthogonal grid, and the center node of each grid is defined as the definition of elevation point. In each clause, we follow the water flow according to the two dimensional shallow water flow equation. In the 10 m resolution all protected inlands are analyzed by two dimensional shallow water flow analysis because it is considered as protected land. In the 50 m resolution, protected inlands are analyzed by two dimensional shallow water flow analysis.

3.Results and discussions

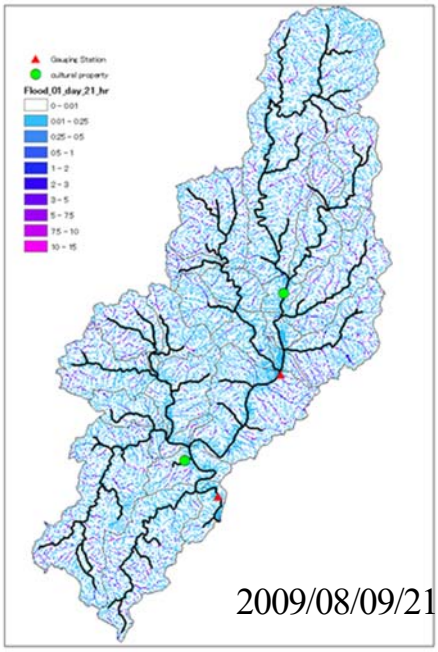

Figure 1. Depth of inundation (50 m resolution) by Sayo river model

Figures 1 and 2 show the inundation depth calculated by the Sayo river inundation model at 50 m resolution and 10 m resolution at 21 o'clock on August 9, 2009, respectively. Both 10 m resolution and 50 m resolution can confirm that the U house is flooded. U house is flooded in case of actual flood in Sayo river. Therefore, it can be said that the reproducibility is high by analysis. For both 10 m resolution and 50 m resolution, O house is not flooded. However, the O house actually flooded in case of flood in the Sayo river..

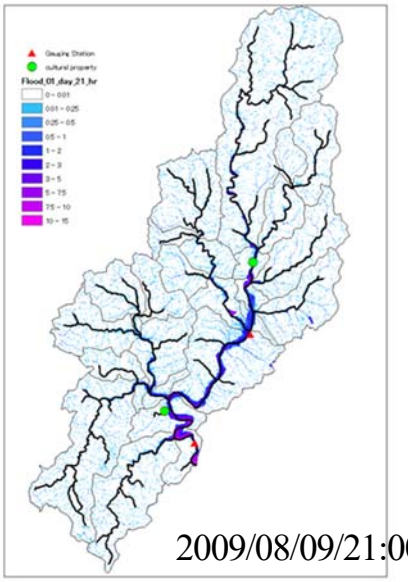

Figure 2. Depth of inundation by Sayo river model (10 m resolution)

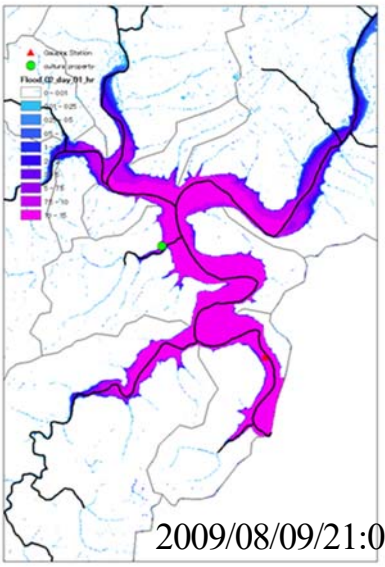

Figure 3. Depth of inundation by the Sayo river model (near O house), 10 m resolution (when raising the downstream water level)

Fig. 3 shows the 10 m resolution image on August 9th and 21st 2009, when raising the water level downstream of the Sayo river. By raising the water level downstream of the Sayo river, it is possible to confirm that the creaking effect occurs, the flooding depth becomes deep, and the O house is flooded. It can be seen that the immersion depth is larger for the 10 m solution with the immersion simulation model of 50 m resolution and 10 m resolution. The reason for this is that 50 m resolution separates the river channel from the embankment of protected land whereas all 10 m resolution is considered as protected land. The simulation is carried out by one-dimensional unsteady flow analysis of river way, and two-dimensional shallow water flow analysis by protected land. From these results, in the case of 50 m resolution, water flows into the river channel from the inside of the embankment and the depth of flooding is decreasing.

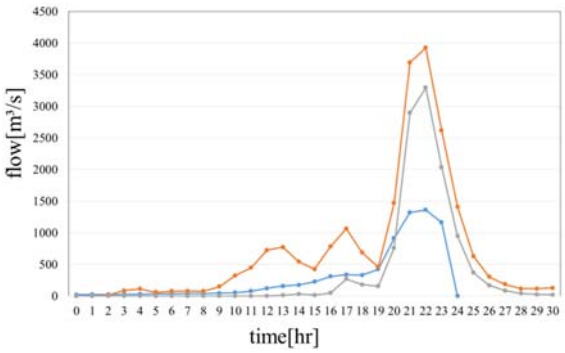

Figure 4. Relationship between time and flow rate of Sayo river model (10 m resolution)

Figure 4 shows the relationship between time and flow rate at the Enkouzi Observatories of the Sayo river model (10 m resolution). Blue line has observation value. Orange line has no soil penetration. Gray line has soil penetration. I will explain it in Chapter 4. Figure 5 shows the comparison between the observed water level and the calculated water level at the point of the temple. Red points express observation value. Black line expresss calculated value(50 m resolution, Nriver=0.08, Nland=0.3, Inf=0), blue line expresss calculated value(10 m resolution, Nriver=0.2, Nland=0.2, Inf=10), green line expresss calculated value(10 m resolution, Nriver=0.2, Nland=0.2, Inf=0). I will explain it in Chapter 4.

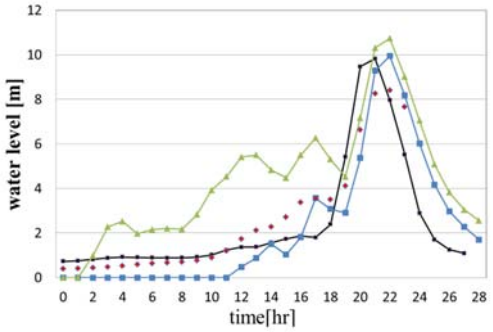

Figure 5. Comparison of observed water level and calculated water level at the location of the yen temple

4.Conclusions

Through model calculations carried out in this study, the flood analysis of the Sayo River could be reproduced roughly. However, when I compared the observed value and the calculated value, there are many differences. Regarding the water depth, it can be said that the difference is small and the reproducibility is high, but regarding the flow rate, there was a time zone in which a large local difference could be seen. Therefore, it is inevitable that the reproducibility is low with respect to the flow rate. Regarding the water level as well, from the comparison of the observed water level and the calculated water level, it was found that the water level rises faster at 50 m resolution and slightly late with respect to 10 m. Therefore, there is still room for improving the reproducibility with respect to the water level. I believe that we could build a model that is sufficiently useful even at present. In this research, there is room for improving the reproducibility such as not considering the condition used land, rain setting, roughness, uniformity of river width, penetration, river runoff etc. It can be said that there is. In the future, it is important to improve these, improve the accuracy of the data, adapt it to the model, calibrate, and improve reproducibility. Even in other areas, creating a model that can be adapted is also an issue. By doing these, we aim to lead to the protection of cultural assets by the model which was able to be made.

DYNAMICS OF CO_2 FLUXES OVER THE HETEROGENEOUS LAND SURFACE

○Masafumi Kon[1*], Daisuke Komori[2], Nanami Sakai[1]

[1]Graduate School of Engineering, Tohoku University, Sendai 980-8579, Japan
[2]Graduate School of Environmental Studies, Tohoku University, Sendai 980-8579, Japan

*E-mail: masafumi.kon.r1@dc.tohoku.ac.jp

Abstract

It is known that the estimates of flux obtained by eddy covariance method are affected by land surface heterogeneity. Therefore, research to quantify its influence is required to improve the accuracy of flux measurements. In this study, the land surface heterogeneity parameter (η), calculated from the coefficient of variation of the flux; and the land use variation index were compared to evaluate the relationship between the flux and the land surface heterogeneity. The result of this study shows that there was a linear relationship between the heterogeneity parameter (η) and the area ratio of vegetation area to fetch area (B).

Keywords: *Eddy Covariance Method, heterogeneity land surface, Join count test*

1. Introduction

The eddy covariance method is the most widely used method for flux estimation. Since it is known that heterogeneous land covers cause errors in measured values of fluxes, flux measurements are generally carried out on homogeneous land covers such as forests or paddy fields. Flux measurements on heterogeneous land covers, including multiple land use remain at the research stage.

Kim et al. 2011 measured long-term fluxes on heterogeneous land covers and developed the parameter η that shows the degree of heterogeneity of the land surface from fluctuations in the flux coefficient.

Since vegetation is the main source of CO2, the ratio of vegetation area to fetch area was calculated from the land use distribution acquired from satellite images; then, they were compared with the parameter η.

The target area of this study is the circular region with a radius of 5 km around the 100 m flux observation tower located in Tak, Thailand. The data for this study consists of the turbulence measurements from the Tak observation tower site and satellite data acquired from MODIS (Resolution: 250 m).

2. Method

First, the influence factor on flux (Fx) and its width X_f were calculated (for detailed formulas see J. H. C. GASH, 1985). Next, the vegetation area included in the fetch is calculated from the satellite data using NDVI. The area ratio of vegetation area to fetch area (B) was obtained by

$$B = \frac{A_v}{A} \quad (1)$$

where A is the area of the fetch, and A_v is the vegetation area which contained in the fetch.

We calculate the heterogeneity parameter η from the turbulence data. η was obtained by

$$\eta = 1 - \frac{\omega}{\varepsilon} \quad (2)$$

where ω is a constant (≈ 0.07), and ε is the relative sampling error, i.e., fractional uncertainty. η ranges from 0 to 1; η = 0 denotes perfect homogeneity. For instrumentation details and the principles of ε and η refer to Kim et al. (2011).

3. Results

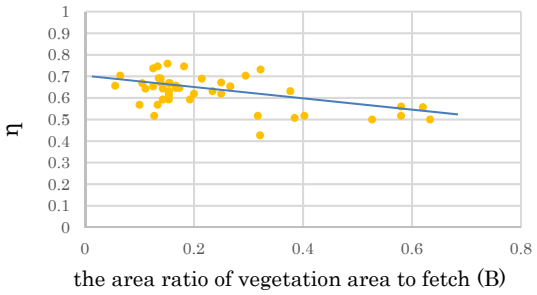

Figure 1. Relationship between the area ratio of vegetation area to fetch and η

Figure 1 shows the relationship between the ratio of vegetation area to fetch (B) and η. A negative linear relationship between the ratio of vegetation to fetch and η was observed. This indicates that the transport of CO2 becomes more stable as the area of vegetation contained in the fetch increases.

4. Conclusion

The result of this study can be summarized as follows.

1) As the ratio of vegetation area to fetch area increases, the land surface heterogeneity parameter (η) approaches to 0, the value corresponding to a homogeneous surface.
2) This study suggests that the heterogeneity of fetch is mainly affected by the area ratio of vegetation area to fetch area (B).

References

1) Wonsik kim ; Long-term analysis of evapotranspiration over a diverse land use area in northern Thailand ; Hydrological Research Letters 8(1), 45–50 , 2014.

Analysis on Instagram data to understand people actions during heavy rainfall period

○Satoshi Anzai[1], So Kazama[2]

[1]Department of Civil Engineering, Tohoku University, Sendai 980-8579, Japan
[2]Graduate School of Engineering, Tohoku University, Sendai 980-8579, Japan

*E-mail: satoshi.anzai.s7@dc.tohoku.ac.jp

Abstract

This study was to analyze people reaction for rivers during heavy rainfall period. Social media has advantages to focus on temporal and spatial distribution. Among various social media, Instagram was chosen for its real-time nature and low-noise. Data was collected by Instagram API detecting hash-tag search with name of rivers such as "#Tama-river". From the results, the number of posts were increasing after the warning, and it might prove that the number of people recognizing the risk were increasing, although many images with posts along a river that time. Generally, the government announces the warning in order to make people aware the danger of flood. However, the results show that the warning can also increase people's interests not only awareness of danger. It is assumed that the warning makes high-risk people increasing.

Keywords: river management, flood, social science, social media

1. Introduction

Many rivers are shorter and have faster flow in Japan than the rivers in foreign[1)]. Floods are easy to occur and cause damage to people living along riverside in Japan. Ushiyama et *al.* surveyed characteristics of victims by heavy rainfall from 2004 to 2009[2)]. As the result, 35.5% of victims were death from approaching dangerous area. Thus it is important to analyze people attention to river during heavy rainfall period and time change of attention.

In past study, Yoshimoto et *al.* analyze characteristics of evacuation from different types of floods[3)]. And, Yabe et *al.* research about process of making decision during river disaster by protocol method[4)]. They used questionnaire results after disasters and speeches data about reaction for imaginary disasters. But, real-time data during real disasters was not used. Therefore, social media data was used to analyze people reaction for rivers during heavy rainfall.

2. Data and Methods

Social media has advantages to focus on temporal and spatial distribution. Among various social media, Instagram data was chosen for their real-time nature with low noise. Data was collected by Instagram Application Program Interface (API) detecting hash-tag search with name of rivers such as "#Tama-river". The study areas were Tama-river, Kinu-river, Edo-river, Tone-river, Sagami-river and Hirose-river, which were struck by a heavy rainfall from 7th Sep 2015 to 11th Sep 2015.

Data was analyzed by three methods. Firstly, time series analysis was made to understand attention changes to the rivers. Time series change of the number of posts were compared with the time of the warning given and canceled. Secondly, text analysis was made to identify for the rivers. Mecab, the open source Japanese language analysis system, was used. It is useful to separate one sentence to each word and obtain frequency for each word. Thirdly, image analysis was made to investigate distance from the poster to the rivers. The distance was manually measured from the river to posters in image.

3. Results

3.1 Result of time series analysis

Each plots are summed the number of posts into each 30 minutes in Fig.1, 2, 3 and 4. Fig.1 shows time series change of the number of posts with #Tama-river and warning given and canceled time in Tama river. The average of the number of posts was approximately 10 posts in Sep 2015. After the warning, the number of posts were increasing promptly. Tama river is located near big city, therefore many people pay attention to the river. Fig.2 shows time series change of the number of posts with #Hirose-river and warning given

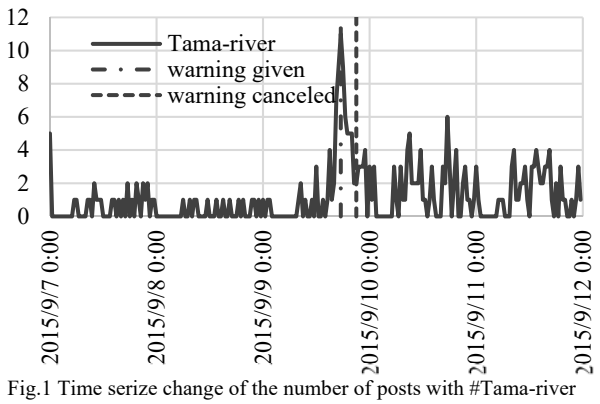

Fig.1 Time serize change of the number of posts with #Tama-river

and canceled time in Hirose river. The average of the number of posts was approximately 6 posts in Sep 2015.After the warning, the number of posts were increasing promptly. Hirose river is located near big city, hence many people pay attention to the river. Fig.3 shows time series change of the number of posts with #Kinu-river and warning given and canceled time in Kinu river and overtopping time. The average of the number of posts was approximately 45 posts in Sep 2015. After the warning, the number of posts were not increasing promptly. Kinu-river is located near small city, thus, few people pay attention to the river. After over topping, the number of posts were increasing. Over topping info was shown on media, so many people pay attention to the river. Fig.4 shows time series change of the number of posts with #Edo-river. The average of the number of posts was approximately 14 posts in Sep 2015. It rained heavily around the rivers, but warning was not given. Though, Edo-river was near to Tama-river, the number of posts were not increasing at same time. People living along the river did not pay attention to the river because warning was not given. As a result, many people concerned for the rivers after warning.

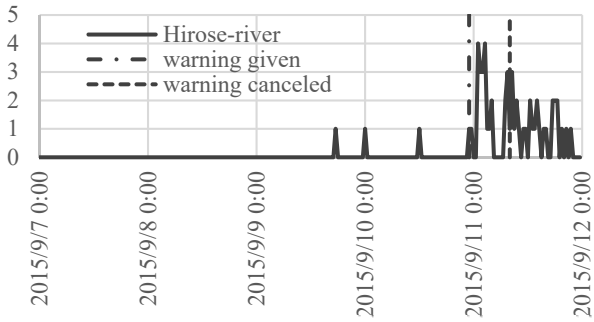

Fig.2 Time series change of the number of posts with #Hirose-river

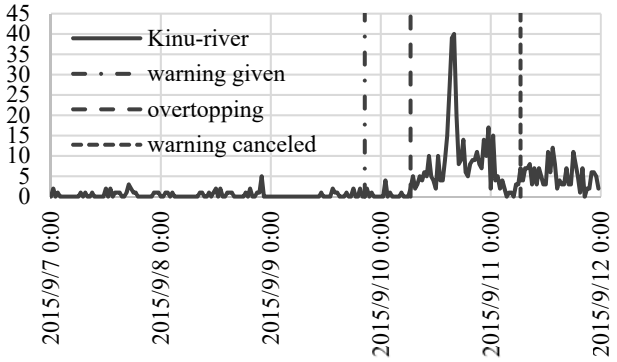

Fig.3 Time series change of the number of posts with #Kinu-river

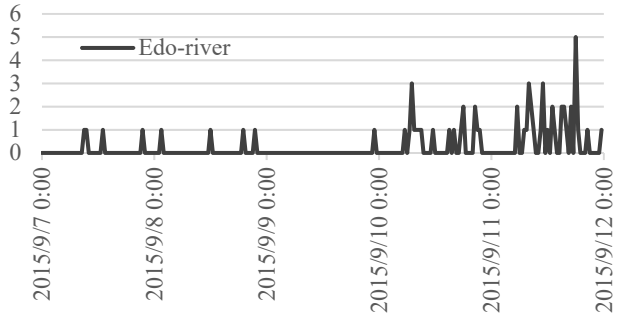

Fig.4 Time series change of the number of posts with #Edo-river

3.2 Result of text analysis and image analysis

Texts and hashtags show recognition for the rivers, and these were analyzed. Table 1 shows ranking of the frequency in use in Tama-river, Kinu-river, Hirose-river and Tone-river. 'Flood' was the 5th most frequently used in Kinu-river. 'High flow' was the 6th most frequently used in Tama-river. 'Flood' was the 3rd most frequently used in Hirose-river. 'Flood' and 'high flow' were the 1st and 3rd most frequently used in Tama-river. Hence, illustrating the change of river conditions such as flood and high flow were frequently used

Images in posts show distance from river to users, and these were analyzed. As a result, under the warning, There are a lot of images near the river. Fig.5 shows the images in posts with #Hirose-river. These images were taken from the riverbank and the bridge under the warning. From the results of text analysis and the results of image analysis people approached river even though knowing the river was dangerous

4. Conclusion

1) After the warning, people pay more attention to the river.
2) People who posted on Instagram recognized the change of river conditions. But a lot of people still obtained images near the rivers. They are being at high risk.
3) The warning can increase people's attention, not only awareness of danger. It is assumed that the warning may increase high-risk to people.

References

1) Rivers which are short and fast flow in Japan. 2015. Japan institute of country-ology and engineering. http://www.jice.or.jp/knowledge/japan/commentary08
2) Motoyuki Ushiyama, Yuka Takayanagi,: Characteristic of death or missing caused by heavy rainfall disaster events from 2004 to 2009, Journal of Natural Disaster Science, 29-3, 355-363, 2010
3) Toshiro Yoshimoto, Toshiharu Fueta, Tetutaro Sumi : Evacuation in flood plains with different characteristic, Annual Journal of Hydraulic Engineering Vol.37, 233-238,1993
4) Hiroki Yabe : Information provision method for river disasters considering decision-making process and perception, Japan Society of Civil Engineers No.800, IV-

Table 1 Word ranking of the frequency in the texts and the hash-tags

river	ranking of frequency	word
Tama-river	7	high flow
Hirose-river	3	flood
Kinu-river	5	flood
Tone-river	1	flood
	3	high flow

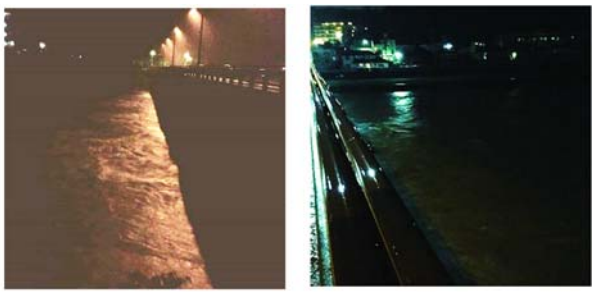

Fig.5 Image in posts with #Hirose-river under the warning

Concentration of Trace Elements in *Corbicula Japonica*

○Koji Iwama[1*], So Kazama[1]
[1]Graduate School of Engineering, Tohoku University, Sendai 980-8579, Japan

*E-mail: koji.iwama.r1@dc.tohoku.ac.jp

Abstract
Lake Ogawara, which is typical brackish lake, is located in eastern part of Aomori prefecture. The environment of Lake Ogawara varies depending on the local characteristic. Therefore, substance concentration of *Corbicula Japonica* in Lake Ogawara is used for understand the difference on the environment. In this study, the change in element concentration inside *Corbicula Japonica* caused by the difference in environment was measured by ICP-AES.
Through ICP-AES, six elements (Ca, Fe, Mg, Mn, Sr, Zn) were measured from the interior of the clams. Ca was largely compared with other elements, and the average value was 4.0098 mg/g. Sr / Ca had a positive correlation with the shell length. In addition, correlation was observed between Sr and Ca, and the correlation coefficient was 0.88.

Keywords: brackish lake, Lake Ogawara, ICP-AES

1. Introduction
Fig.1 shows the peripheral view of Lake Ogawara. Lake Ogawara is located in the eastern part of Aomori Prefecture, facing the Pacific Ocean. The lake is one of the habitats of *Corbicula Japonica*. *Corbicula japonica* is one of important fishery resources in Japan. Recently the stock biomass are decreasing, and the catch is also decreasing accordingly[1)]. Also, there is a declining trend in stock biomass and the catch in Lake Ogawara. Bottom sediment has greatly influenced by the habitat condition of *Corbicula Japonica*[2)]. However, due to differences in bottom sediments, it has not been clarified what affects to the clams. Therefore, by measuring the concentration of elements in the interior of the clams and by comparing with the sediment, it is considered that the influence on the clams due to the difference in the environment can be understood. The change in element concentration inside *Corbicula Japonica* caused by the difference in environment was measured by ICP-AES (Inductively Coupled Plasma Atomic Emission Spectroscopy). The sediment quality (mud fraction, ignition loss) at the sampling point was compared with the measured element concentration.

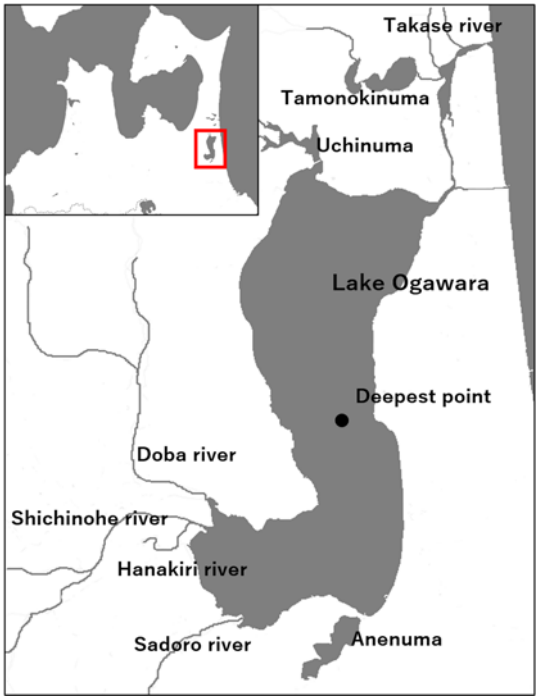

Fig.1 The peripheral view of Lake Ogawara

2. Survey and analysis method
Corbicula Japonica was collected at nine points in Lake Ogawara (water depth 1m: 6 points, water depth 3 m: 3 points), and the shell length was measured. Samples of clams used for the analysis were prepared as a set of 5 individuals at each site, and here 9 sets totally. Measurement was carried out using ICP-AES for the concentration of elements in the interior of clams.

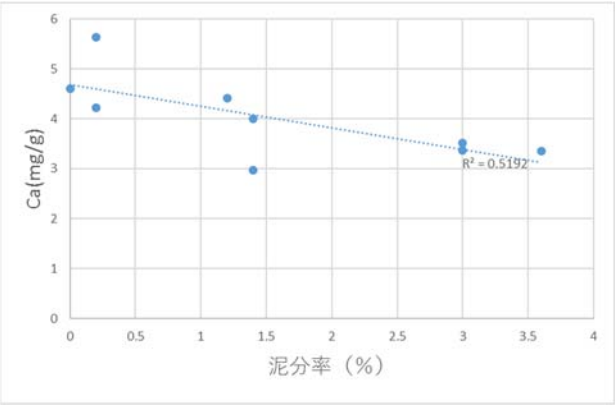

Fig.2 relationship between Ca and mud fraction

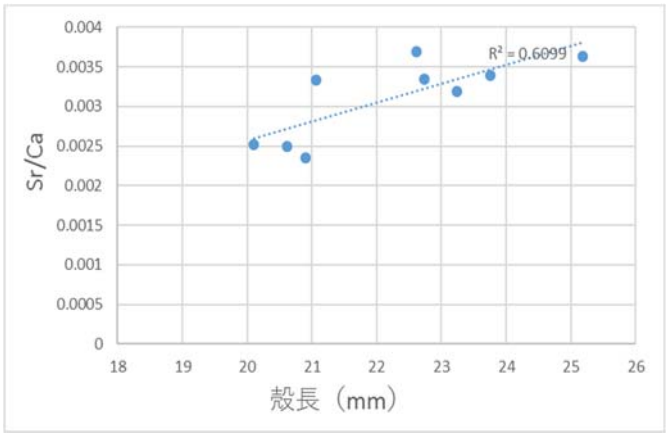

Fig.3 The relationship between (Sr/Ca) and shell

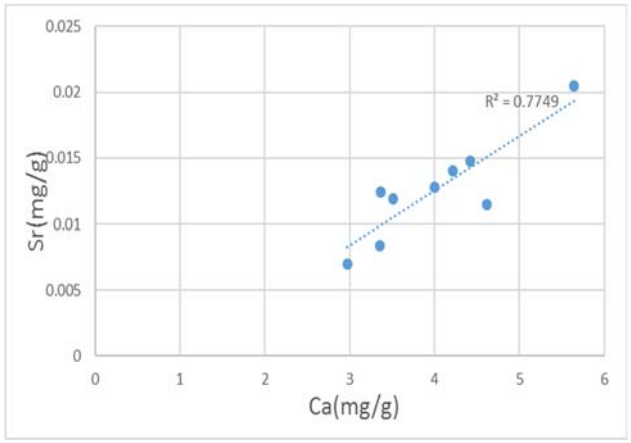

Fig.4 The relationship between Ca and Sr

Table.1 The values of Sr in each district

District	Ikato(1m)	Misawanada(1m)	Semoda(1m)	Takatori(1m)	Shimaguchi(1m)
Sr(mg/g)	0.012440794	0.011480729	0.020481168	0.008423105	0.012757852
District	Ikato(3m)	Funagasawamae(1m)	Semoda(3m)	Takatori(3m)	
Sr(mg/g)	0.014749148	0.011908764	0.014047176	0.006986357	

The sediment data is based on the data obtained from the sediment survey conducted in 2015. Sediment collection was carried out by Ekmanbage sampler. The measured values were converted per 1 g of dry weight.

3.Results

Through ICP-AES, six elements (Ca, Fe, Mg, Mn, Sr, Zn) were measured from the interior of the clams. The average values of Ca, Fe, Mg, Mn, Sr and Zn are 4.00978 mg/g, 0.21209 mg /g, 0.89363 mg/g, 0.49394 mg/g, 0.01258 mg/ g , 0.09277 mg/g, respectively. Fig.2 shows the relationship between Ca and mud fraction. As the mud component increased in the sand particle composition, Ca tended to decrease.

Fig.3 shows the relationship between Sr/Ca and shell length. Fig.2 shows the relationship between Sr/Ca and the shell length has a positive correlation. Sr/Ca and the growth rate are found to have a negative correlation in many cases[3]. *Corbicula Japonica* has been found to grow slowly as the shell length increases. Therefore, the relationship between Sr/Ca and shell length has a positive correlation.

Table 2 shows the values of strontium in each district. From this, it can be seen that the measured value of Sr is small in the Takatori area. Seawater contains 400 times more Sr than in freshwater[3]. In fact, comparing a freshwater bivalve and a marine bivalve there is a report that marine bivalve incorporates more Sr. In Lake Ogawara, the salt concentration in normal condition is low. Salt water intrusion in the lake only when the tide level becomes larger than the water level of the lake. Therefore, it is considered that the value of Sr decreased in the Takatori area far from the lake where saltwater intrusion occurs.

Fig. 3 shows the relationship between Ca and Sr. There was a correlation between Ca and Sr. The correlation coefficient was 0.88.

Future prospects

In this research, we used *Corbicula Japonica* in Lake Ogawara. As a result, it is conceivable that clams get results peculiar to Ogawara Lake. In the future, it is necessary to collect *Corbicula Japonica* in various parts of the country and analyze it. By analyzing the clams in various parts of the country, it will be clear how the internal element of the clams changes depending on the environment. Also, it is necessary to measure the bottom mud and the water quality of the lake as well as the sample of clams.

There are possibilities that internal elements of *Corbicula Japonica* are subject to change according to the season. In fact, there is a report on the seasonal fluctuation of the internal elements of *Corbicula Japonica* by past research. As a result, it is conceivable that the result will change greatly. Therefore, it is necessary to consider seasonal variation.

References

1) Akira komaru: Causes and countermeasures for decrease of fishery of clams, The 4th National Symposium of Shizimi in Lake Ogawara, p.1, 2003.
2) Akira tamai, Hirokazu fujiwara, Mitsuhiko kubota, Masayasu nagasaki, Masataka hamada, Masahumi sakaki: Correlation between water quality in the Lake Ogawara and hatching of Corbicula Japonica, Annual Journal of Hydraulic Engineering, JSCE, Vol. 52, pp.1255-1260, 2008.
3) Akira komaru, Knji onouchi, Yasuhiro yanase, Teruyoshi narita, Tsuguo otake: Sr / Ca ratio of shells of Corbicula Japonica collected in water areas with different salt concentrations by EPMA (Electron Probe Micro Analyzer), Nippon Suisan Gakkaishi 75(3), pp.443-450, 2009.
4) Yuji koizumi, Fujiwara hirokazu, Yusuke matsuo, Takuma numayama: Characteristics of water quality in Lake Ogawara in recent years, The Journal of Japan Society of Civil Engineers, Ser. B1 Vol.70, No4, I_1579-I_1584, 2014.

Start-up of a Novel Single-stage Anammox Progress for Treating Sewage

○Yujie Chen[1], Rong Chen[1,2], Jiayuan Ji[1], Satoshi Sakuma[1], Yu-You Li[1]

[1]Department of Civil and Environmental Engineering, Tohoku University, Sendai, Miyagi 980-8579, Japan
[2]Xi'an University of Architecture and Technology, Xi'an, Shaanxi 710055, P.R.C.
*E-mail: gyokuyu.ri.a5@tohoku.ac.jp

Abstract

Anammox progress is considered to be a cost-effective biological nitrogen removal way in wastewater treatment. Some wastewater treatment plants (WWTPs) have already applied anammox process. However, the start-up of anammox treatment process needs to take much time due to the anammox bacteria's long generation period and sensitivities. Most of the WWTPs used the anammox process under the condition of relatively high temperature to treat high strength ammonia nitrogen. While in order to treat wastewater under a lower or room temperature as well as to extend the application of anammox process even to the low strength ammonia nitrogen contained wastewater such as the municipal sewage, this study was focused on the start-up of the a novel single-stage anammox progress for removing nitrogen from low concentration ammonia sewage at room-temperature.

Keywords: anammox, nitrogen removal, nitritation-anammox, single-stage anammox, aeration control

1. Introduction

Anammox process was first found in 1990s by scientists in Netherland. Since then, it has been being focused on by many researchers as anammox could let the ammonium and nitrite converted into nitrogen gas in a short-cut way.

Among the processes, single-stage anammox is a process that nitritation and anammox reaction occurred in the same tank then achieved nitrogen removal. The reactions for the whole process are shown below:

Nitritation (Partial Nitrification):

$$1.3NH_4^+ + 1.95O_2 \rightarrow 1.3NO_2^- + 2.6H^+ + 1.3H_2O \quad (1)$$

Anammox Reaction:

$$NH_4^+ + 1.3NO_2^- \rightarrow 0.26NO_3^- + 1.02N_2 + 2H_2O \quad (2)$$

Single-stage Anammox (1+2):

$$NH_4^+ + 0.85O_2 \rightarrow 0.11NO_3^- + 0.445N_2 + 1.13H^+ + 1.43H_2O \quad (3)$$

During the single-stage anammox process, aeration is used for both providing dissolved oxygen (DO) to achieve nitritation and stirring in the reactor tank. In the meanwhile, given the slow growth rate and low yield of anammox bacteria, biofilms have been shown to be a more effective way because of their enhanced capacity to retain biomass within the reactor system compared to suspended sludge processes. The aim of this study was to achieve single-stage anammox process for treating low strength ammonia nitrogen wastewater at room temperature as well as investigate the shortest HRT or the highest nitrogen loading rate (NLR) based on the performance of nitrogen removal.

2. Materials and Methods

Facilities used in this study are shown as figure 1 while the operating conditions during the experiment are shown in table 1. The carriers used for biofilm growth were hollow cylinders made of hydrophobic polypropylene resin, with a size of 4 mm Φ×4 mm L, a specific gravity of 0.98 g/cm^3 and a specific surface area of 1500 m^2/m^3 and filling rate is 30 %.

In order to inhibit the nitrification reaction and promote the anammox reaction, DO in the reactor was controlled below 0.3 mg/L and the aeration rate (AR) was controlled between 0.1 – 0.2 L/min.

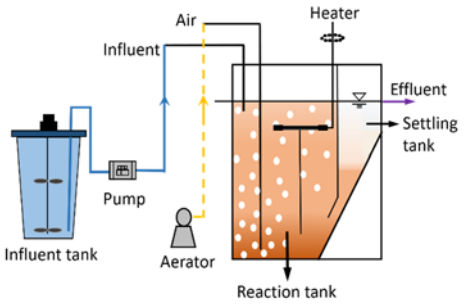

Fig. 1 The schematic picture of experimental facilities

Table 1 Operating conditions

Days	1-41	42-61	62-91	92-120	121-223
HRT(h)	6	3	2	1	2
NH_4^+-N (mg/L)	100	50	50	50	50
NLR (kg N/m^3/d))	0.4	0.4	0.6	1.2	0.6

The seed sludge (high-strength anammox sludge, MLVSS=2.2 g/L, MLSS=3.8 g/L) was collected from a PN/A reactor fed continuously by relatively high-strength synthetic wastewater containing 250 mg/L NH_4^+-N. Therefore, the anammox reactor was started up under a HRT of 6h and the NH_4^+-N concentration in the influent was set as 100 mg/L, before the extremely low-strength (50 mg/L NH_4^+-N) influent was fed. Influent pH ranged from 7.41 to 7.94.

3. Results and Discussion

Figure 2 shows kinds of nitrogen concentration in effluent, AR, DO and nitrogen removal efficiency (NRE) during the operation.

When the HRT decreased to 3 h, though the NLR was unchanged, the ammonium concentration in effluent decreased slightly and the NRE was about 61.96 % as the effect of faster flow velocity which resulted low utilization of the substrate.

Then as HRT was decreased to 2 h, the ammonium concentration in effluent became low and the NRE was improved to 76.56 % due to the higher NLR resulted the increased of the available substrate for microorganisms.

However, since the HRT was further decreased into 1 h, ammonium concentration became very high and nitrite concentration also increased lead to the NRE was as low as 25 %. The reason to be considered is that ammonium nitrogen volumetric loading was so high that AOB couldn't catch enough oxygen to transform ammonium nitrogen to nitrite nitrogen properly and there wasn't enough time for anammox process finally caused NRE decreased rapidly.

Therefore, AR was regulated higher gradually to enhance the transform from ammonium to nitrite by AOB. With DO increasing, AOB could use more oxygen which caused obviously decrease of ammonia, slightly increase of nitration in the effluent and NRE improved to about 40 % but still lower than that HRT was 2 h. On day 118, AR was recovered to 0.25 while the NRE still decreased.

During the last phase, HRT was returned to 2 h again, ammonium concentration in the effluent was decreased gradually and NRE improved gradually finally stabled at around 72 %. Meanwhile nitrite concentration was also at a extremely low level. Though nitrate concentration was higher than the first HRT 2 h phase and the NRE was also a little lower, it is reasonable as the second HRT 2 h phase was controlled by AR higher than the first one. As a conclusion of the long-termed operation, single-stage anammox process was successfully achieved for treating a low strength nitrogen wastewater at room temperature.

During HRT ranged from 3 h to 1 h in the experiment, the highest NRE was achieved in the phase of HRT was 2 h, thus the shortest HRT as well as a relatively high NRE was obtained as HRT was 2 h, and the NRE was 0.6 kg N/(m^3·d) in this study.

In a late period, the symbiotic relation of anammox bacteria and anammox oxidizing bacteria (AOB) by fluorescence in situ hybridization (FISH) was studied. The results (Figure 3) showed that there was an obvious symbiotic relation between the two kinds of bacteria. And the quantitative proportion of anammox to AOB is 1:1.1.

4. Conclusions

The results of this study were concluded as below:

1) This study demonstrated that anammox process can remove nitrogen from low strength ammonia nitrogen sewage at room temperature by the aeration rate controlled around 0.1 L/min.

2) The HRT condition was achieved as short as 2 hours with a nitrogen loading rate of 0.6 kg N/(m^3·d), acted out the nitrogen removed efficiency kept at 74+15%.

3) According to the results of FISH experiment, anammox bacteria and AOB can be cultured together in the sludge and presented the quantitative proportion of anammox to AOB was 1:1.1 in this study.

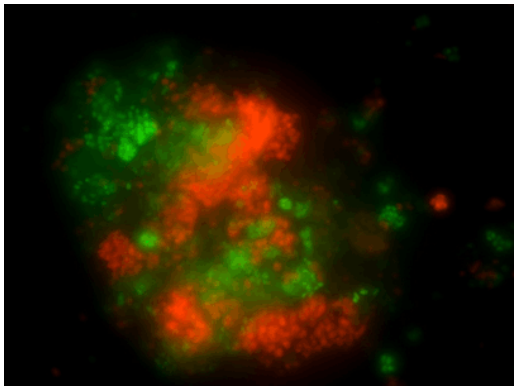

Fig. 3 Anammox-AOB association in the biofilm (Red represents anammox bacteria and green represents AOB)

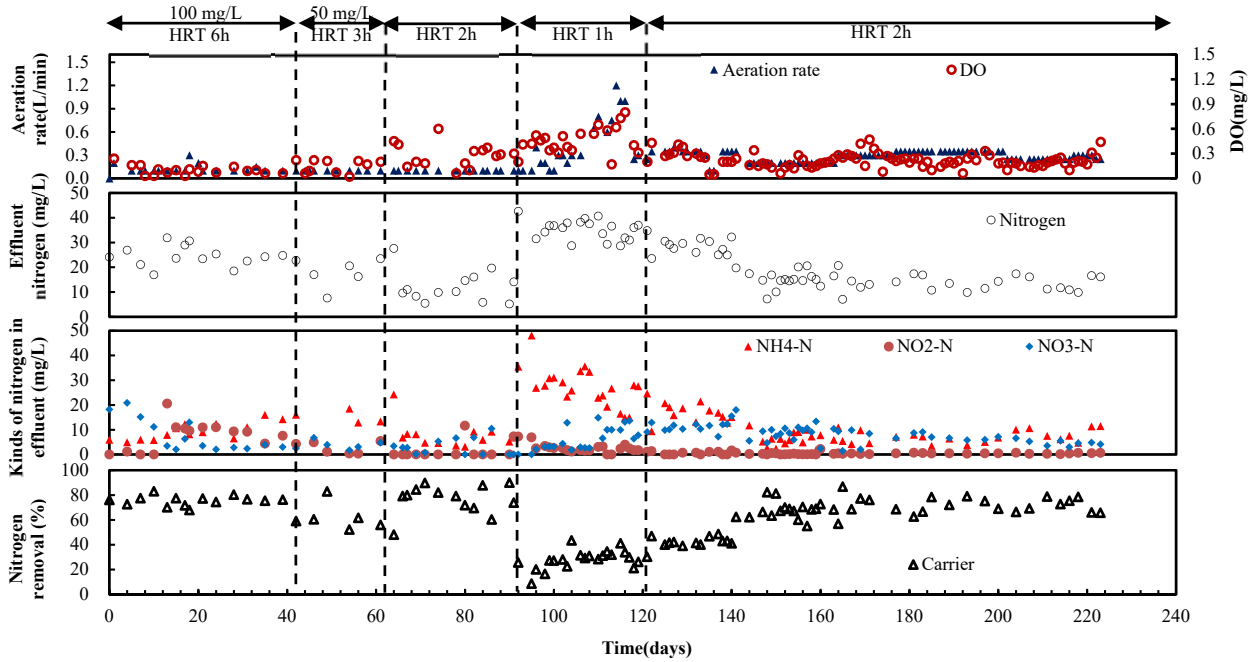

Fig. 2 Treatment performance on nitrogen removal

How do the facultative DMF degradation bacteria play their roles in anaerobic conditions

○Lu Li[1], Zhe Kong[1], Kengo Kubota[1], Yu-You Li[1]*

[1]Department of Civil and Environmental Engineering, Tohoku University, Sendai, Miyagi 980-8579, Japan
*E-mail: gyokuyu.ri.a5@tohoku.ac.jp

Abstract

12 samples were taken from a series of process in the decomposition of *N*, *N*-Dimethylformamide (DMF) to reveal the difference of microbial community between aerobic condition and anaerobic conditions. Through aeration, *Paracoccus* increased rapidly and generate DMFase to degrade DMF into dimethylamine (DMA) and formic acid (HCOOH). The intermediate products can be used as carbon resource to generate methane by methanogenic archaea in anaerobic sludge. By mix the aerobic and anaerobic sludge, DMF degrading bacteria and methanogenic archaea generate a symbiotic system thus DMF can be degraded into methane in anaerobic condition.

Keywords: DMF, DMFase, anaerobic, co-culture

1. Introduction

N, *N*-Dimethylformamide (DMF) [$(CH_3)_2NCHO$] has been widely employed in variety of chemical and manufacturing industries owing to its excellent water-miscibility. According to the statistics data from Pollutant Release and Transfer Resister, DMF contained emissions rank third in newly added toxic pollutants in 2014 and approximately 5.36×10^3 tons of DMF were either discharged or transferred in 2015. DMF is poisonous and hazardous to human due to its hepatotoxicity and carcinogenicity. Thus, effective treatment of DMF-containing wastewater has become a great concern worldwide. Traditional physical and chemical methods were unfeasible or unfriendly to environment. To massively treat DMF-containing wastewater, biodegradation was considered as an appropriate alternative. Since aerobic degradation takes lots of energy for aeration, we want to investigate whether the toxic DMF can be degraded in anaerobic condition and produce methane.

Degradation of DMF in anaerobic conditions had been realized in our previous studies by artificially mixed the aerobic sludge and anaerobic sludge, but the mechanisms is still unclear.

Our study aims to: (1) identify predominant microorganisms in aerobic and anaerobic conditions; (2) clarify the changes in community structure between different conditions; (3) explain the role of functional bacteria in DMF decomposition system.

2. Materials and Methods

2.1 Experimental design and Sampling

A 62-day batch experiment was conducted to verify whether DMF can be degraded in anaerobic conditions by artificially mixed an aerobic sludge (Sample ID: K4) and an anaerobic sludge (Sample ID: K5). In the whole process, totally 4 parts were contained. Part I aerated anaerobic sludge to promote the growth of DMF-degrading bacteria (Red line in Fig. 1). Part II conducted a 62-day anaerobic domesticated culture from the mixed sludge (Sample ID: K10) by batch experiment (Blue line in Fig. 1). Part III was a batch control started from sample K5 while Part IV is a long-term reactor control (Green line).

2.2 DNA extraction, PCR and Illumina sequencing

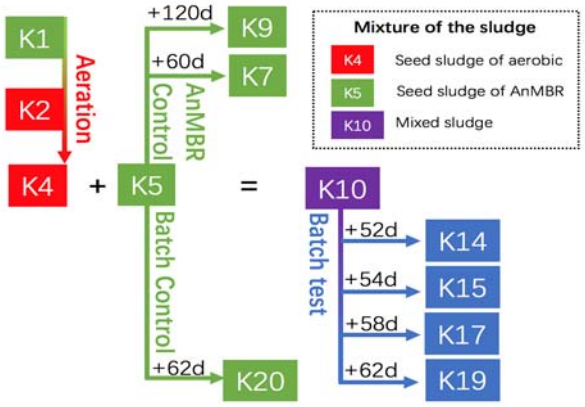

Fig. 1 Relationship between samples.

DNA was extracted with ISOIL for Beads Beating kit (Nippon gene, Japan), then measured the concentration by NanoDrop 2000 (Nanodrop Inc., USA) and diluted to 10 ng/μl for PCR. V3-V4 fragment of 16S rRNA gene were amplified with the foward primer 341F and mixed reverse primer 806R/806R-P. PCR condition was as follows: 30 cycles of 94 °C for 5 secs, 50 °C for 30 secs, 68 °C for 10 secs, and a final extension at 68 °C for 7 min with Low DNA Ex Taq® (TaKaRa, Japan). The purity and concentration of amplified DNA was verified by DNA chip 7500 with Bioanalyzer (Agilent Technologies, USA) and then purified with Agencourt® AMPure® XP (Beckman Coulter, Inc., USA) according to the manufacturers' instructions. Purified DNA was measured by Qubit 3.0 ® (Life technologies, USA) and diluted to 2 ng/μl. Barcode added PCR products were sequenced by Illumina Miseq platform.

2.3 Data processing

Raw data were filtered to remove short and low-quality sequences, as well as demultiplexing were done with split_libraries_fastq.py in QIIME (version 1.8.0). OTUs were generated based on 97% identity, then Chimeras were removed with ChimeraSlayer. Singleton OTUs were removed and sequences were randomly selected to unified the sequence number of each sample to 40,000. LEfSe analysis was proceeded online in Galaxy website.

3. Results and discussion

3.1 Proportion analysis

The relative proportions of main phyla are shown in figure 2, the phyla which occupied less than 1% of total sequences is summarized as "Others". We can see that in Prat I (Include samples of K1, K2 and K3), phylum Proteobacteria increased rapidly. In Part II (Include samples from K10 to K14-19), phylum Euryarchaeota, the only main phylum of archaea, rarely appeared in both aerobic conditions but bloomed in the mixed sludge. In Part III (Include samples from K5 to K7 and K9) and Part IV (from K5 to K20), the community structures are similar.

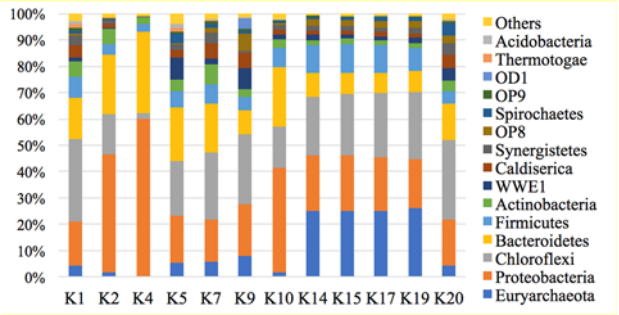

Fig. 2 Main phyla of 12 samples.

3.2 Cluster analysis

12 samples were analyzed for PCoA (Principal Coordinates Analysis) with weighted calculation method (Fig. 3). Significant changes have taken place in different types of samples. With aeration, the anaerobic sludge K1 transform into K2 and K4, the red arrow represents the community structure changed with aeration. Than we mixed the K5 and K4 to generate the mixed sludge of K10 thus K10 located in the position which is between K5 and K4. After 60 days anaerobic co-cultivation, the new symbiosis community structure formed and seems stable. While the control group, nether the batch control group nor the reactor control group can generate a new symbiosis community structure which can effectively degrade DMF.

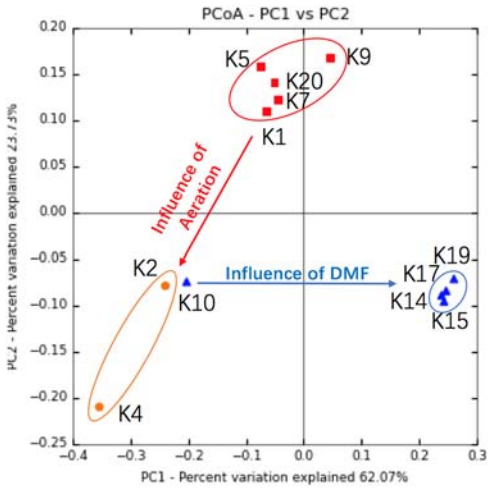

Fig. 3 Principal Coordinates Analysis.

3.3 Function analysis

LEfSe analysis were based on top 43 OTUs which represent 80% of total sequence in 12 samples. In level of Genus, *Paracoccus* increased rapidly when anaerobic sludge turned into aerobic one, this genus had been proved to have the ability to degrade DMF into dimethylamine (DMA) and formic acid (HCOOH) in aerobic condition by produce DMFase and this genus was identified as facultative anaerobes. In our research, in Part I, *Paracoccus denitrificans* increased rapidly and the relative ratio reached to 20% in K4. While in Part II, the relative ratio keeps at 5%.

The right blue part in LEfSe (Fig. 4) shows that archaea bloomed and comes to the dominate ones after mixed the sludge. Methane production rate increased and the DMF concentration decreased based on the experimental data. In control groups, the methanogenic archaea cannot proliferate without carbon resource of DMA and MMA which is the intermediate products in the degradation of DMF to methane.

Based on this, we propose that by mix the aerobic sludge which can generate DMFase and the anaerobic sludge which harbors methanogenic archaea, the degradation of DMF can be realized in anaerobic condition.

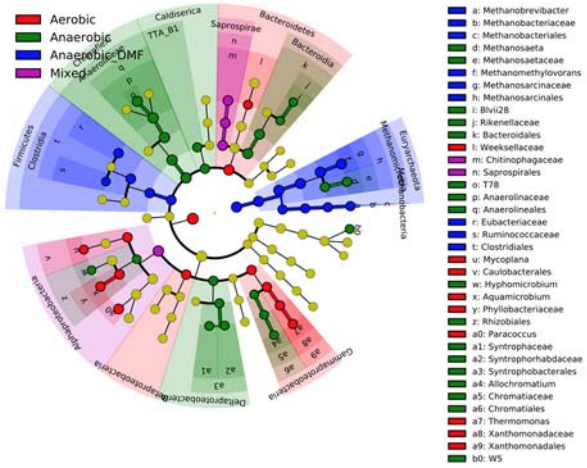

Fig. 4 LEfSe analysis of total samples based on 4 groups.

4. Conclusions

(1) Phylum Proteobacteria increased rapidly when aerobic sludge turned into anaerobic one. Only mixed sludge can harbor a certain number of archaea which is associate with methane fermentation.

(2) In total 4 parts of cultivation, only two pathways can be inducted as the evolution of bio-community structure. One is from anaerobic to aerobic condition, another one is from a simply artificial mixed sludge to a symbiosis system.

(3) Specific species from aerobic sludge degrade DMF into DMA by produce DMFase while methanogenic archaea from anaerobic degrade DMA to MMA than to methane. A mutualistic symbiosis generated in anaerobic condition.

5. Acknowledgements

The authors would like to thank their advisors and workmates in the lab of Tohoku University, this article was supported by Tohoku University Division for Interdisciplinary Advanced Research and Education.

Effect of HRT on Thermophilic Anaerobic Digestion of Paper Waste Containing OFMSW

○Aijun ZHU[1]*, Jing WU[1], Yu Qin[2] & Yu-You Li,[1,2]
[1] Department of Frontier Science for Advanced Environment, Graduate School of Environmental Sciences, Tohoku University, 6-6-20 Aoba, Aramaki-Aza, Aoba-Ku, Sendai, Miyagi 980-8579,
[2] Department of Civil and Environmental Engineering, Graduate School of Engineering, Tohoku University, 6-6-06 Aoba, Aramaki-Aza, Aoba-Ku, Sendai, Miyagi 980-8579, Japan;
*E-mail: zhu.aijun.t4@dc.tohoku.ac.jp

Abstract
The aim of this study was to investigate the effect of hydraulic retention time (HRT) on methane production using a single-stage anaerobic process. One continuously stirred tank reactors (CSTRs) were used under thermophilic conditions (55±2ºC) in order to enhance methanogenesis. A mixture of paper waste and OFMSW (1:1:1, v/v/v) was utilized. The reactor was operated at three different HRTs of 30, 20 and 10 days. The maximum CH_4 production rate of 6.99 L/L d was achieved at HRT of 10 d. The TS, VS, carbohydrate and COD removal efficiency was almost same at different HRT and protein showed negative removal efficiency.

Keywords: Single-stage anaerobic digestion; paper waste; OFMSW; Hydraulic retention time

1. Introduction
Renewable energy sources have received great interest from the international community during the last decades. Organic fraction of municipal solid waste (OFMSW) is one of the most promising energy sources. However, despite its high carbohydrate content, the anaerobic treatment of OFMSW is quite problematic due to its low bicarbonate alkalinity high COD concentration and tendency to rapid acidification. Except for the resistant to biodegradation, the low C/N ratio of algal sludge is also a serious problem to the anaerobic digestion. Although, an optimum C/N range in feedstock for the anaerobic digestion is still debatable in the literature, 20/1–30/1 is a most acceptable range (Parkin and Owen, 1986).

One method to avoid excessive ammonia accumulation is to adjust low feedstock C/N ratios by adding high carbon content materials, thereby improving the digestion performance. Most OFMSW consists of paper material (including office paper and newspaper), which has a C/N ratio ranging from 173/1 to greater than 1000/1 (Stroot et al., 2001). Both wastes are produced in large quantities and in many places, and much research has focused on this particular issue. Co-digestion using paper waste containing OFMSW as substrate may enhance the performance of the AD due to better carbon and nutrients balance. That is, the use of a co-substrate that in most cases improves the biogas yields due to positive synergisms established in the digestion medium and the supply of missing nutrients by the co-digestion.

A series of operational parameters including pH (Dareioti et al.,2014), temperature, reactor configuration (Nasir et al., 2012), Among them, hydraulic retention time (HRT) has been reported as one of the most important parameters significantly affecting microbial ecology in CSTR digesters and must be thus optimized for the particular feedstock fermented in the digester. Organic loading rate (Mariakakis et al., 2011) and hydraulic retention time (Rincon et al., 2008) have been investigated in the literature due to their effect on biogas production. More specifically, our aim was to study the effect of HRT, as one of the most critical operating parameters on methane production. The purpose of this work was to assess the possibility of co-digestion of OFMSW and high carbon content of waste paper at different HRT to produce methane on the methane production.

2. Materials and Methods

2.1 Materials
The compositions of OFMSW used as substrate in the test based on previous study which consisted of 30% fruits, 36% vegetables, animal 14% and staple food 20%. (Li et al. 2003). The collected OFMSW were ground and homogenized to less than 5 mm with tap water in a blender and were stored at 4°C before feeding. FW was supplemented with the cardinal elements, Fe, Co and Ni: 100 mg/L of Fe ($FeCl_2{\cdot}4H_2O$), and 10 mg/L of both Co ($CoCl_2{\cdot}6H_2O$) and Ni ($NiCl_2{\cdot}6H_2O$) (Wu et al. 2015).

The paper waste was consisted of office paper toilet paper and newspaper which are the most amount of recycle paper in Japan. The ratio of three paper waste was 1 : 1 : 1, cut by shredder before mixing with OFMSW for feeding.

Seed sludge was from a mesophilic sewage sludge digester at the Sendai municipal sewage treatment plant located along Sendai, Japan.

2.2 Analysis methods
Daily biogas production is measured by wet gas meter, and the composition of biogas (CH_4, CO_2 and N_2) were measured by a ShimadzuGC-8A gas chromatograph. The

pH, COD, TS, ammonium nitrogen, alkalinity, VS and VSS were measured according to Standard Methods (APHA, 1995). Sludge samples were sampled twice a week from the digesters and the substrate tank to determine the total and soluble parameters. Samples for the analysis of soluble items, such as soluble COD (SCOD), total ammonia nitrogen (TAN), VFAs and alkalinity, were centrifuged at 8,000 rpm for 15 min and then filtered with 0.45 μm filters before they were analyzed. A GC, equipped with a flame ionization detector ((GC-FID, Shimadzu GC-14B) and a DB-WAXetr column, was utilized to detect VFAs and ethanol. A 0.5 mL filtrate was collected in a 1.5 mL GC vial, and 0.5 mL 0.1 mol/L HCl solution was also added to achieve an acidic pH.

2.3 Reactors start-up and operation

A mixture of paper waste and OFMSW (in a ratio of 1:1v/v) was used, based on our previous experiment. Experiments were carried out in a single-stage continuous anaerobic process. The anaerobic reactors were cylindrical in shape, made with a double wall, having an operating volume of 3 L, and were operated at constant temperature (55±2°C) via a heaters and water jackets. The feedstock was stored in a tank maintained constant temperature at 4 °C.

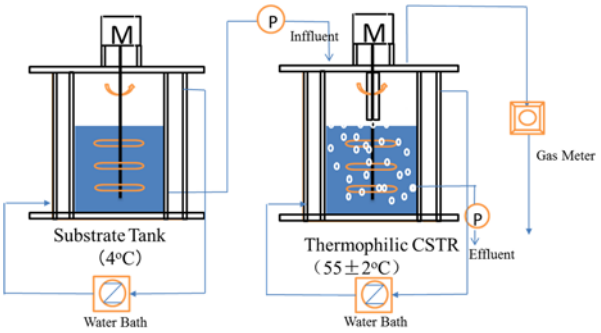

Fig. 1. Schematic diagram of the single-stage system used in this study for methane production

The continuous operation of the reactor started at HRT of 30 d. Sludge samples were sampled twice a week from reactors under continuous stirring conditions and analysed, for monitoring each reactors performance. Experiments were conducted successively to determine the optimum HRT for methane production. Organic loading rate (OLR) was increased by decreasing the operating HRT. The reactor was operated at three different HRTs of 30, 20 and 10 d with a feeding mixture of paper waste and OFMSW. The tested operating conditions in the two-stage system are summarized in Table 1.

Table 1 Operating conditions in the digester

Run NO.	HRT(d)	OLR (g VS/L d)	OLR (g COD/L d)
1	30	7.27	4.3
2	15	14.5	8.6
3	7.5	29.1	17.3

3. Results and Discussion

The changes of reactor performance in the three HRT were measured and the results are summarized in Figure 2. As shown in Figure 2, pH remained practically constant at each HRT values (30, 20 and 10 d), with values 7.47 ±0.02, 7.31±0.06 and 7.15±0.07, respectively. The TAN and alkalinity decreased significantly with the decrease of HRT, but finally it can keep a stable level. There is no change about methane contents in each HRT. During the all operation time, there is no VFA accumulation observed, indicating process stability. The average biogas production in each HRT was 2.18 3.41 and 6.99 L/L/d respectively, as shown in Fig. 2.

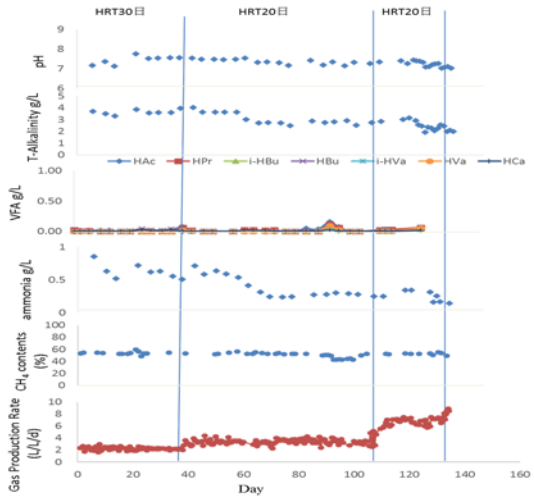

Fig. 2. Time course for thermophilic reactor

Figure 3 **presents** the experimental results about organic removal efficiency obtained at steady-state conditions for the different HRTs. The TS, VS , carbohydrate and COD removal efficiency was almost same at different HRT, s the the all best performance as positive removal was achieved in HRT＝30 days, TS(77.3%), VS(81.6%) , carbohydrate (91.5%) and COD(78.9%)Meanwhile, protein showed negative removal of 13.4% , 21.4%, and 29.5% respectively. The single-stage continuous anaerobic process was a promising way to treat the paper waster and OFMSW. And there is possible for single-stage continuous anaerobic process operating at more shorter HRT .

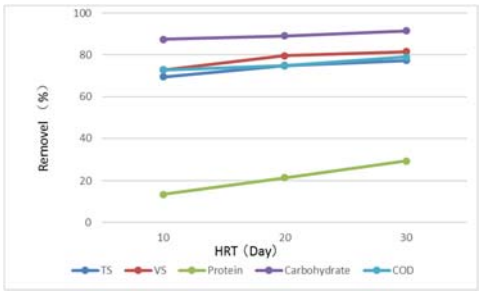

Fig. 3. Effect of HRT on removal efficiency of COD, TS, VS, carbohydrates and protein